

AN ABSTRACT OF THE THESIS OF

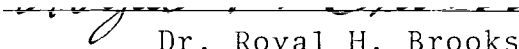
Chong-Guang Su for the degree Ph.D.

in Civil Engineering presented on March 29, 1976

Title: Hydraulic Functions of Soils from Physical
Experiments and Their Applications

Redacted for Privacy

Abstract approved:


Dr. Royal H. Brooks

Based upon the Pearson Type VIII distribution function, a general retention function which relates the saturation to the capillary pressure in disturbed soils has been discovered. This simple and yet complete function has been shown to describe precisely the imbibition as well as the drainage branch of the retention curve. It is defined by four readily assessed parameters that either have physical significance themselves or may be used to determine some hydraulic properties of the soil.

With the assumption that the Burdine integrals are adequate, a relative permeability function has been derived through the substitution of the retention function for the integrands in the Burdine integrals. The permeability function is expressed in terms of the incomplete Beta

function ratio whose value may be conveniently found in some mathematical tables.

Further, a general pore-size distribution function of soils has been obtained from the retention function. The derivation of the pore-size distribution function enables more rigorous examination and further exploration of the theories concerning water movement in partially saturated soils. In this respect, an explanation of the phenomenon of air entrapment during imbibition has been offered through an energy concept based upon the pore-size distribution function along with the retention function.

Two criteria of affinity have been established for porous media. Media are said to be affine if their corresponding pore-size distribution parameters are identical. The scaling factor for the external dimension of the model has been chosen to be the capillary pressure head at the inflection point of the retention curve, whose value is always finite.

The effect of the pore-size distribution parameters upon the retention, permeability and diffusivity curves has been analyzed. The analysis shows the parameter governing the downward concavity of the retention curve is as important as that governing the upward concavity when it comes to computing the permeability values from the retention data.

A new and simple apparatus and procedure for obtaining the retention data of soil water in the laboratory have been developed. The technique can expedite the acquisition of the data for either the drainage or the imbibition branch of the retention curve.

Hydraulic Functions of Soils
from Physical Experiments
and Their Applications

by

Chong-Guang Su

A THESIS

submitted to

Oregon State University

in partial fulfillment of
the requirements for the
degree of

Doctor of Philosophy

Completed March 29, 1976

Commencement June 1976

APPROVED:

Redacted for Privacy

Associate Professor of Agricultural and Civil Engineering
in charge of major

Redacted for Privacy

Head of Department of Civil Engineering

Redacted for Privacy

Dean of Graduate School

Date thesis is presented March 29, 1976

Typed by Barbara McVicar for Chong-Guang Su

ACKNOWLEDGMENTS

The author wishes to thank Dr. Royal H. Brooks, his major adviser, for the encouragement and assistance received during the years of his graduate study towards the doctorate. Dr. Brooks's inspiring suggestion and constructive criticism throughout the course of the development of this thesis are valuable. The author is fortunate to have such an adviser.

Appreciations are also extended to Dr. Peter C. Klingeman, under whose altruistic guidance the author earned his M.S. degree, and Dr. John R. Davis for their assistance at the preliminary stage of this doctoral study, and to Dr. John W. Wolfe, whose help is always remembered, and Prof. Leonard J. Weber for their service as members of the author's doctoral committee. For the special review and criticism of this thesis by Drs. Catherine E. K. Rovey and Charles H. Ullery, the author is grateful.

A special gratitude is due to the author's aunt and sisters. Their perennial affection helps make a cherished wish come true.

Acknowledgments are also expressed to Barbara McVicar of the Department of Agricultural Engineering, OSU for her typing the manuscript and to Pete Lyngstrand for his drawing the figures.

Finally, the financial support of this research from the Office of Water Resources and Technology, U.S. Department of the Interior through Grant No. 14-31-0001-4218, is gratefully acknowledged.

To the Memory of My Parents

TABLE OF CONTENTS

	<u>Page</u>
ABSTRACT	i
ACKNOWLEDGMENTS	vi
LIST OF FIGURES	xii
CHAPTER I -- INTRODUCTION	1
CHAPTER II -- REVIEW OF LITERATURE	5
A. Water Retention Functions	5
B. Computational Schemes for Determining Partial Hydraulic Conductivity	11
1. Statistical approach	12
2. Hydraulic radius theory	21
C. Methods of Obtaining Retention Data in the Laboratory	26
CHAPTER III -- THEORY	30
A. Retention Function	30
B. Permeability Function	39
C. Diffusivity Function	43
CHAPTER IV -- CRITERIA OF AFFINITY FOR POROUS MEDIA	46
A. Scaled Hydraulic Functions	47
1. Scaled retention function	47
2. Relative permeability function	50
3. Scaled diffusivity function	50
B. Pore-Size Distribution Function	52
CHAPTER V -- EXPERIMENTAL PROCEDURE	55

TABLE OF CONTENTS (Continued)

	<u>Page</u>
CHAPTER VI -- RESULTS AND DISCUSSION	62
A. Determination of the Parameters of the Retention Function from Retention Data	62
B. Comparison of the Retention Function with Experimental Data	64
C. Comparison of the Permeability Function with Experimental Data	70
D. Physical Significance of the Parameters of the Retention Curve	73
1. The inflection point	73
2. The boundary effect of the retention cell	76
E. Effect of the Pore-Size Distribution Parameters upon the Retention Function and the Probability Density Function of Pores	78
F. Effect of the Pore-Size Distribution Parameters upon Permeability and Diffusivity	84
G. Hysteresis and Air Entrapment	90
H. The Concept of Energy	93
CHAPTER VII -- CONCLUSIONS	97
A. Summary	97
B. Significant Findings	101
C. Needs of Future Research	103
BIBLIOGRAPHY	104
APPENDICES	
A. Nomenclature	110

TABLE OF CONTENTS (Continued)

	<u>Page</u>
B. Steps to Reduce the System of Four Equations to a Single Nonlinear Equation with S_r as the Unknown	114
C. Computer Program for Determining the Parameters of the Retention Function	120
D. Experimental Data Pertaining to the Figures	124

LIST OF FIGURES

<u>Figure</u>		<u>Page</u>
1	Definitive retention curves depicting the relationships of the parameters in the theoretical retention function.	33
2	Schematic of the apparatus for obtaining the retention data.	57
3	Comparison of the theoretical (or computed) retention curves with retention data of two media, where the dots represent measured values.	67
4	Comparison of the theoretical (or computed) retention curves with retention data on the first drainage (initially vacuum-saturated) and imbibition branches for two media, where the points represent measured values.	68
5	Comparison of the theoretical (or computed) retention curves with retention data on the second drainage (initially apparently saturated) and imbibition branches for two media, where the points represent measured values.	69
6	Comparison of the theoretical (or computed) relative permeability curve with experimental data obtained from Corey (1959), where the corresponding retention data and curve are shown in (A).	71
7	Comparison of the theoretical (or computed) relative permeability curve with experimental data obtained from Corey (1959), where the corresponding retention data and curve are shown in (A).	72
8	Scaled saturation and scaled frequency of pore sizes as functions of scaled capillary pressure for two media with widely different pore-size distributions.	75
9	Comparison of the theoretical (or computed) retention curves with retention data on the first drainage branch, where the theoretical curves were determined by using the four data points indicated by solid circles.	77

LIST OF FIGURES (Continued)

<u>Figure</u>		<u>Page</u>
10	Hypothetical retention and pore-size distribution curves of media with various values of m .	80
11	Theoretical curves of scaled saturation and scaled frequency of pore sizes as functions of scaled capillary pressure for hypothetical media having various values of b/a and $m = 0.5$.	81
12	Comparison of the theoretical pore-size distribution function, $dS./dr.$, and the function, $dS./dP$. for $m = 0.5$ and $b/a = 0.25$.	83
13	Theoretical relative permeability curves for hypothetical media having various values of m and $b/a = 0.25$.	86
14	Theoretical relative permeability curves for hypothetical media having various values of b/a and $m = 0.5$.	87
15	Theoretical scaled diffusivity as a function of scaled saturation for various values of m and for $b/a = 0.25$.	88
16	Theoretical scaled diffusivity as a function of scaled saturation for various values of b/a and for $m = 0.5$.	89
17	(A) Theoretical scaled retention curves forming the hysteresis envelope and (B) the scaled frequency of pore sizes as a function of scaled capillary pressure for the hysteresis envelope shown in (A).	91
18	Theoretical scaled retention curves and theoretical scaled pore-size distribution curves for the hysteresis envelope.	92

HYDRAULIC FUNCTIONS OF SOILS FROM PHYSICAL EXPERIMENTS AND THEIR APPLICATIONS

CHAPTER I INTRODUCTION

Engineers dealing with watershed hydrology, land drainage, and irrigation are often confronted with difficulty of accurately describing the complex soil-water system. Not only is the soil-water system in nature complicated by the variability of soil properties in space, but the chemical and biological interactions on these properties as functions of time defy description. In spite of the difficulty, much can be gained by considering the soil-water system as one in isothermal, stable and homogeneous conditions. But even for this ideal soil-water system, it is still not a facile task to describe water movement in soils, owing to the strong nonlinearity among the variables that control the storage and movement of water in the porous space.

With today's high-speed, large-capacity computers and with the modeling technique presently available, it is not impossible to investigate thoroughly the subsurface water movement for a particular set of boundary conditions provided the properties of the soil-water system can be defined in functional or tabular forms. But it will be difficult to construct a generalized model and predict its performance

for a wide range of soil properties when little is known about the range that may be encountered in the field.

The functional forms of general relationships among the variables governing water movement and storage in soils are highly desirable, particularly if the functions involve meaningful and measurable hydraulic properties of the soil. One advantage of the functional relationships is that computation time and computer storage space for the solutions of flow problems are greatly reduced, and the input data to the computer need only to consist of a few hydraulic parameters of the soil. Furthermore, if the range of the values of soil hydraulic parameters is known, one may deduce a family of solutions that would approach what is obtainable from analytical solutions.

In particular, the functional forms are needed in the solutions of problems that employ Darcy's law for either steady or unsteady flow. After Darcy (1856) first proposed his empirical law governing the flow of water in saturated sands, Buckingham (1907) suggested that Darcy's law would be valid for partially saturated media as well. His supposition was later verified experimentally by Childs and Collis-George (1950). Therefore, in partially saturated media, the constant hydraulic conductivity needs to be redefined as a function of soil-water content. The combination of Darcy's law with the variable hydraulic con-

ductivity and the equation of continuity brings about a general partial differential equation for water movement in partially saturated soils. The flow equation may be solved analytically or numerically depending upon the complexity of the system. For complex systems, analytical solutions are not obtainable owing to the strong nonlinearity of the equation.

Inasmuch as the relationship between hydraulic conductivity and soil-water content is difficult to obtain experimentally, many researchers have resorted to predictive methods of evaluating this relation from the measured water retention curve. Some of the methods have been experimentally verified and seem to give reasonably good approximations. Thus, if a general relationship is available for the water retention curve, it follows that a general expression may be obtained for the relation between hydraulic conductivity and soil-water content, which includes the properties or constants of the water retention curve.

Functions for both hydraulic conductivity and retention of water have been proposed independently. In a few cases, researchers have proposed dependent relationships only to become either oversimplified approximations or highly complex, exact expressions that lose their practicality. In the latter case, too many constants make the relationships difficult to assess by indirect methods, and it becomes

prohibitive to relate the constants to easily visualized or measurable properties of the soil.

It is the first objective of this thesis to present simple and yet complete functional relationships among soil-water content, hydraulic conductivity and capillary pressure. The relationships include meaningful properties or parameters of the soil, which will be useful in characterizing the soil hydraulically. The second objective is to develop a new apparatus and procedure which will expedite the acquisition of the retention data in the laboratory.

CHAPTER II

REVIEW OF LITERATURE

A. Water Retention Functions

Brooks and Corey (1964) appeared to be the first to develop a convenient function that relates capillary pressure to saturation for media with relatively wide ranges of pore-size distribution. In their equation,

$$S_e = \left(\frac{P_b}{P} \right)^\lambda \quad \text{for } P \geq P_b$$

$$\text{and } S_e = 1.0 \quad \text{for } P \leq P_b \quad (2-1)$$

where S_e is the effective saturation defined as $(S - S_r)/(1 - S_r)$, S_r is the residual saturation, P_b is the bubbling pressure related to the largest pore size forming a continuous network of flow channels within the medium, P is the capillary pressure, and λ is an index to the pore-size distribution. The derivation of this function emanated from a large number of experimental data of the drainage branch of the retention curve. The two parameters of the function, namely, P_b and λ , have physical significance and have been used as criteria of similitude. Since Equation (2-1) is a step type function, it fails to describe the downward concavity of the retention curve in the region of high saturation. In general, the function can describe reasonably

well the experimental data in the portion of the curve showing upward concavity. For the media with ill-defined bubbling pressure, i.e., with a P_b being practically zero, the use of P_b as a characteristic length for scaling presents difficulty.

King (1965) developed a complicated equation for describing both the drainage and imbibition branch of the retention curve. To enable the "plateau" of the retention curve for small values of capillary pressure to be equally well described, he managed to produce the hyperbolic function,

$$S = \delta \left\{ \frac{\cosh \left[\left(\frac{P}{P_0} \right)^\beta + \epsilon \right] - \gamma}{\cosh \left[\left(\frac{P}{P_0} \right)^\beta + \epsilon \right] + \gamma} \right\} \quad (2-2)$$

where β , δ , ϵ , γ and P_0 are parameters whose values depend upon the properties of the water and the soil, and the hysteresis. Each of these parameters is subject to a certain constraint such that $P_0 > 0$, $\beta < 0$, $\cosh \epsilon \geq \gamma > 0$, $1 \geq \delta > 0$, and $\epsilon \geq 0$. Furthermore, as P approaches zero, S approaches δ , and as P approaches infinity, S approaches

$$\frac{\delta(\cosh \epsilon - \gamma)}{\cosh \epsilon + \gamma}$$

or $\lim_{P \rightarrow \infty} S = \frac{\delta(\cosh \epsilon - \gamma)}{\cosh \epsilon + \gamma} .$

King pointed out that the lower limit of S should correspond closely to the residual saturation defined by Brooks and Corey (1964). Also, the function may be transformed so that the capillary pressure becomes the dependent variable. The transformation yields

$$P = P_0 \left\{ \ln \left[\gamma \left(\frac{\delta + S}{\delta - S} \right) + \sqrt{\gamma^2 \left(\frac{\delta + S}{\delta - S} \right)^2 - 1} \right] - \epsilon \right\}^{\frac{1}{\beta}}. \quad (2-3)$$

To determine the parameters of Equation (2-2) or (2-3) is by no means a simple task as King admitted. With its strong nonlinearity and dealing with experimental data, even a system of five simultaneous equations in terms of the five unknown constants would be difficult to solve because of the uncertainty of the five initial guesses and the possible experimental errors in the data. A nonlinear regression analysis would be even more difficult. The application of Equations (2-2) and (2-3) is undoubtedly limited.

Upon examining several distribution laws available from general probability theory such as the incomplete gamma distribution, the lognormal distribution, and the first asymptotic distribution for the largest values, Brutsaert (1966) concluded that although the use of a given probability law might be justified on a theoretical basis, the preference of one law to another in most cases rested upon purely heuristic grounds. According to Brutsaert, from a practical

viewpoint, the selection of the probability law should depend upon not only the porous medium but also the nature of the problem. The mathematical manipulations of these probability density functions, by and large, cannot be easily performed. The problem in assessing the parameters of those functions appears prohibitive. Thus, Brutsaert proposed a simple empirical distribution function of his own. He presented the relation:

$$S_e = \frac{a}{a + (c/r)^b} \quad (2-4)$$

where S_e is the effective saturation, r is the pore radius, and a , b , and c are constants. This function is somewhat similar to that of Brooks and Corey (1964) if the variable of pore radius is replaced by that of capillary pressure. He claimed without giving substantial evidence that a much better fit with experimental data could be obtained with Equation (2-4) than those proposed by Brooks and Corey (1964). It should be noted that no physical significance was attached to the constants of the equation.

Laliberte (1969) presented a pore-volume probability density function, $s_e(r)$, which would yield some mathematical expressions for the relation between capillary pressure and saturation. He postulated that $\xi(r)$, a transformation of $s_e(r)$, was normally distributed such that

$$\int_0^r s_e(r) dr \approx \frac{1}{\sqrt{\pi}} \int_{-\infty}^{\xi} \exp(-\xi^2) d\xi \quad (2-5)$$

$$\text{where } \xi(r) = \frac{\alpha}{(r_b/r) + \gamma} - \beta \quad (2-6)$$

$$\text{or } \xi(P.) = \frac{\alpha}{P. + \gamma} - \beta$$

and α , β , and γ are constants depending upon the porous material, r is the radius of pores, r_b is the radius of pores corresponding to the bubbling pressure, and $P.$ is the scaled capillary pressure with the bubbling pressure as scaling factor. When the pore-size distribution function,

$$\frac{dS_e}{dr} = s_e(r),$$

is combined with Equation (2-5), then

$$S_e(r) = \frac{1}{\sqrt{\pi}} \int_{-\infty}^0 \exp(-\xi^2) d\xi + \frac{1}{\sqrt{\pi}} \int_0^{\xi} \exp(-\xi^2) d\xi . \quad (2-7)$$

The first term on the right-hand side is equal to 0.5 whereas the second term is one half the nonelementary probability integral whose solution is the error function. Since the error function is an even function, it is necessary to rewrite Equation (2-7) as follows:

$$S_e = 0.5(1 - \operatorname{erf} \xi) \quad S_e \leq 0.5$$

$$\text{and } S_c = 0.5(1 + \operatorname{erf} \xi) \quad S_c \geq 0.5 . \quad (2-8)$$

To find the corresponding values of capillary pressure and saturation, Equation (2-8) together with Equation (2-6) is used. With respect to the evaluation of the constants, α , β , and γ , Laliberte presumed a correlation between those constants and λ , the pore-size distribution index given by Brooks and Corey (1964). Also, he assumed the retention curves defined by his functions and by Brooks and Corey's function would become merged for large values of capillary pressure. It is not surprising that a better fit has been found with Laliberte's function for sands since the values of α , β , and γ are based upon a well defined value of λ , the pore-size distribution index. However, for soils with wide ranges of pore-size distribution, either the correlation between the parameters and λ breaks down, or λ itself is not sufficiently descriptive. At any rate, it seems that the proposed probability density function should employ other independent methods for evaluating its parameters in order to determine its generality. Apparently, the evaluation of the parameters is not a simple operation to perform.

To offer physical justification for the relation between capillary pressure and saturation, White (1970) introduced several physical models. He partitioned the drainage branch of the retention curve into four parts and named them: (1) the boundary effect zone, (2) primary

transition zone, (3) secondary transition zone, and (4) residual desaturation zone. For each of those four "zones" a theory was set forth to interpret the desaturation mechanism within it. He then formulated those theories in such a way that the resultant equations represented the relation between saturation and capillary pressure. A total of thirteen parameters are required to define the entire drainage branch of the retention curve. It is obvious that his functions are of little practical value owing to the large number of parameters to be determined. However, the theoretical relations fitted experimental data quite well as White pointed out. One may conclude the high contact portions of the curve on either side of the inflection point are inherent properties of the retention curve.

B. Computational Schemes for Determining Partial Hydraulic Conductivity

To evade the difficulty of directly measuring hydraulic conductivity as a function of saturation in the laboratory, numerous attempts have been made to formulate some sort of computational scheme so that the partial hydraulic conductivity may be acquired through the knowledge of other properties of a porous medium which are easier to measure. Such properties should be representative of the geometry of pores and their distribution in space. Since the micro-

scopic structure of a porous medium is too complicated to deal with in exact mathematical terms, simplifying assumptions on the disorder existing in the medium are necessary.

1. Statistical approach

Childs and Collis-George (1950) adopted an approach for finding the relation between hydraulic conductivity and the pore-size distribution of a porous medium by assuming that pores of various sizes were randomly distributed in the medium. Their approach was based upon the concept of a pore sequence that was obtained by cutting the medium into two sections and then rejoining the two sections at random. They then proceeded to evaluate the contribution to the hydraulic conductivity made by the pore sequence. Childs and Collis-George considered the group of pores on one section having an average size ρ and range of size δr , and the group of pores on the other section having a mean size σ . Then the area of the pores with average size ρ was given by

$$A_{\rho} = F(\rho) \delta r$$

while the area of the pores on the other surface by

$$A_{\sigma} = F(\sigma) \delta r$$

where $F(r)$ is a pore-size distribution function. Since the two sections come together randomly, the area of the junction

occupied by the pore sequence is simply the product of A_ρ and A_σ , or

$$A_{\rho \rightarrow \sigma} = F(\rho) \delta r \cdot F(\sigma) \delta r \quad .$$

It was further assumed that the resistance to flow increased rapidly as the pore size decreased, the resistance of the larger pore in the sequence could be neglected, and only the contribution of the direct pore sequence to the hydraulic conductivity should be considered. If one takes σ to be smaller than ρ in the sequence, the number of pore sequences occupying the area $A_{\rho \rightarrow \sigma}$ is proportional to $A_{\rho \rightarrow \sigma} / \sigma^2$. According to Poiseuille's equation, the rate of flow through each pore sequence with σ as its controlling pore size is proportional to σ^4 when the hydraulic gradient is taken as unity. Consequently, the contribution of this controlling pore size to the hydraulic conductivity is

$$\delta K = M \sigma^2 F(\rho) \delta r \cdot F(\sigma) \delta r$$

where M is a constant of proportionality to be determined experimentally. Summing up the contribution of all possible pore sequences whose controlling sizes cover the entire spectrum of the pore-size distribution, one may obtain the hydraulic conductivity function,

$$K = M \sum_{\rho=0}^R \sum_{\sigma=0}^R \sigma^2 F(\rho) \delta r \cdot F(\sigma) \delta r \quad (2-9)$$

where R is the largest pore size which remains full of water in a partially saturated medium. The pore-size distribution function is determined from the retention curve which is divided into a number of divisions of capillary pressure values. The greater the number of divisions, the more accurate the computed values of the conductivity should be. In this case, the pore-size distribution was treated as a discrete model although it could have been treated as a continuous function. It should be noted that M in Equation (2-9) is a matching factor obtained by matching the experimental and theoretical curves at a given point.

Marshall (1958) also presented an equation for the relation between permeability and the pore-size distribution of a porous medium. He assumed that the necks connecting the pores in the medium controlled the flow rate. Since the alignments of pores were often imperfect, allowance was made for a reduction in the cross-sectional area of the necks. On a fractured section of the medium where A and B are the two exposed surfaces, the area of A or B is regarded as consisting of n sub-units of area $1/n$. Each sub-unit of surface B is further subdivided into n sub-units of area $1/n^2$. Each of these sub-units has the same volumetric water content, θ , and contains pores of the same radius.

The magnitudes of the pore radii are arranged in descending order, i.e., $r_1 > r_2 > r_3 \dots > r_n$. The sub-unit of surface A which has pores of radius r_1 comes into contact with one of the larger sub-units of surface B. On the average, the cross-sectional area of the neck of the connecting pores would be θ times the area of the smaller pore. Hence, the area of the neck for each of the smaller sub-units of surface B in contact with the first sub-unit of surface A would be, $\theta\pi r_1^2$, $\theta\pi r_2^2$, $\theta\pi r_3^2$, ..., $\theta\pi r_n^2$. Similarly, the second sub-unit of A containing pores of radius r_2 would give neck areas of $\theta\pi r_2^2$, $\theta\pi r_2^2$, $\theta\pi r_3^2$, $\theta\pi r_4^2$, ..., $\theta\pi r_n^2$. The series continues in this way until the n th sub-unit of surface A is counted. This last sub-unit would provide a neck area of $\theta n\pi r_n^2$. The average cross-sectional area of the necks for all the smaller sub-units of surface B with area $1/n^2$ is

$$\begin{aligned} & \theta\pi \left[(r_1^2 + r_2^2 + r_3^2 + \dots + r_n^2) \right. \\ & + (r_2^2 + r_2^2 + r_3^2 + r_4^2 + \dots + r_n^2) \\ & + (r_3^2 + r_3^2 + r_3^2 + r_4^2 + r_5^2 + \dots + r_n^2) \\ & + (r_4^2 + r_4^2 + r_4^2 + r_4^2 + r_5^2 + r_6^2 + \dots + r_n^2) \\ & \left. + \dots + nr_n^2 \right] / n^2 , \end{aligned}$$

$$\text{or } \theta\pi n^{-2} \left[r_1^2 + 3r_2^2 + 5r_3^2 + \dots + (2n - 1)r_n^2 \right] .$$

Equating the above series to πr_t^2 and substituting for r_t^2 in Poiseuille's equation, i.e.,

$$U = - \frac{\theta r_t^2}{8\eta} \frac{d\psi}{dl} ,$$

one obtains

$$U = - \frac{\theta^2 n^{-2}}{8\eta} \frac{d\psi}{dl} \left[r_1^2 + 3r_2^2 + 5r_3^2 + \dots + (2n - 1)r_n^2 \right] . \quad (2-10)$$

According to Darcy's law,

$$U = \frac{-k}{\eta} \frac{d\psi}{dl} . \quad (2-11)$$

Equating Equation (2-10) to Equation (2-11) yields

$$k = \frac{\theta^2}{8n^2} \left[r_1^2 + 3r_2^2 + 5r_3^2 + \dots + (2n - 1)r_n^2 \right] \quad (2-12)$$

where k is the permeability at a certain volumetric water content, θ .

To develop further the model of pore sequence originated by Childs and Collis-George, Millington and Quirk (1961) arrived at a basic equation which could be used to describe permeability as a function of porosity, water content, and pore-size distribution. They envisaged a porous medium as consisting of solid spheres which interpenetrated each other and were separated by spherical pores which also interpenetrated. The solid and pore systems were therefore symmetrical. Based upon this model, it was possible to

derive a generalized relation between the porosity and the cross-sectional area which controlled the flow rate of water in the medium. They assumed that the area of pores on a fractured section might be represented by porosity of an isotropic porous medium, ϕ , and if an interaction model was adopted to include the probability of continuity of pores in space, the pore area resulting from interaction would be between ϕ and ϕ^2 . They then proceeded to find the interacting pore area. If the area from interaction is ϕ^{2x} , then $\phi > \phi^{2x} > \phi^2$. Since $\phi < 1$, $1 > x > 0.5$. Furthermore, ϕ^x might be regarded as a maximum pore area in space whereas ϕ^{2x} a minimum. If ϕ^{2x} was obtained on a single plane, it would be associated with a maximum solid area which would be given by $(1 - \phi)^x$. Hence the minimum pore area in the absence of interaction was given by $1 - (1 - \phi)^x$. Both the minimum pore area obtained in the above way and the minimum pore area obtained through interaction should be identical. Therefore, $1 - (1 - \phi)^x = \phi^{2x}$. For values of ϕ between 0.1 and 0.6, the values of x lie between 0.6 and 0.7, and for the sake of simplicity x may be taken as $2/3$. Assuming there were m classes of pores in the porous medium and each class occupied the same proportion of the total porosity, the interacting areas of these classes on a plane were denoted by $a_1, a_2, a_3, \dots, a_m$ and the radii of these pore classes were $r_1 > r_2 > r_3 > \dots > r_m$. For Poiseuille's

flow, both pore area and radius interactions would contribute to the flow. The resistance to flow in a pore sequence was determined by the square of the smaller pore radius.

Thus the permeability was given by

$$k_1 = \frac{1}{8} \begin{bmatrix} a_1 a_1 r_1^2 & a_1 a_2 r_2^2 & a_1 a_3 a_3^2 & & a_1 a_m r_m^2 \\ a_2 a_1 r_2^2 & a_2 a_2 r_2^2 & a_2 a_3 a_3^2 & & a_2 a_m r_m^2 \\ a_3 a_1 r_3^2 & a_3 a_2 r_3^2 & a_3 a_3 a_3^2 & \dots & a_3 a_m r_m^2 \\ \vdots & \vdots & \vdots & & \vdots \\ a_m a_1 r_m^2 & a_m a_2 r_m^2 & a_m a_3 a_m^2 & & a_m a_m r_m^2 \end{bmatrix} .$$

Since $a_1 = a_2 = a_3 = \dots = a_m = \phi^{2/3}/m$, then

$$k_1 = \frac{1}{8} \phi^{4/3} m^{-2} \left[r_1^2 + 3r_2^2 + 5r_2^2 + \dots + (2n - 1)r_m^2 \right] . \quad (2-13)$$

For the partial permeability, the value of ϕ was replaced by that of the volumetric water content, and the r^2 series began with the largest pore radius occupied by water.

Attempts by a number of investigators to evaluate the success of the proposed computational schemes have been made. Nielsen, et al. (1960) compared the values of partial hydraulic conductivity calculated with Childs and Collis-George's, and Marshall's procedures with measured values for four field soils. They concluded that Childs and Collis-George's method appeared superior to the others over a

narrow range of capillary pressure. In contrast to that, Jackson, et al. (1965) tested three individual methods and found that the methods of Childs and Collis-George, and Marshall did not predict the shapes of the hydraulic conductivity curves, and that if a matching factor was used, Millington and Quirk's method gave good results over a wide range of saturation.

Kunze, et al. (1968) reported that Millington and Quirk's method with a matching factor did not produce the best fit with their experimental data. They claimed a better fit could be obtained if the volumetric water content in Equation (2-13) was not raised to $4/3$ power but to 1.0 power. This change brought about a slightly higher hydraulic conductivity at lower degree of saturation and required a smaller matching factor. They stated, however, that the change was only a step in the right direction, but was still not sufficient to correct the discrepancy between measured and calculated values of hydraulic conductivity at low saturations.

In an evaluation of some predictive methods, Green and Corey (1971) tested both Marshall's, and Millington and Quirk's methods with matching factors which were the ratios of measured total hydraulic conductivity to calculated total hydraulic conductivity. They proposed a modified version of Marshall's method, in which the values of θ and n in Equation (2-12) were held constant regardless of the degree of

saturation. They discovered all three methods including the one of their own gave reliable predictions of measured hydraulic conductivity, and suggested they be used routinely for field applications. They pointed out that to characterize the variation in the water retention curves from many sites in a field might be more important than to accurately measure the $K(\theta)$ values on a very limited number of cores or field sites. They also investigated the hydraulic conductivity computed from absorption branch of the retention curve, and reported that the computed values of hydraulic conductivity were always smaller than the measured values. They thought this discrepancy was due to the inadequacy of the absorptive branch for characterizing the pore-size distribution of the porous medium. They felt the desorptive branch was preferable in this respect.

Jackson (1972) reviewed the predictive methods of Marshall, and Millington and Quirk with matching factors. He demonstrated that the procedures of calculation for those two methods were similar except for the exponent of the pore interaction term. He reasoned that since both Marshall's, and Millington and Quirk's derivations were based upon an idealized model of the porous medium, the values of the exponent appeared arbitrary. He then tried to determine the optimum value of the exponent with which the methods would best predict experimental hydraulic conductivity. The

would-be optimum value of the exponent obtained by method of least squares for several media varied around unity. Therefore, he suggested that a value of unity would be adequate.

2. Hydraulic radius theory

Based upon a simplified hypothesis, Purcell (1949) derived an equation which related the retention curve and the porosity to the permeability of a saturated porous medium. He first considered the medium as a system composed of a large number of parallel cylindrical capillaries of equal length but random radii. The total rate of flow through this system is equivalent to the sum of the contributions made by each of the individual capillaries. He then equated Darcy's law to Poiseuille's equation and substituted the capillary pressure for the radius by use of the Laplace's surface tension equation to produce an equation for permeability, i.e.,

$$k = (\sigma \cos \alpha)^2 \phi \sum_{i=1}^n \frac{\Delta S_i}{P_i^2} \quad (2-14)$$

where σ is the coefficient of surface tension, α is the contact angle, ϕ the porosity of the medium, S_i the portion of saturation in the capillary of radius r_i and P_i the capillary pressure. Purcell realized that Equation (2-14)

was too idealistic because its derivation was based upon a system consisting of non-interconnected capillaries of circular cross-section and equal length. Certainly the occurrence of such a system in porous medium is rarely approached. Accordingly, he introduced a so-called lithology factor, F , to account for difference between the flow in the idealistic porous medium and that in naturally occurring materials. Thus Equation (2-14) became

$$k = F(\sigma \cos \alpha)^2 \phi \sum_{i=1}^n \frac{\Delta S_i}{P_i^2} . \quad (2-15)$$

The summation of $\Delta S_i/P_i^2$ in Equation (2-15) might best be evaluated through the retention curve. If integral form is adopted, Equation (2-15) becomes

$$k = F(\sigma \cos \alpha)^2 \phi \int_0^1 \frac{dS}{P^2} . \quad (2-16)$$

Gates and Lietz (1950) suggested that Purcell's equation be extended to the partially saturated media. It was noted that at complete saturation the limits of integration in Equation (2-16) were from zero to unity. They reasoned that for any saturation other than unity the upper limit of integration in Equation (2-16) would be the saturation itself. Although they recognized Purcell's lithology factor would

not be the same at an intermediate saturation as at a saturation of unity, they had no independent method of estimating those factors.

Wyllie and Spangler (1952) combined Kozeny's fundamental postulates with the retention curve to obtain another expression for the relative permeability of a partially saturated porous medium. They proposed on the basis of a dichotomy originally suggested by Carman that the Kozeny constant for any porous medium with a random distribution of pores was obtainable if the tortuosity of the porous medium could be measured. That is to say, there exists a relation between the Kozeny constant and tortuosity. Wyllie and Spangler pointed out that Carman was responsible for writing the following expression:

$$c = c_0 (L_e/L)^2 \quad (2-17)$$

where c is the Kozeny constant, c_0 is the shape factor of pores which generally falls within the range between 2.0 and 3.0, L_e the actual length of sinuous path taken by a fluid flowing through the porous medium, L the linear external dimension, and $(L_e/L)^2$ is the tortuosity T_e of the porous medium at a certain saturation. They went on to derive an equation for the relative permeability given by

$$k_r = \frac{1}{\frac{T_e}{T}} \frac{\int_0^S \frac{dS}{P^2}}{\int_0^1 \frac{dS}{P^2}} \quad (2-18)$$

where T is the tortuosity at saturation equal to unity.

They further proposed to determine the ratios of tortuosity, T_e/T , from electrical resistivity measurements.

Recognizing the unsuccess in measuring the ratios of tortuosity by electrical resistivity index analogy, Burdine (1953) analyzed experimental data of permeability and found that to a first approximation, $(T/T_e)^{1/2}$ might be assumed as a linear function of saturation. He wrote

$$\sqrt{\frac{T}{T_e}} = \frac{S - S_r}{1 - S_r} \quad (2-19)$$

where S_r is the residual saturation. Substituting Equation (2-19) into Equation (2-18) yields

$$k_r = \left(\frac{S - S_r}{1 - S_r} \right)^2 \cdot \frac{\int_0^S \frac{dS}{P^2}}{\int_0^1 \frac{dS}{P^2}} \quad (2-20)$$

which is known as Burdine's equation. A detailed description of the theory leading to the Burdine equation has been given by Brooks and Corey (1964). It is interesting that Wyllie and Gardner (1958) developed a statistical model of porous

media similar to that of Childs and Collis-George (1950), and arrived at the same equation given by Burdine.

By substituting Equation (2-1), a simple retention function of their own, into Equation (2-20) and changing the lower limit of integration from zero to S_r , Brooks and Corey (1964) were able to produce a simple expression for relative permeability,

$$k_r = \left(S_e \right)^{\frac{2+3\lambda}{\lambda}} \quad (2-21)$$

or

$$k_r = \left(\frac{P_b}{P} \right)^{\eta} \quad \text{for } P \geq P_b \quad (2-22)$$

where $\eta = 2 + 3\lambda$. They expected this equation was valid only for isotropic media and possibly only for drainage cycle. However, they claimed it held true for any pore-size distribution according to experimental evidences.

Brust, et al. (1968) compared Brooks and Corey's method with that of Millington and Quirk, and concluded that the former gave better results than the latter when compared with hydraulic conductivity measured in the field. Nielsen, et al. (1970) pointed out that in general, the computational methods for obtaining the partial hydraulic conductivity or permeability appeared most successful for soils with narrow

ranges of pore-size distribution. In a highly aggregated soil, a considerable portion of the total water content is retained as relatively immobile water. Under such circumstances better results were obtained if the concept of effective saturation as used in Equation (2-21) was adopted. Bouwer and Jackson (1974) stated that although the computational procedure of Brooks and Corey's method was relatively simple, care ought to be exercised to obtain the best value of residual saturation. They concluded the calculated hydraulic conductivity compared favorably with other methods and with measured data.

C. Methods of Obtaining Retention Data in the Laboratory

There are many techniques for obtaining retention data in the laboratory. Almost all techniques have been developed to obtain the drainage branch of the retention curve. According to Bear (1972), there are two general methods for obtaining retention data: (1) displacement, and (2) dynamic methods. Of these two groups, the displacement method is the one most commonly used by agronomists and soil scientists. It is suitable for fragile disturbed or undisturbed samples. Basically, all the techniques pertaining to the displacement group establish successive states of static equilibrium and data are taken of the equilibrium water content and capil-

lary pressure. The most common techniques of the displacement group are: (1) increasing the pressure of the non-wetting phase and holding the pressure of wetting phase constant, and (2) decreasing the pressure of the wetting phase and holding the pressure of the non-wetting phase constant. Both techniques require the use of a saturated capillary barrier that is permeable only to the wetting phase. The capillary barrier must have a uniform pore-size distribution and pores that will not allow the non-wetting phase to penetrate the barrier. The capillary barrier is initially saturated with the same fluid to be displaced in the medium.

To obtain data by the first technique indicated above, a pressure plate or pressure membrane equipment is used. The sample is subjected to non-wetting phase pressure within a pressure cooker or pressure cell that contains the capillary barrier. An outflow tube is connected to one side of the capillary barrier for measuring volume displaced and detecting equilibrium condition at a particular pressure of the non-wetting phase. Usually one soil sample is required for each equilibrium pressure measurement. For example, if one desires to obtain five data points, five samples are required, and each of them is subject to a different non-wetting phase pressure. When retention data are needed for a large number of samples, the technique is valuable.

However, the time required for equilibrium may be considerable, e.g., 10-40 days, depending upon the range of capillary pressure desired.

The technique which lowers the pressure of the wetting phase is limited to the low range of capillary pressure, i.e., less than 1 bar. When one desires a retention curve on only one or two soils over the range of 1 bar, this technique appears superior to the pressure plate technique. Nevertheless, it is time-consuming and tedious also. The technique involves reducing the pressure of the wetting phase in increments and measuring the displaced volume of wetting fluid in equilibrium.

Other displacement methods include mercury injection and centrifuge methods. The former is used by the petroleum industry where consolidated samples are dealt with. Mercury is used as the non-wetting phase and forced into pores of the medium in an evacuated chamber. The centrifuge method causes the wetting fluid to leave the sample by subjecting it to normal accelerations in a centrifuge. This is equivalent to subjecting the sample to increased gravitational force. Data may be obtained in a relatively short time, but it is not particularly suitable for the low range of capillary pressure.

Imbibition retention data may be acquired by methods similar to the displacement type methods, in which fluid is

allowed to imbibe through the capillary barrier as opposed to drainage from the sample. However, no satisfactory techniques have been established.

CHAPTER III

THEORY

A. Retention Function

After reviewing the mathematical expressions in the literature for soil-water retention curves, it was found that the one originated by Brooks and Corey (1964) had the simplest form and yet could approximate experimental data reasonably well under certain circumstances. However, their function fails to describe an inflection in the curve. Precisely, it completely ignores the downward concavity of the retention curve and assumes that retention data can be approximated by a curve that is entirely concave upward. In some cases, this over-simplification results in an unrealistic approximation especially for soils with ill-defined bubbling pressures.

It was further discovered that when Brooks and Corey's function underwent a simple mathematical manipulation, it took the form of the Pearson Type VIII distribution function (Pearson, 1916). It will be assumed herein that the capillary pressure of the soil-water system is related to the geometry of the interfaces between water and air within the porous matrix by Laplace's surface tension equation (Encyclopaedia Britannica, 1969),

$$P = \sigma \left(\frac{1}{r} + \frac{1}{r'} \right) \quad (3-1)$$

or

$$P = \frac{2\sigma}{r}, \text{ if } r' = r \quad (3-2)$$

where P is the capillary pressure, σ the surface tension coefficient and r and r' are the radii of curvature of any two normal sections of the interface at right angles to each other. Therefore, one may consider the soil-water retention curve as an indication of the pore-size distribution of the porous medium. In other words, one can obtain the probability density function of pores by taking the derivative of saturation, which connotes percentage volume, with respect to capillary pressure, or with respect to pore size. In this connection, the Pearson Type VIII distribution function suggests that there be no pores in the medium, which have sizes larger than the one corresponding to the bubbling pressure. Observations of experimental data indicate this is not always the case and a more general expression should be developed.

Upon close examination of numerous experimental data of capillary pressure versus saturation, it became clear that the plotting of the data generally exhibited three common features. The data approach a vertical asymptote at both residual saturation and saturation equal to unity, and

between these two extremes of saturation there exists an inflection point. If the pore-size distribution is assumed to be of the same type on either side of the inflection point, then by reversing the concavity of the curve at the inflection point, perhaps a more suitable expression of capillary pressure versus saturation may be obtained. With this in mind, the Pearson Type VIII distribution function was written for these two portions of the curve and then matched at a fictitious inflection point. The resulting expression is given by

$$P = P_f \left(\frac{S - S_r}{a} \right)^{-m} \left(\frac{1 - S}{b} \right)^{\frac{bm}{a}} \quad (3-3)$$

where P is the capillary pressure, P_f is the capillary pressure at the fictitious inflection point, S is the saturation, S_r the residual saturation, m the shape factor of the retention curve and therefore a pore-size distribution parameter of the medium, and a and b are the domains of saturation separated by the fictitious inflection point. Figure 1(A) shows a typical soil-water retention curve and gives the definitions of the symbols in Equation (3-3) graphically. It can be seen from Figure 1(A) that the sum of a , b and S_r must equal unity, i.e.,

$$a + b + S_r = 1.0 \quad . \quad (3-4)$$

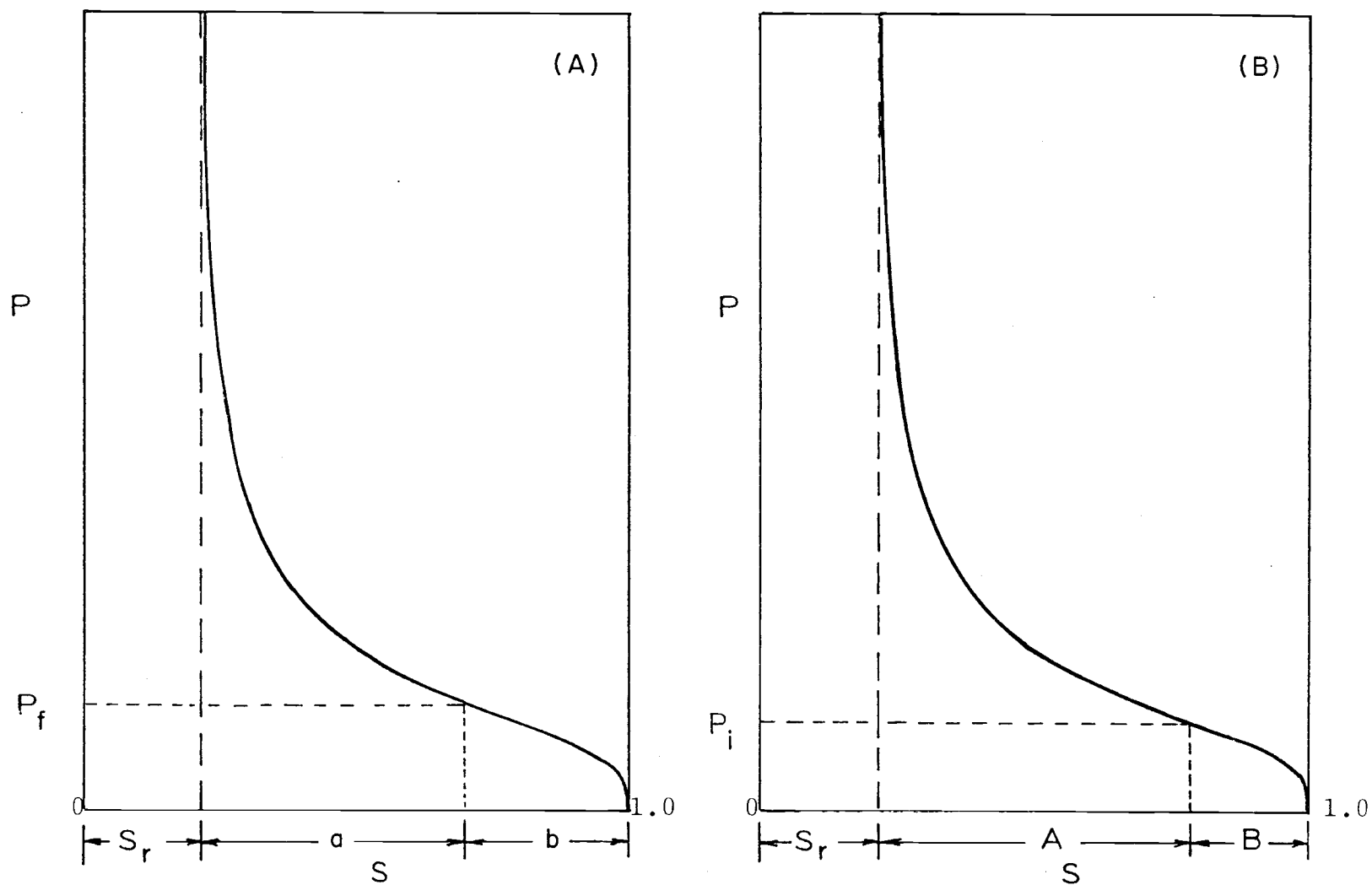


Figure 1. Definitive retention curves depicting the relationships of the parameters in the theoretical retention function.

Therefore, the only constants needed to define the soil-water retention curve are a , b , m and P_f . Since the sum of a and b is the domain of saturation that is of greatest concern to engineers in the fields of irrigation, drainage and hydrology, the theory will be confined to this domain.

It is worthwhile recalling the definition of effective saturation, S_e , given by Corey (1954), i.e.,

$$S_e = \frac{S - S_r}{1 - S_r} \quad (3-5)$$

When S_r is replaced by a and b by use of Equation (3-4), one may transform Equation (3-5) into

$$S_e = \frac{S - (1 - a - b)}{a + b} \quad (3-6)$$

and thus exclude the immobile water content from consideration. This is expedient because the water content below residual saturation is believed hydraulically insignificant. By making use of Equation (3-4) and Equation (3-6), Equation (3-3) becomes

$$P = P_f \left(\frac{S_e}{\frac{a}{a+b}} \right)^{-m} \left(\frac{1 - S_e}{\frac{b}{a+b}} \right)^{\frac{bm}{a}} \quad (3-7)$$

By using new notation defined as

$$P_s = \frac{P}{P_f}, \quad S. = S_e = \frac{S - S_r}{1 - S_r}, \quad a. = \frac{a}{a+b} \text{ and } b. = \frac{b}{a+b}, \quad (3-8)$$

Equation (3-7) becomes

$$P_s = \left(\frac{S.}{a.} \right)^{-m} \left(\frac{1 - S.}{b.} \right)^{\frac{b.m}{a.}} \quad (3-9)$$

with $a. + b. = 1.0$.

Equation (3-9) may be transformed into an expression in terms of the ratio of $b.$ to $a.$

Hence

$$P_s = \left[S. \left(1 + \frac{b.}{a.} \right) \right]^{-m} \left[(1 - S.) \left(1 + \frac{a.}{b.} \right) \right]^{\frac{b.m}{a.}} \quad (3-10)$$

So far, the constants in Equation (3-3) or (3-10) do not convey any physical significance. It should be emphasized here that the fictitious inflection point which is used to define a and b should not be mistaken for the true inflection point of the retention curve. In Figure 1(B) the true inflection point is defined along with the domains of saturation associated with the inflection point. The "A" domain of saturation corresponds to the upward concavity while the "B" domain corresponds to the downward concavity of the retention curve. To find the real inflection point, Equation (3-10) must be differentiated twice and equated to zero. The operation brings about a quadratic equation, $f(S.) = 0$ or

$$\left(1 - \frac{b}{a}\right) \left(1 + m - \frac{bm}{a}\right) S.^2 - 2 \left(1 + m - \frac{bm}{a}\right) S. + (1 + m) = 0 . \quad (3-11)$$

The solutions of Equation (3-11) are given by the quadratic formula, i.e.,

$$S. = \frac{\left(1 + m - \frac{bm}{a}\right) \pm \sqrt{\frac{b}{a} \left(1 + m - \frac{bm}{a}\right)}}{\left(1 - \frac{b}{a}\right) \left(1 + m - \frac{bm}{a}\right)} . \quad (3-12)$$

In light of the physical constraints, the roots cannot be imaginary. This requires the discriminant of the quadratic equation be positive or zero. Based upon experimental data, the inflection point nearly always lies within the bounds of saturation, $0 < S. < 1$. The possibility that the discriminant may be equal to zero can be eliminated. The most important solution of Equation (3-11) is the one where the roots are real and unequal. The following will further show that there is only one appropriate solution to Equation (3-11).

According to the definitions of a and b , it is obvious that $\frac{b}{a} > 0$. Since the discriminant of Equation (3-12) should be greater than zero, it follows that $\left(1 + m - \frac{bm}{a}\right) > 0$. Then,

$$\sqrt{\frac{b}{a} \left(1 + m - \frac{bm}{a}\right)} > 0 > - \frac{b}{a} \left(1 + m - \frac{bm}{a}\right) .$$

By adding $(1 + m - \frac{bm}{a})$ to the members of the above inequality, one has

$$(1 + m - \frac{bm}{a}) + \sqrt{\frac{b}{a} (1 + m - \frac{bm}{a})} > (1 - \frac{b}{a})(1 + m - \frac{bm}{a}).$$

Now, if $(1 - \frac{b}{a}) > 0$, then

$$\frac{(1 + m - \frac{bm}{a}) + \sqrt{\frac{b}{a} (1 + m - \frac{bm}{a})}}{(1 - \frac{b}{a})(1 + m - \frac{bm}{a})} > 1. \quad (3-13)$$

Next, if $(1 - \frac{b}{a}) < 0$, then

$$\frac{(1 + m - \frac{bm}{a}) + \sqrt{\frac{b}{a} (1 + m - \frac{bm}{a})}}{(1 - \frac{b}{a})(1 + m - \frac{bm}{a})} < 0. \quad (3-14)$$

The left-hand members of inequalities (3-13) and (3-14) are one of the two roots of Equation (3-11), but their values transgress the physical bounds of $S_{.i}$. Therefore, the only valid solution having physical significance is

$$S_{.i} = \frac{(1 + m - \frac{bm}{a}) - \sqrt{\frac{b}{a} (1 + m - \frac{bm}{a})}}{(1 - \frac{b}{a})(1 + m - \frac{bm}{a})} \quad (3-15)$$

where $S_{.i}$ is the effective saturation at the true inflection point of the retention curve. To find the unscaled satura-

tion at the inflection point, Equation (3-6) is used. Thus,

$$S_i = (a + b) \frac{(1 + m - \frac{bm}{a}) \cdot \frac{b}{a} - \sqrt{\frac{b}{a} (1 + m - \frac{bm}{a})}}{(1 - \frac{b}{a}) (1 + m - \frac{bm}{a})} + 1 \quad (3-16)$$

is the expression for the unscaled saturation at the inflection point. For the value of the capillary pressure P_i corresponding to S_i , Equation (3-3) is recalled and S_i is substituted for the independent variable S . Thus,

$$P_i = P_f \left[\left(1 + \frac{b}{a}\right) (1 - H) \right]^{-m} \left[\left(1 + \frac{a}{b}\right) H \right]^{\frac{bm}{a}}$$

where

$$H = \frac{\sqrt{\frac{b}{a} (1 + m - \frac{bm}{a})} - \frac{b}{a} (1 + m - \frac{bm}{a})}{(1 - \frac{b}{a}) (1 + m - \frac{bm}{a})} . \quad (3-17)$$

It is postulated from statistical standpoint that S_i may be the critical saturation beyond which the air phase becomes discontinuous on the imbibition branch because the frequency of pores is maximum at the inflection point of the retention curve. In other words, it is quite possible that the air phase may become blocked and isolated as the liquid phase invades and fills those pores related to P_i , which possess the most significant amount of pore volume in the porous

medium. On the other hand, as the liquid phase leaves those pores having greatest frequency, the air phase may first become continuous and potentially mobile. This phenomenon was in effect observed and pointed out by White (1968). The verification of the above postulate of P_i and S_i should be of paramount importance to drainage engineers inasmuch as aeration of soils may be defined in terms of soil properties.

Regarding the above presentation, it is noteworthy that the constants in Equation (3-9) are hydraulic properties of the media and each of them is physically significant. This complete retention function makes possible the study of the retention of fluids in porous media for both the imbibition and drainage branches of the retention curve.

B. Permeability Function

Based upon the review of functional forms suitable for computing the permeability of porous media given in Chapter II, the equation of Burdine [Equation (2-20)] was found to have several advantages over the others. These advantages include: (1) its demonstrated accuracy is at least equal or better than other computational schemes, and (2) relative permeability may be expressed by a simple mathematical form. The latter advantage makes it possible to arrive at an analytical expression for relative perme-

ability, which is as accurate as the Burdine integrals, provided an accurate retention function is available and it can be integrated. Of course, if the retention function does not represent the true retention relationship, the permeability function will be in error accordingly. The work of Brooks and Corey is an example of what has been done in this regard. It will be assumed in this thesis that the Burdine integrals are adequate and that if the retention function accurately represents the retention of water in soils during drainage, the permeability obtained from the retention function will be as accurate as the Burdine integrals themselves. The result of inserting the retention function proposed herein, i.e., Equation (3-9), into the Burdine integrals, Equation (2-20), to obtain the ratio of partial hydraulic conductivity to the total hydraulic conductivity (or relative permeability) is given below.

Recalling Equation (2-20) and the definition of residual saturation, the Burdine integrals are transformed into

$$k_r = (S_c)^2 \frac{\int_0^{S_c} 1/(P_s)^2 dS_e}{\int_0^1 1/(P_s)^2 dS_e} . \quad (3-18)$$

The transformation to the definition of effective saturation implies that the water in the soil at saturation less than S_r is immobile or that the permeability at $S = S_r$ is zero.

Substituting Equation (3-9) for P_s in the integrands of Equation (3-18) gives

$$\frac{\int_0^{S_e} \frac{1}{(P_s)^2} dS_e}{\int_0^1 \frac{1}{(P_s)^2} dS_e} = \frac{\int_0^{S_e} (S_e)^{2m} (1 - S_e)^{-\frac{2bm}{a}} dS_e}{\int_0^1 (S_e)^{2m} (1 - S_e)^{-\frac{2bm}{a}} dS_e} . \quad (3-19)$$

The denominator on the right-hand side of the equal sign is a definite integral whose value is readily expressed in terms of the Beta function, i.e.,

$$\int_0^1 (S_e)^{2m} (1 - S_e)^{-\frac{2bm}{a}} dS_e = \beta(2m + 1, -\frac{2bm}{a} + 1) . \quad (3-20)$$

The numerator can also be expressed in terms of the incomplete Beta function, i.e.,

$$\int_0^{S_e} (S_e)^{2m} (1 - S_e)^{-\frac{2bm}{a}} dS_e = \beta_{S_e}(2m + 1, -\frac{2bm}{a} + 1) . \quad (3-21)$$

The relative permeability as a function of effective saturation is obtained by combining Equations (3-18) and (3-19) with Equations (3-20) and (3-21), i.e.,

$$k_r = (S_e)^2 \frac{\beta_{S_e}^{(2m+1, -\frac{2bm}{a}+1)}}{\beta_{(2m+1, -\frac{2bm}{a}+1)}} \quad (3-22)$$

Since

$$\frac{\beta_{S_e}^{(2m+1, -\frac{2bm}{a}+1)}}{\beta_{(2m+1, -\frac{2bm}{a}+1)}} = I_{S_e}^{(2m+1, -\frac{2bm}{a}+1)} \quad (3-23)$$

where I_{S_e} is the incomplete Beta function ratio with its arguments given in the parentheses (Abramowitz and Stegun, 1970), Equation (3-22) becomes

$$k_r = (S_e)^2 I_{S_e}^{(2m+1, -\frac{2bm}{a}+1)} \quad (3-24)$$

Of course, if absolute rather than relative values of permeability are desired, one may use the equation,

$$k = k_1 (S_e)^2 I_{S_e}^{(2m+1, -\frac{2bm}{a}+1)} \quad (3-25)$$

where k_1 and k are respectively the total permeability and partial permeability for any given saturation in the interval, $1 > S \geq S_r$. Similarly, for partial hydraulic conductivity, one may substitute the partial hydraulic conductivity, K , for partial permeability and the total hydraulic conductivity, K_1 , for the total permeability and Equation (3-25) becomes

$$K = K_1 (S_e)^2 \left[I_{S_e} (2m + 1, -\frac{2bm}{a} + 1) \right]. \quad (3-26)$$

C. Diffusivity Function

In a soil water-air system, it is generally acceptable to regard the pressure of air everywhere in the porous medium as a constant being equal to the atmospheric pressure. It is also possible to ignore the flow of air because of its relatively low resistance due to its low viscosity. With these in mind, Darcy's law may be written in terms of the pressure of water to describe the flow in partially saturated media, i.e.,

$$\bar{q} = -K \nabla \left(\frac{P_w}{\gamma} + z \right) \quad (3-27)$$

where \bar{q} is the volume flux, K is the partial hydraulic conductivity, ∇ is the vector differential operator, P_w the pressure of the soil-water, γ the specific weight of water and z is the elevation above an arbitrary datum. Combining Equation (3-27) with the equation of continuity,

$$\nabla \cdot \bar{q} = -\phi \frac{\partial S}{\partial t} , \quad (3-28)$$

yields

$$\nabla \cdot \left[-K \nabla \left(\frac{P_w}{\gamma} + z \right) \right] = -\phi \frac{\partial S}{\partial t} , \quad (3-29)$$

where ϕ is the porosity of the soil, S is the saturation and t is the time. Equation (3-29) is called the Richards' equation named after its originator (Richards, 1931). If P_w is a single-valued function of S , then

$$\nabla \left(\frac{P_w}{\gamma} \right) = \frac{\partial \left(\frac{P_w}{\gamma} \right)}{\partial S} \nabla S ,$$

and Equation (3-29) may be written as

$$\nabla \cdot \left[-K \frac{\partial \left(\frac{P_w}{\gamma} \right)}{\partial S} \nabla S \right] - \frac{\partial K}{\partial z} = -\phi \frac{\partial S}{\partial t} \quad (3-30)$$

or

$$\nabla \cdot (D \nabla S) - \frac{\partial K}{\partial z} = -\phi \frac{\partial S}{\partial t} \quad (3-31)$$

in which

$$D = -K \frac{\partial \left(\frac{P_w}{\gamma} \right)}{\partial S} \quad (3-32)$$

is known as the soil-water diffusivity (Klute, 1965) or here to be designated as the diffusivity function, and Equation (3-31) is called the diffusion equation for flow in partially saturated media.

If the specific weight of water is removed from the differential operator, the diffusivity function, Equation (3-32), becomes

$$D = \frac{K}{\gamma} \frac{\partial P}{\partial S}, \text{ where } P = -P_w.$$

Differentiating Equation (3-3) with respect to S and substituting into the above produces

$$D = K \frac{P_f}{\gamma} \frac{m}{a} \left(\frac{S - S_r}{a} \right)^{-m} \left(\frac{1 - S}{b} \right)^{\frac{bm}{a}} \left(\frac{a}{S - S_r} + \frac{b}{1 - S} \right) \quad (3-33)$$

which when combined with Equation (3-26) becomes

$$D = K_1 (S_e)^2 \left[I_{S_e} \left(2m+1, -\frac{2bm}{a}+1 \right) \right] \frac{P_f}{\gamma} \frac{m}{a} \left(\frac{S - S_r}{a} \right)^{-m} \left(\frac{1 - S}{b} \right)^{\frac{bm}{a}} \left(\frac{a}{S - S_r} + \frac{b}{1 - S} \right). \quad (3-34)$$

CHAPTER IV

CRITERIA OF AFFINITY FOR POROUS MEDIA

There are two recognized approaches to establishing similitude criteria for flow fields. One approach, called dimensional analysis, transforms the original variables into a set of similarity numbers which are dimensionless. These numbers are subsequently used to determine the size of the model. The second approach which is called inspectional analysis requires that the differential equation describing the flow field be known. By transforming the differential equation into one that is dimensionless or scaled, a set of standard units of scaling is obtained. If the transformation procedure is properly followed, the differential equation will yield identical particular solutions for two flow fields provided the initial and boundary conditions in terms of scaled variables and the relationships among the scaled variables are identical. Actually, any set of standard units may be chosen; however, a set that is physically meaningful and measurable is highly desirable.

In the porous medium flow field, the second approach is to be applied for establishing proper criteria. Two porous media are said to be *affine* if the relationships among scaled hydraulic variables, e.g., capillary pressure, hydraulic conductivity, diffusivity and saturation are identical. Furthermore, two flow fields are said to be

similar if there is affinity between the porous media, their initial and boundary conditions in terms of scaled variables are identical, and there is similarity between the size and orientation of the flow field.

The term *affine* is preferable to *similar* for describing porous media since for affine media a transformation may be used to produce identical scaled relationships among the hydraulic variables even though the media may not, in a physical sense, appear geometrically similar.

The requirements of affinity for porous media are deduced in this section by scaling the relationships among the hydraulic variables.

A. Scaled Hydraulic Functions

1. Scaled retention function

Since the water content related to saturation less than the residual is assumed to be immobile, the saturation may be normalized so that the immobile water is excluded from consideration. This may be accomplished by using the concept of effective saturation and residual saturation introduced by Corey (1954), i.e.,

$$S_e = \frac{S - S_r}{1 - S_r} \quad (4-1)$$

where S_r is the residual saturation and S_e is the effective saturation.

The two domains of saturation associated with the fictitious inflection point have been denoted as a and b where $a = S_f - S_r$, $b = 1 - S_f$, and S_f is the saturation at P_f . These two domains may be normalized to obtain their scaled forms by way of the same normalization factor as used for saturation, i.e.,

$$a_e = \frac{S_f - S_r}{1 - S_r} = \frac{a}{a + b} \quad (4-2)$$

$$b_e = \frac{1 - S_f}{1 - S_r} = \frac{b}{a + b} \quad (4-3)$$

where a_e and b_e are the scaled domains of saturation associated with the fictitious inflection point.

Substituting Equations (4-1), (4-2), and (4-3) into Equation (3-3), one obtains

$$P = P_f \left(\frac{S_e}{a_e} \right)^{-m} \left(\frac{1 - S_e}{b_e} \right)^{\frac{b_e}{a_e} m}$$

or

$$P = P_f \left[\left(1 + \frac{b_e}{a_e} \right) S_e \right]^{-m} \left[\left(1 + \frac{a_e}{b_e} \right) (1 - S_e) \right]^{\frac{b_e}{a_e} m} \quad (4-4)$$

The P_i at the actual inflection point of the retention function appears more suitable as a standard scaling unit of pressure than the pressure P_f particularly when the function is viewed in terms of a pore-size distribution function. Therefore, the scaled retention function becomes

$$P. = \frac{P}{P_i} = \frac{P_f}{P_i} \left[\left(1 + \frac{b.}{a.} \right) S. \right]^{-m} \left[\left(1 + \frac{a.}{b.} \right) (1 - S.) \right]^{\frac{b.}{a.} m} . \quad (4-5)$$

Since

$$\frac{P_f}{P_i} = \left[\left(1 + \frac{b.}{a.} \right) (1 - H) \right]^m \left[\left(1 + \frac{a.}{b.} \right) H \right]^{-\frac{b.}{a.} m} \quad (4-6)$$

where H is given by Equation (3-17), the scaled retention function may be further simplified. Thus,

$$P. = \left(\frac{S.}{1 - H} \right)^{-m} \left(\frac{1 - S.}{H} \right)^{\frac{bm}{a}} . \quad (4-7)$$

Equation (4-7) is completely defined in terms of m and b/a . It is clear that any two porous media will be affine provided they have the same values of m and the same ratios of $b.$ to $a.$, or b to a . It is obvious from Equations (4-2) and (4-3) that the scaled ratio of $b./a.$ is identical to the unscaled ratio of b/a .

Apparently, only one additional affinity criterion is required when the retention function is represented by a continuous function beginning with $P = 0$, compared with that specified by Brooks and Corey (1964) from their step type function.

2. Relative permeability function

Inasmuch as the relative permeability function has already been derived in Chapter III, it needs only to be rewritten here in the dot notation. If $k.$ is the ratio of partial permeability to total permeability, then Equation (3-25) can be rewritten as

$$k. = (S.)^2 I_{S.} (2m + 1, -\frac{2bm}{a} + 1) . \quad (4-8)$$

It can be seen from Equation (4-8) that any two soils with the same values of m and the ratio b/a possess the same relative permeability function. That is to say, any two soils which fulfill the criteria of affinity set forth previously from the retention function will behave similarly also with respect to permeability or other dynamic relations.

3. Scaled diffusivity function

The definition of the diffusivity function is the product of hydraulic conductivity and the slope of the soil-water retention curve. The scaled form of the dif-

fusivity function may be defined in the same manner as the unscaled form except the definientia are now scaled variables. Hence,

$$D. = -K. \frac{\partial P.}{\partial S.} \quad (4-9)$$

where K. and P. are single-valued functions of S. By differentiating Equation (4-7) with respect to S. and combining the derivative with Equation (4-8), one obtains the scaled diffusivity function

$$D. = (S.)^2 \left[I_{S.} (2m + 1, -\frac{2bm}{a} + 1) \right] \left(\frac{S.}{1 - H} \right)^{-m} \left(\frac{1 - S.}{H} \right)^{\frac{bm}{a}} \cdot \left[\frac{m}{S.} + \frac{bm}{a(1 - S.)} \right] \quad (4-10)$$

where H is given by Equation (3-17).

The scaling factor for the diffusivity may be deduced from the scaled definientia in the scaled diffusivity function. From Equation (4-9) and the definitions of K., P., and S., one has

$$D. = - \frac{K}{K_1} \frac{d\left(\frac{P}{P_i}\right)}{d\left(\frac{S - S_r}{1 - S_r}\right)} = - K \frac{d\left(\frac{P}{Y}\right)}{dS} \left[\frac{\gamma (1 - S_r)}{P_i K_1} \right]. \quad (4-11)$$

Let the scaling factor for D be designated as D_0 . Then

$$D. = \frac{D}{D_0} = \frac{-K \frac{d\left(\frac{P}{\gamma}\right)}{dS}}{\frac{P_i K_1}{\gamma(1 - S_r)}} \quad (4-12)$$

and

$$D_0 = \frac{P_i K_1}{\gamma (1 - S_r)}$$

or

$$D_0 = \frac{P_i K_1}{\gamma (a + b)} \quad (4-13)$$

B. Pore-Size Distribution Function

A generalized pore-size distribution function of the porous medium can be derived from Equation (4-7). The development begins with taking the first derivative of P. with respect to S.. The result is

$$\frac{dP.}{dS.} = -P. \frac{m}{a.} \left(\frac{a.}{s.} + \frac{b.}{1 - S.} \right) \quad (4-14)$$

If it is assumed that a pore radius may be related to capillary pressure by the relation

$$P = \frac{2\sigma \cos \alpha}{r}$$

where σ is the coefficient of surface tension of the fluid, α is the angle of contact between the fluid and solid boundary and r is the radius of the pore, then

$$P. = \frac{P}{P_i} = \frac{2\sigma \cos \alpha / r}{2\sigma \cos \alpha / r_i} = \frac{r_i}{r}$$

where r_i is the radius of pores characterized by P_i .

Since

$$P. = \frac{r_i}{r} = \frac{P_f}{P_i} \left(\frac{S.}{a.} \right)^{-m} \left(\frac{1 - S.}{b.} \right)^{\frac{b.m}{a.}}$$

and

$$r = \frac{r_i}{\frac{P_f}{P_i} \left(\frac{S.}{a.} \right)^{-m} \left(\frac{1 - S.}{b.} \right)^{\frac{b.m}{a.}}} \quad (4-15)$$

when Equation (4-6) is substituted into Equation (4-15), one has

$$r = r_i \left(\frac{1 - H}{S.} \right)^{-m} \left(\frac{H}{1 - S.} \right)^{\frac{b.m}{a.}} \quad (4-16)$$

Equation (4-16) may be scaled by dividing through by r_i .
This produces

$$r. = \left(\frac{1 - H}{S.} \right)^{-m} \left(\frac{H}{1 - S.} \right)^{\frac{b.}{a.}m} \quad (4-17)$$

where $r. = r/r_i$.

Differentiating Equation (4-17) with respect to $S.$
yields

$$\frac{dr.}{dS.} = \frac{m}{a.} \left(\frac{1 - H}{S.} \right)^{-m} \left(\frac{H}{1 - S.} \right)^{\frac{b.}{a.}m} \left(\frac{a.}{S.} + \frac{b.}{1 - S.} \right) \quad (4-18)$$

where H is given by Equation (3-17). The inverse of Equation (4-18) in conjunction with Equation (4-17), is the generalized probability density function for pores. In other words, the frequency of pores with a certain scaled radius $r.$ is represented by $dS./dr.$. It should be noted that the probability density function of pores is completely defined by $a.$, $b.$ and m . It is also evident that any two affine media fulfilling the criteria set forth in the previous section possess identical pore-size distribution functions.

CHAPTER V

EXPERIMENTAL PROCEDURE

In general, it is time-consuming and tedious to obtain retention curves by using techniques in which a pressure difference is arbitrarily set across the capillary barrier and the sample is allowed to equilibrate. This technique is primarily used to obtain the drainage branch of the retention curve. Furthermore, there are no well-established techniques for acquiring the imbibition branch of the retention curve. It is the second objective of this thesis to develop a rapid technique for measuring both the drainage and imbibition branch of the retention curve on disturbed soil samples. Such measurement techniques will not only permit the theories already presented to be tested but they will be valuable to researchers interested in obtaining the hydraulic properties of soils quickly.

The equipment pertaining to the procedure consists of four parts: 1) the retention cell that includes a capillary barrier, 2) a capillary tube-burette apparatus for determining equilibrium and the volume of liquid drained, 3) a vacuum-pressure regulator, and 4) manometers for pressure readings. A photograph of the equipment and its schematic arrangement are shown in Exhibit 1 and Figure 2.

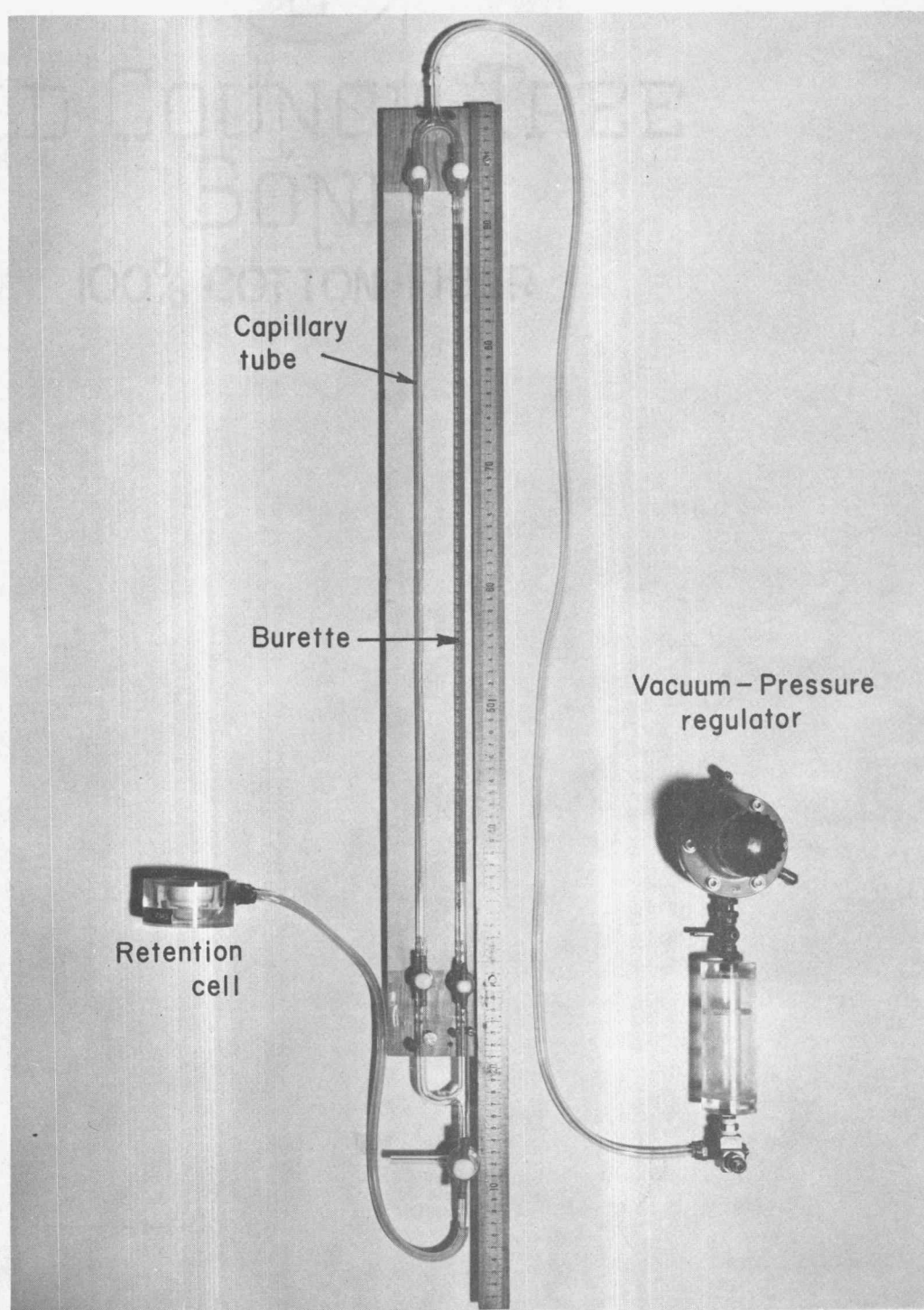


Exhibit 1. Apparatus for obtaining retention data.

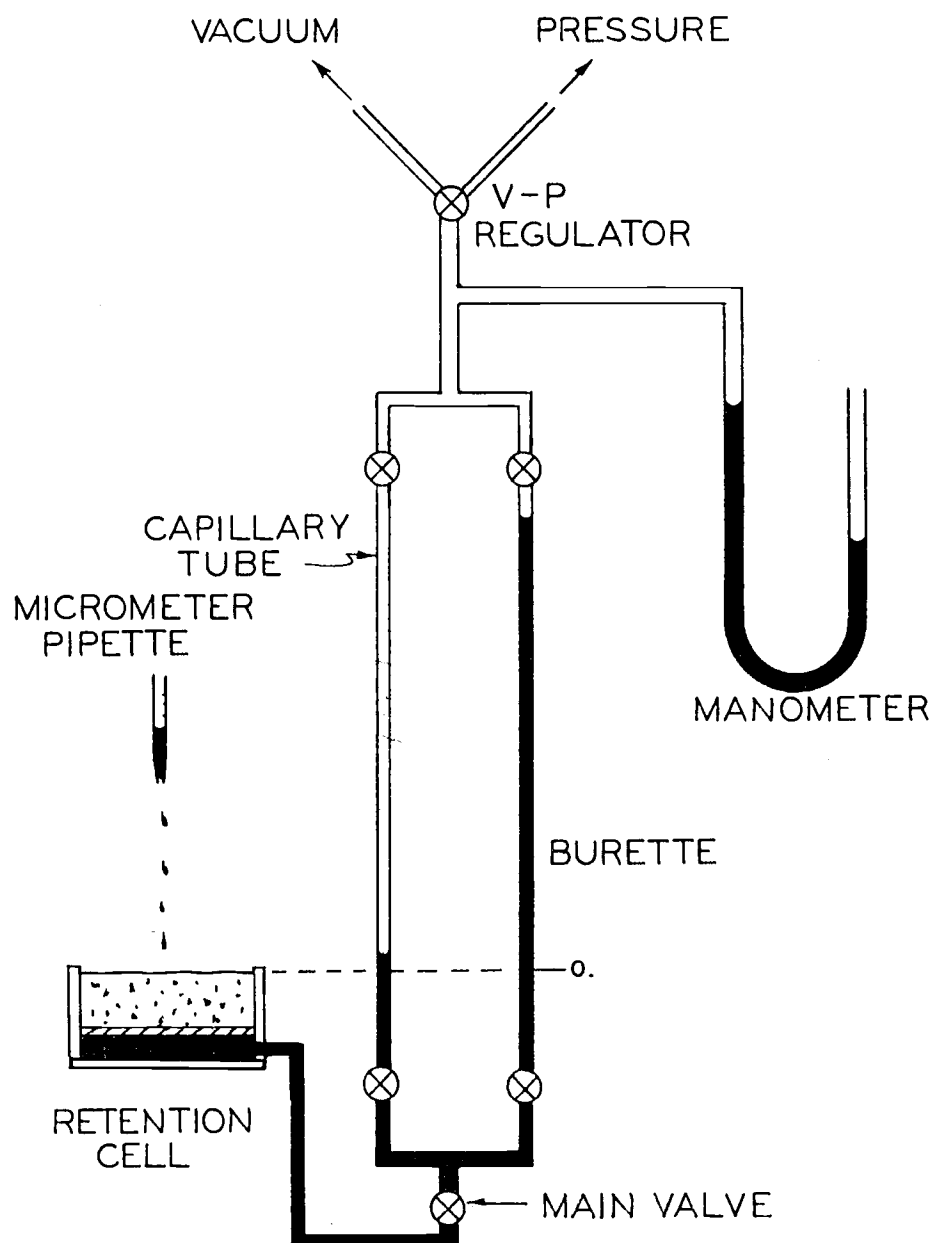


Figure 2. Schematic of the apparatus for obtaining the retention data.

To avoid the so-called boundary effect, the retention cell consists of the end of a ceramic candle that is installed in a recessed block of acrylic plastic. The ceramic was completely sealed into position by epoxy. A pressure tap was installed in the plastic block in order to connect the wetting fluid to the capillary tube-burette apparatus. After soil was packed uniformly into the ceramic candle, the entire cell was vacuum-saturated to exclude air from the soil pores as well as from the capillary barrier. In some cases, the samples were brought to maximum saturation by submerging the cell with soil sample into the wetting fluid for several hours.

After saturating the soil and the capillary barrier by either of the two procedures described above, the retention cell was connected to the capillary tube-burette apparatus through a semi-rigid tube that had been filled with liquid while the vacuum-pressure regulator was set at zero pressure (gage). By setting the top of the cell at the same elevation as the zero volume mark on the burette, a liquid-air interface was established in the burette and capillary tube at that mark.

The elevation of the interface in the capillary tube could be measured by the attached meter stick shown in Exhibit 1. The capillarity of the tube was 1.0 cm. The specific volume of the capillary tube was 0.0174 cm^3 per

cm of length. Both the burette and the capillary tube were connected jointly to the vacuum-pressure regulator. Liquid could be drained from the soil by increasing the pressure difference across the interfaces in the burette and the capillary tube. The volume drained at any particular capillary pressure in equilibrium was equal to the volume in the burette plus the product of the height of the interface in the capillary tube above the zero datum and the specific volume of the capillary tube.

The procedure that was followed to obtain the drainage branch of the retention curve was to create a pressure difference across the interface in the burette by the vacuum-pressure regulator. After a specified volume had drained into the burette from the soil, the burette valve was closed and the interface in the capillary tube was noted. The pressure difference across the interface was then reduced so that the interface remained stationary in the capillary tube. If the pressure difference across the interfaces in the soil pores were not in equilibrium with the pressure difference across the interface in the capillary tube, flow would occur either into or from the sample. Since the specific volume of the capillary tube was small, equilibrium conditions could be easily detected. Care was taken during the experiment on the drainage branch to insure that the wetting fluid always drained away from the soil into the

burette or the capillary tube. Because the capillary tube-burette apparatus was mounted in a vertical plane, the pressure difference across the interface for non-equilibrium condition which would cause liquid to move in the capillary tube was automatically adjusted (decreased) by the rising interface in the capillary tube. This combination of manual and automatic adjustment of the pressure difference across the interface of the small capillary tube greatly decreased the time required to obtain the retention data.

After true equilibrium was reached, the elevation of the interface in the capillary tube and the liquid volume in the burette were noted. The capillary tube valve was then closed and the pressure was decreased (or the pressure difference increased) through the vacuum-pressure regulator by an arbitrary amount. The burette valve was then opened and followed by the opening of the capillary tube valve. The procedure for equilibrium was repeated for each drainage volume. Of course, the time required to determine true equilibrium increases progressively after each increment of drainage. Care must be exercised in allowing sufficient time for determining the movement of the interface in the capillary tube to be certain of equilibrium.

When the saturation of the soil sample had been reduced to that corresponding to the steep portion of the drainage curve, the imbibition branch of the retention curve was

started. The burette was not used any longer. A given volume of liquid was added to the soil surface by use of a micrometer pipette. After the liquid was added to the soil surface, the air pressure in the capillary tube was increased to prevent drainage from occurring, but not sufficient enough to cause a large volume of liquid in the capillary tube to retreat toward the soil. Pressure readings in equilibrium were obtained in a manner similar to that for the drainage branch. Flow under non-equilibrium conditions always moved into the sample. Equilibrium conditions for imbibition were always reached much more rapidly than for drainage.

After the equilibrium at zero capillary pressure, another drainage branch was started. Once one or more branches of the retention curve have been obtained, the sample was removed from the retention cell. To prevent any flow from occurring during the removal of the sample, the main valve for the capillary tube-burette apparatus was closed. The soil was weighed, dried in the oven, and weighed again in order to determine the total pore volume or the apparent pore volume.

CHAPTER VI

RESULTS AND DISCUSSION

In this section the retention function will be fitted to the experimental data obtained by the procedure previously discussed as well as fitted to published data found in the literature. These data include both the drainage and imbibition branch of the retention curve.

The hydraulic properties of porous media for affinity from the retention curve will be discussed and also their effect upon permeability, diffusivity and pore-size distribution. The retention function will be used as a base for the discussion on the mechanism pertaining to air entrapment during imbibition.

A. Determination of the Parameters of the Retention Function from Retention Data

Regardless of how well a function may fit experimental data, if the parameters in the function are difficult to obtain, the function may well be only of academic interest and probably will not be very useful. However, if the parameters are easy to assess and have physical meaning, the function will have great utility.

In order to obtain the parameters for the retention function developed in this thesis, a method was derived to

force the function to go through four experimental data points since four parameters are needed to define the function, i.e., a , b , m , and P_f . Theoretically, the parameters may be found by solving a system of four simultaneous equations formed by four pairs of P and S values. The solutions of these equations depend upon not only the accuracy of the experimental data but also upon the criterion established for convergence in solving the system of equations. Strictly speaking, the four-point forcing method is not the best one to use because of the constraints imposed. Of course, methods of nonlinear regression analysis are superior to the forcing method since they can take more data into account and obtain a best-fit through experimental data. Unfortunately, no efficient method of nonlinear regression analysis has been found. It is interesting to note, however, that little or no difficulty has been experienced in finding the parameters by the forcing method for all the retention data that have been analyzed. This is regarded as a strong evidence of the exactness of the retention function. The selection of the four pairs of P and S values should be made in such a way that they cover a wide range of saturation, and unreliable data are excluded from consideration.

The derivation of the equation used to determine the parameters by the forcing method is given in Appendix B.

A Fortran program was written to solve the nonlinear equation through the teletype time-sharing communication system with a CDC 3300 computer. The computer program and an example of the teletype print-out are shown in Appendix C. The criterion for convergence was set as 10^{-10} in the program.

The most efficient way of determining the four best data points to be used in the program is to plot the data and draw a best-fit-by-eye smooth curve through the data points. Those points that fall precisely on the curve are first choice. If the system fails to converge, one or more other data pairs are substituted for those initially used.

In addition to selecting four pairs of data for use in the forcing program, an initial guess of residual saturation must be made. Convergence of the numerical scheme is relatively insensitive to the initial guess. If the raw data are plotted and extend over the steep portion of a curve passing through the data, the first guess of residual saturation will be close to its final value.

B. Comparison of the Retention Function with Experimental Data

In all cases, the fitness of the theoretical retention curve to the experimental retention data was excellent no matter whether the data were from experiments on the im-

bibition or drainage branch. The function also fits experimental data of either vacuum-saturated or apparently saturated samples. The apparent saturation is defined as volume of liquid in the pores divided by the total pore volume less volume of air entrapped in the pores at zero capillary pressure. In other words, the entrapped air is treated as part of the solid matrix of the porous medium. Thus,

$$\text{Apparent saturation} = \frac{\text{Volume of liquid}}{\left(\text{Total pore volume} \right) - \left(\text{Volume of entrapped air at zero capillary pressure} \right)} .$$

The definition of apparent saturation is probably a more realistic one for field situations since the soil profile in a field is not likely to be exclusively filled with liquid. If the total pore volume of the medium is used as a base, Equation (3-3) needs to be modified in order to describe the imbibition branch which ends at a saturation less than unity. The retention function should be written as

$$P = P_f \left(\frac{S - S_r}{a} \right)^{-m} \left(\frac{S_m - S}{b} \right)^{\frac{bm}{a}} \quad (5-1)$$

with $S_r + a + b = S_m$, where S_m is the maximum saturation at which the capillary pressure is zero on the imbibition branch. It should be noted that Equation (5-1) is essentially

the same as Equation (3-3) except the domain of saturation is changed from unity to a smaller value. Illustrations comparing the theoretical or computed retention curve with experimental data for the imbibition branch are given in Figure 3, where the dots represent the experimental data while the lines represent theoretical curves. Figures 3(A) and 3(C) are for two sands, where capillary pressure head is plotted against saturation. Figures 3(B) and 3(D) are for the same sands but plotted as functions of apparent saturation. It is noteworthy that the values of m , P_f and the ratio of b/a are identical for both definitions of saturation.

In Figure 4 the theoretical curves are compared with experimental data obtained from samples that were initially vacuum-saturated before drainage was started. After the last data point was obtained for drainage, the imbibition branch began. The wetting fluid used to obtain the data in Figure 4(A) was water while that in Figure 4(B) was oil. The theoretical curves are in excellent agreement with the experimental data. The data for these figures and others shown herein are tabulated in Appendix D along with the parameters of the retention function. Figure 5 shows the theoretical curves and experimental data for the imbibition and drainage branch where maximum saturation is less than unity. The agreement between theoretical curves and the experimental data is also excellent.

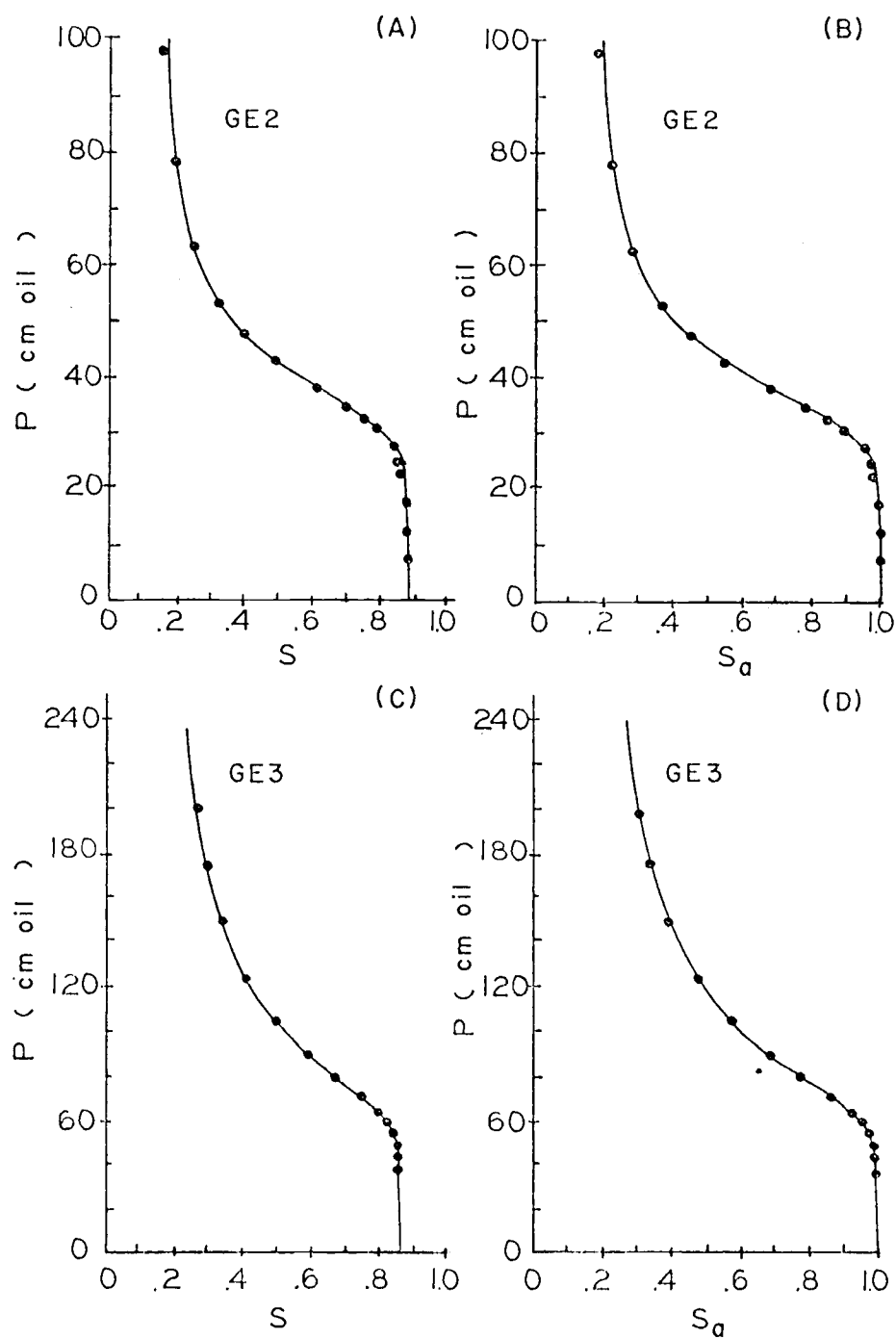


Figure 3. Comparison of the theoretical (or computed) retention curves with retention data of two media, where the dots represent measured values.

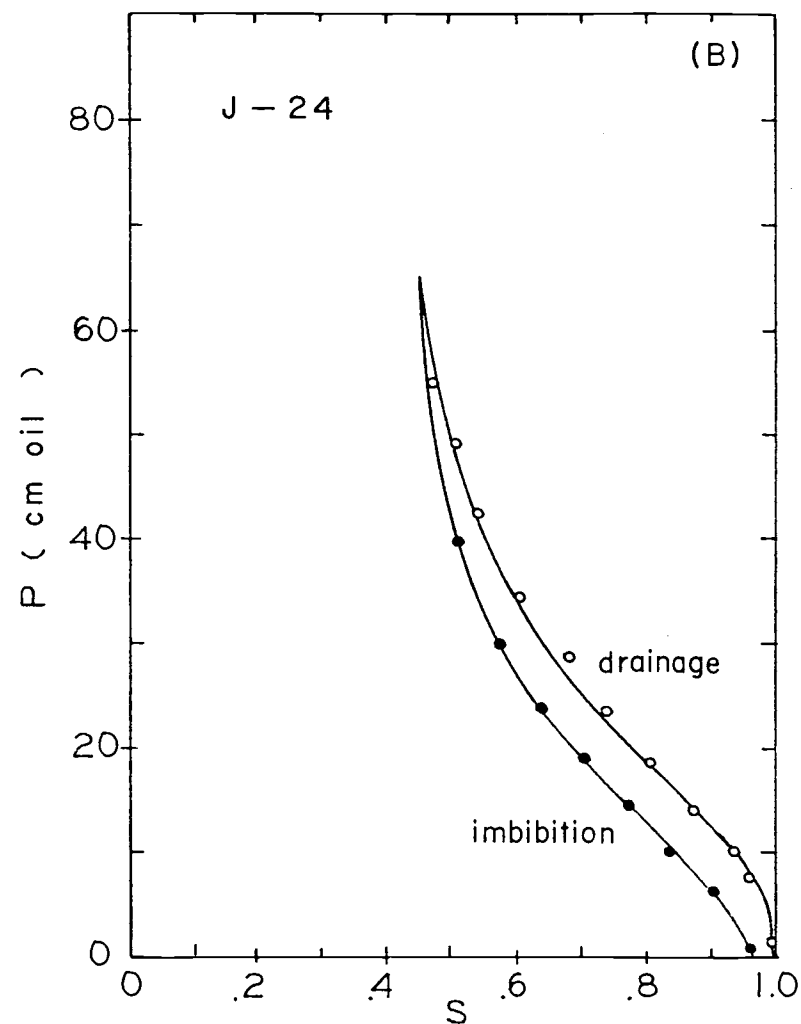
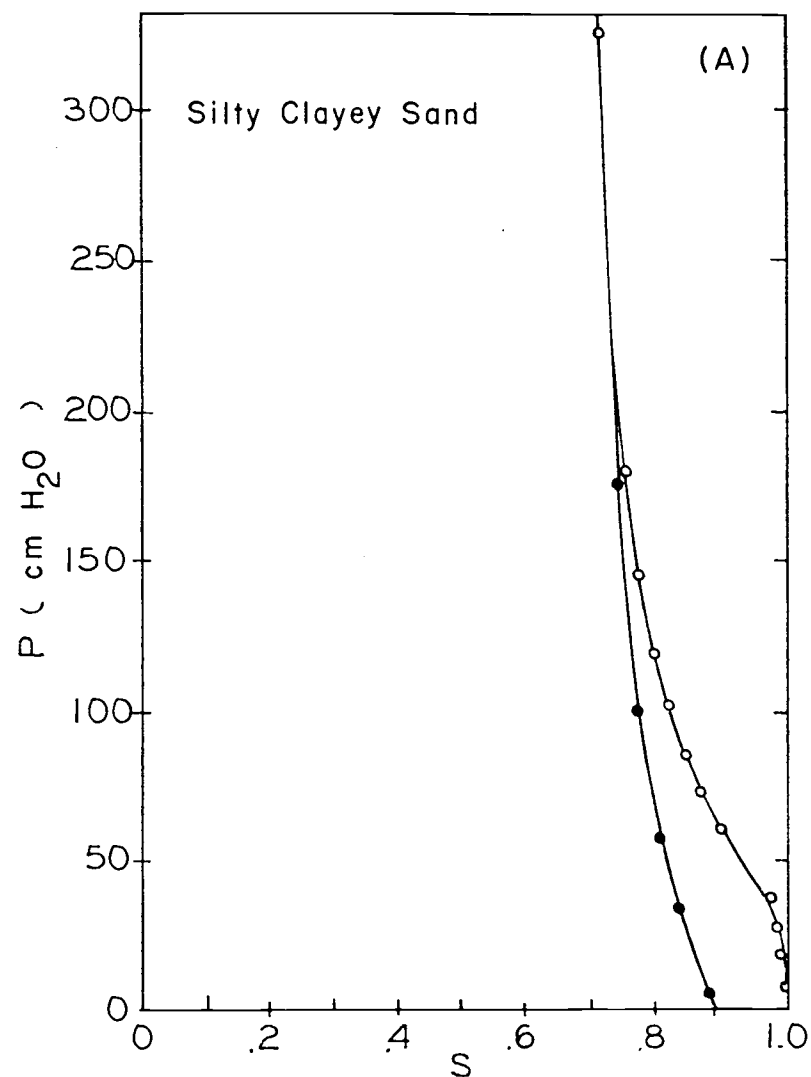


Figure 4. Comparison of the theoretical (or computed) retention curves with retention data on the first drainage (initially vacuum-saturated) and imbibition branches for two media, where the points represent measured values.

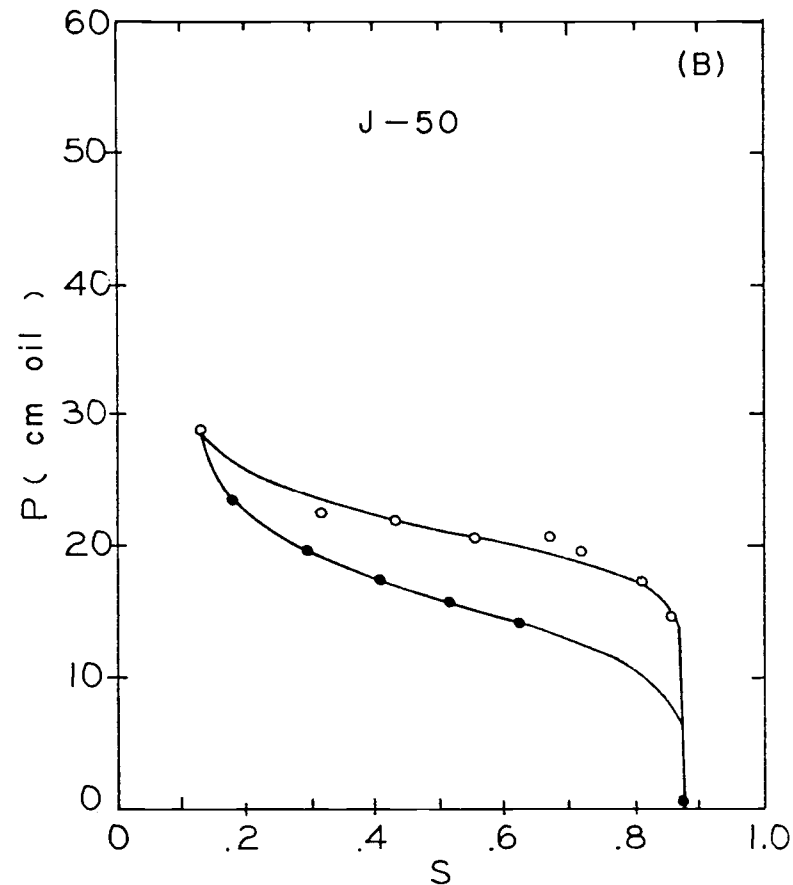
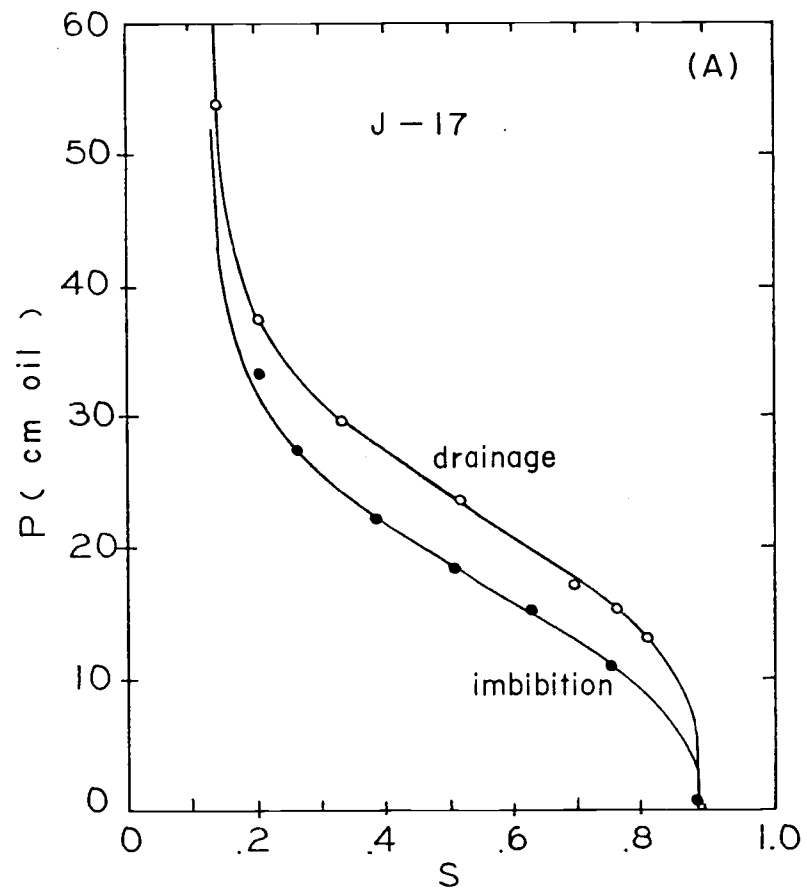


Figure 5. Comparison of the theoretical (or computed) retention curves with retention data on the second drainage (initially apparently saturated) and imbibition branches for two media, where the points represent measured values.

C. Comparison of the Permeability Function with Experimental Data

According to the derivation in Chapter III, permeability may be calculated from the pore-size distribution parameters obtained from the retention function. No attempt has been made to measure permeability for the purpose of verifying the Burdine integrals. However, the theoretical relative permeability computed from Equation (3-24) has been compared with published experimental data in which capillary pressure retention curves are available.

A comparison of theoretical and measured relative permeabilities is shown in Figures 6 and 7 where relative permeability is plotted as a function of saturation. The measured data are presented as points while the computed values are represented by a solid curve. The retention curves are shown adjacent to the permeability curves. The samples were obtained from consolidated petroleum reservoir rocks. The retention data were acquired by the mercury injection method commonly employed by petroleum reservoir engineers. The agreement between measured and computed permeability values is reasonably good. In the case of core G-1, the permeability is underestimated while for core G-4, the permeability is over-estimated, even though the retention function fits the retention data almost exactly.

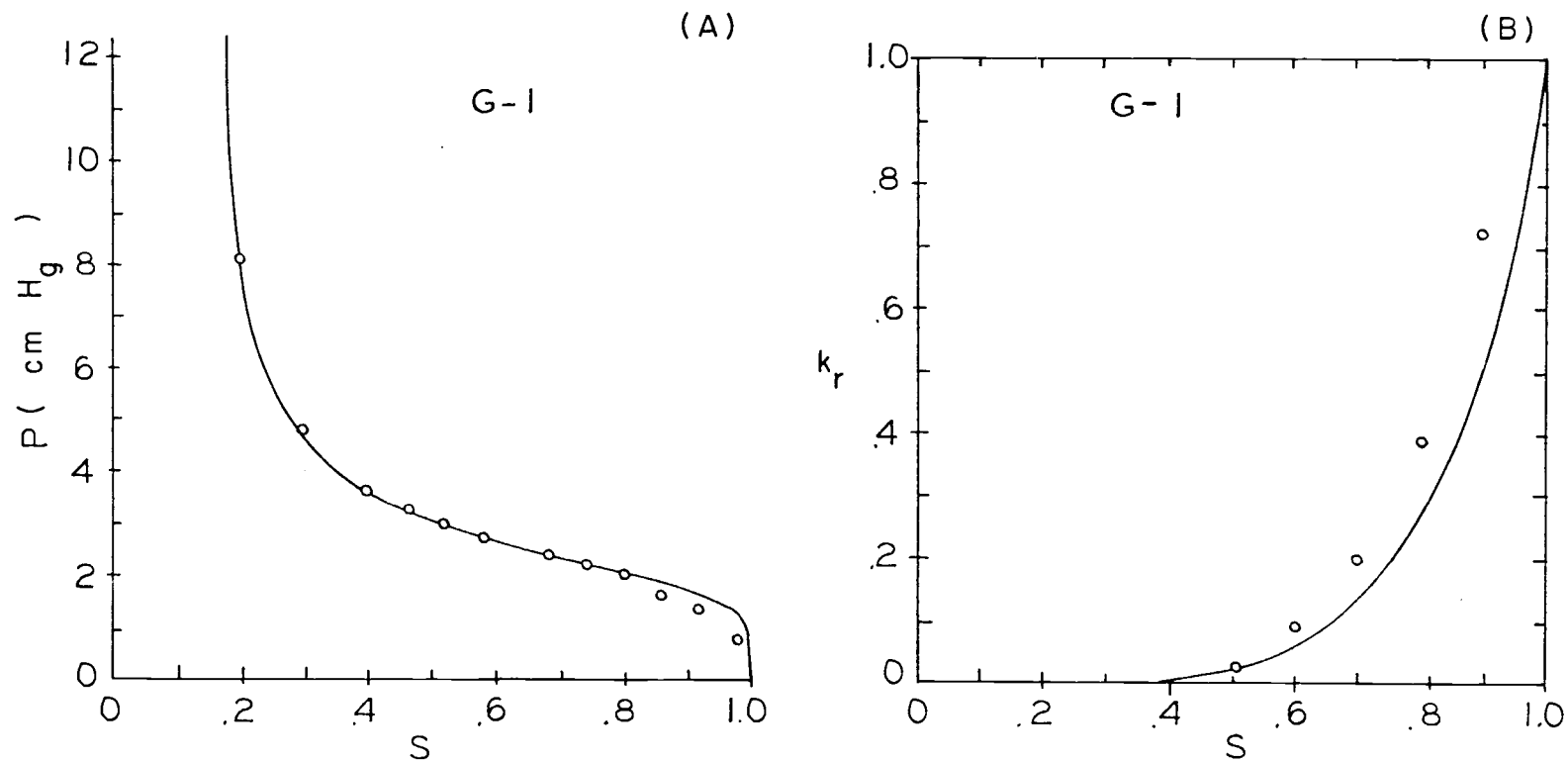


Figure 6. Comparison of the theoretical (or computed) relative permeability curve with experimental data obtained from Corey (1959), where the corresponding retention data and curve are shown in (A).

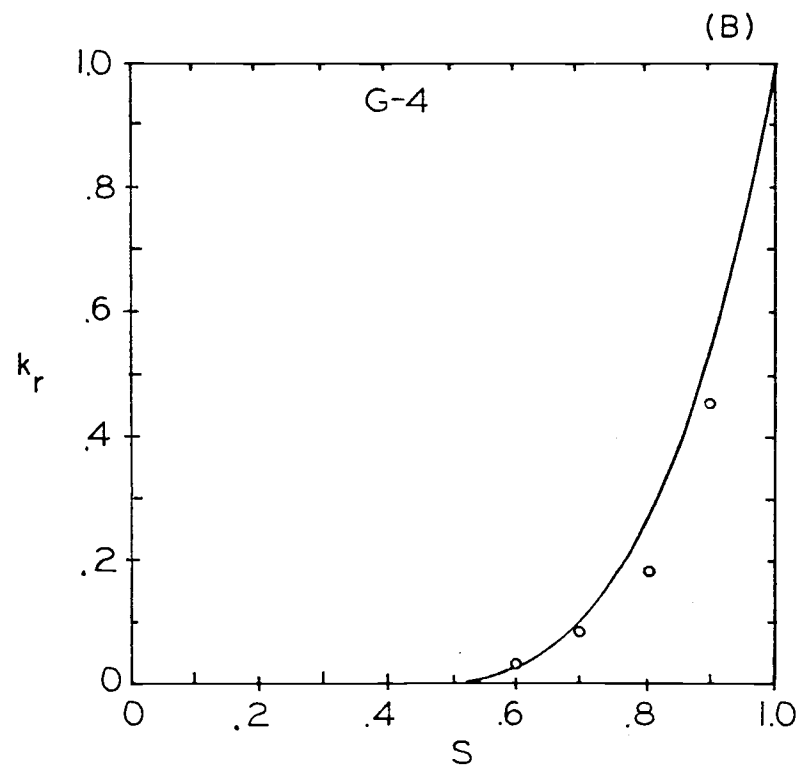
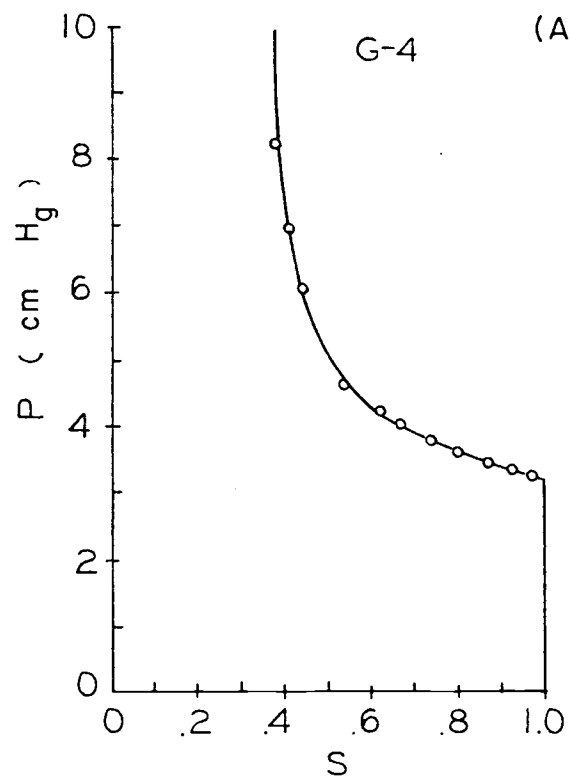


Figure 7. Comparison of the theoretical (or computed) relative permeability curve with experimental data obtained from Corey (1959), where the corresponding retention data and curve are shown in (A).

D. Physical Significance of the Parameters of the Retention Curve

1. The inflection point

The fictitious matching point with the coordinates (P_f, S_f) should not be mistaken for the real inflection point of the retention curve. The location of the inflection point depends upon the values of a , b , and m . More precisely, the abscissa of the inflection point can be calculated through Equation (3-16), and the ordinate through Equation (3-17).

The capillary pressure, P_i , and the saturation at the inflection point, S_i , are regarded as very significant properties of the porous medium. Although the physical significance of the saturation at the inflection point has not been studied in this thesis, it may be the critical saturation at which the non-wetting phase becomes continuous or discontinuous. Based upon the work done by White (1968) dealing with media having narrow pore-size distributions, this postulate appears to be valid. The rationale for this postulate may be developed through the consideration of the pore size associated with P_i by the relation $r_i = 2\sigma/P_i$, in which r_i is the radius of the pores, and σ is the surface tension of the wetting fluid. The frequency of r_i is the

greatest of the entire spectrum of the pore-size distribution. That is to say, the number of pores with the radius r_i is maximum. In view of the interconnectivity of pores, one may infer that this group of pores possesses the greatest potentiality of blocking the non-wetting phase on the imbibition branch, because pores of this size are scattered to the greatest extent throughout the medium. When the wetting phase occupies these pores, the non-wetting phase becomes discontinuous. On the other hand, when the wetting phase drains from these pores, their interconnectivity provides the first possible continuous path for the non-wetting phase.

Figure 8 shows the scaled retention curves and the scaled pore-size distribution curves for the drainage branch of two different media. The inflection points of the retention curves are located at $P. = 1$ where $P.$ is the capillary pressure scaled by the respective P_i . It is clear from Figure 8(B) that the pore associated with $P. = 1$ is the mode of the pore-size distribution.

Since P_i/γ is the characteristic scaling length for modeling, it is important to recognize that P_i/γ is always finite.

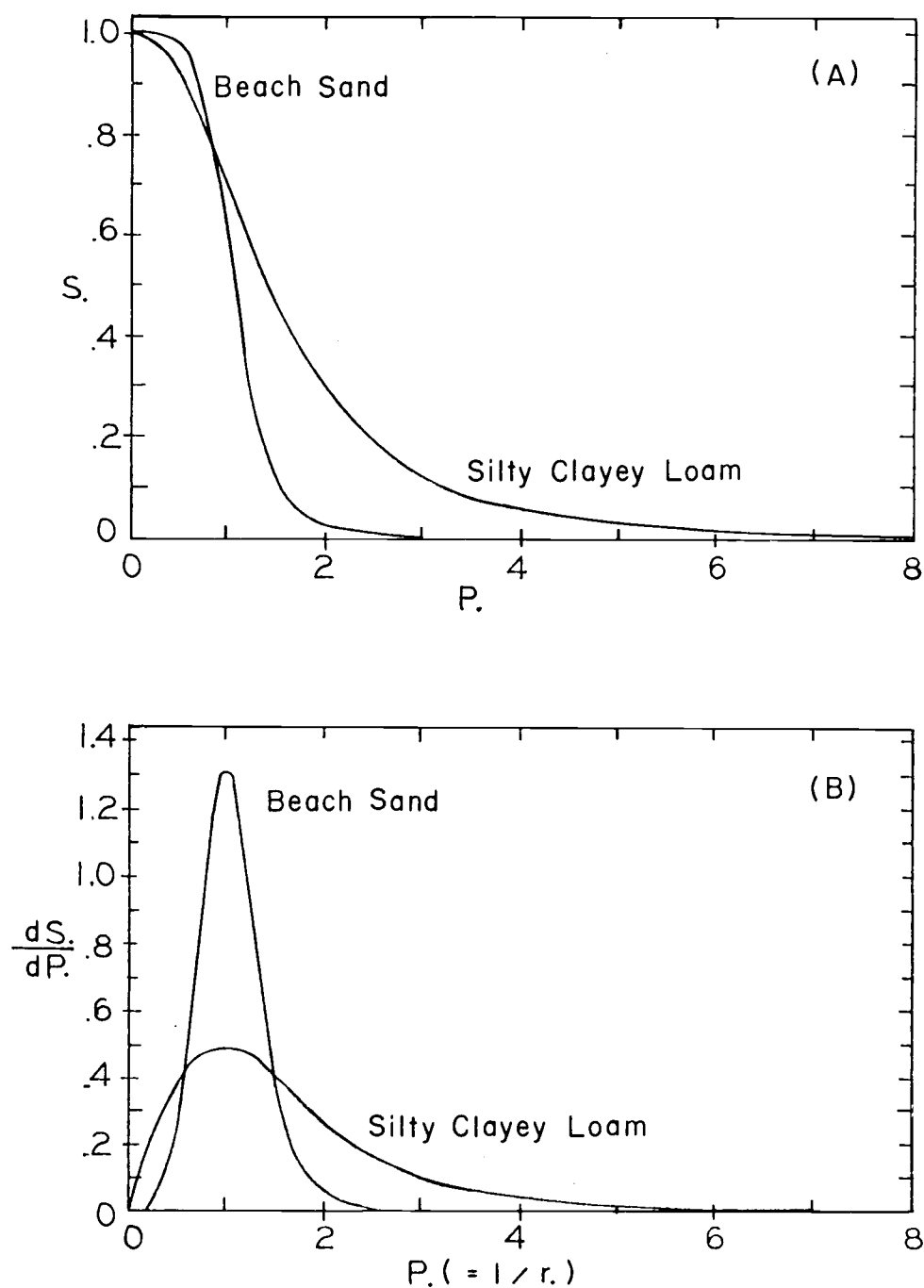


Figure 8. Scaled saturation and scaled frequency of pore sizes as functions of scaled capillary pressure for two media with widely different pore-size distributions.

2. The boundary effect of the retention cell

For soils that have a very narrow range of pore sizes, e.g., sands, as the capillary pressure is increased and the capillarity of the boundary is broken, the fluid at the boundary floods some of the interior pores that have already drained and causes imbibition to occur. The phenomenon has been explained in the recent work of Corey and Brooks (1975). The boundary effect upon the "B" domain of saturation or the downward concavity of the retention curve is to make it steeper than it would be if the liquid at the boundary drained in the same manner as the interior portions of the soil. In other words, if the boundary effect was not present, the slope of the retention curve would be less steep and the downward concavity would be more pronounced. Of course, the degree of the drainage retardation at the boundary is proportional to the area of the non-porous surface of the retention cell and inversely proportional to the drainable porosity.

The effect of the boundary upon the parameters of the retention function may be eliminated by simply ignoring those data in the "B" domain of saturation. The parameters of the retention function can be easily obtained by using data solely from the "A" domain of saturation. The curves computed for the data shown in Figure 9 were obtained

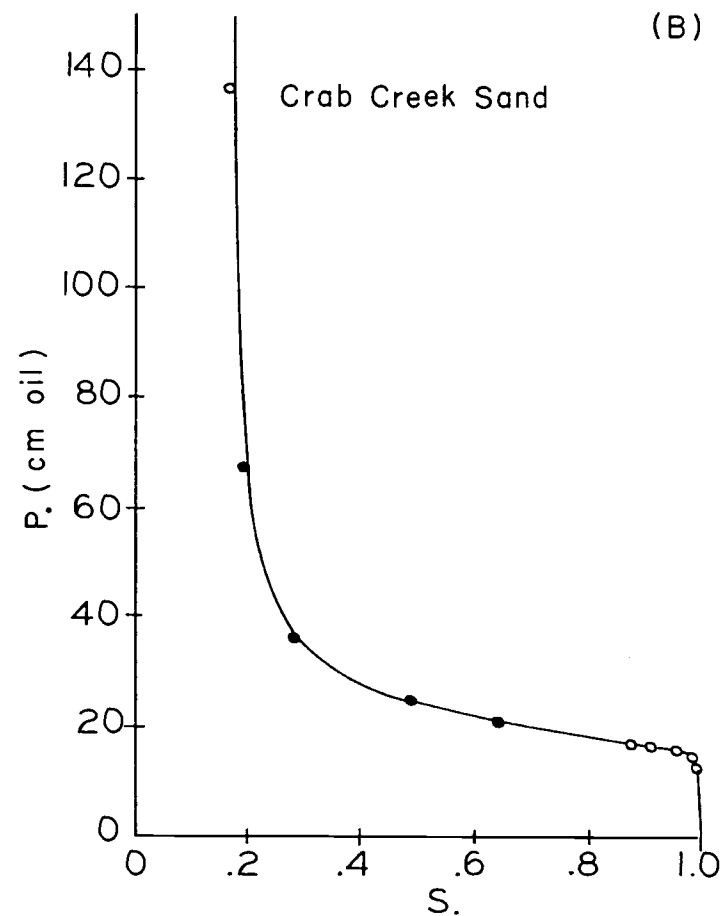
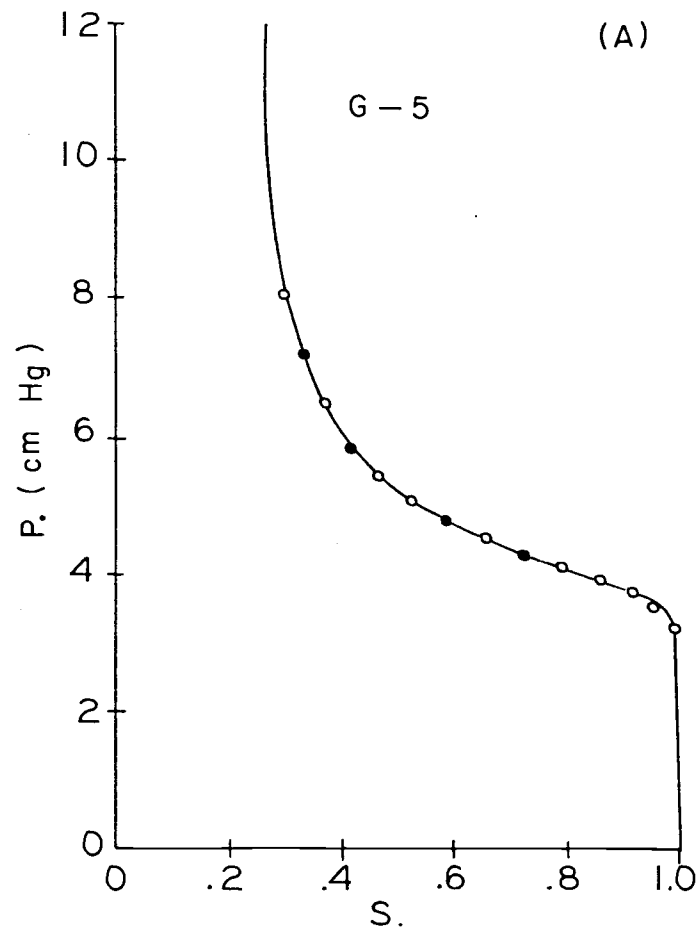


Figure 9. Comparison of the theoretical (or computed) retention curves with retention data on the first drainage branch, where the theoretical curves were determined by using the four data points indicated by solid circles.

in that manner. Under conditions in which apparent initial saturation is involved, there is no boundary effect upon the "B" domain of saturation.

In particular, the "B" domain of saturation is affected by the type of retention cell used to obtain the data. A cell in which the capillary barrier is located only at the bottom of the sample may influence the "B" domain of saturation if the soil sample is initially vacuum-saturated. The effect is particularly pronounced on fine textured media, and is due to the small space between the non-porous surface of the cell and the soil. At the early stages of drainage, liquid progressively drains from the soil surface as air begins to intrude farther and farther into the interior of the soil. During this period of drainage, the boundary remains saturated as observed through the clear acrylic plastic. This phenomenon leads one to believe that if the liquid at the boundary is free from retardation at the early stage, there should be more liquid drained away from the sample.

E. Effect of the Pore-Size Distribution Parameters
Upon the Retention Function and the Probability
Density Function of Pores

The parameters m and b/a are designated as pore-size distribution parameters. It is only when $b/a = 0$ that m may

be referred to as a pore-size distribution index. When $b/a = 0$, the retention function reduces to the step type function proposed by Brooks and Corey (1964) and m is the reciprocal of their index. However, when b/a is not zero, the relationship between the Brooks-Corey pore-size distribution index and m is lost and the pore-size distribution becomes a function of b/a and m . In other words, pore-size distribution cannot be expressed in terms of a single parameter since both b/a and m affect the distribution frequency of pores.

The effect of these two pore-size distribution parameters upon the retention function and the probability density function of pores is shown in Figures 10 and 11. In Figure 10(A) scaled saturation is plotted as a function of scaled capillary pressure while in Figure 10(B) the derivatives of the curves in Figure 10(A), i.e., $dS./dP.$, are plotted as functions of scaled capillary pressure. The derivative of $S.$ with respect to $P.$ is not precisely the probability density function of pores defined in Chapter IV, but is related to $dS./dr.$ by the relation $dS./dr. = P.^2 |dS./dP.|$. The magnitudes of either derivative is not particularly meaningful except they are indications to the frequency of pore sizes and the area under the curves of $dS./dr.$ vs $r.$, and $dS./dP.$ vs $P.$ are equal to unity. The derivative $dS./dP.$ is more useful when plotted on the same

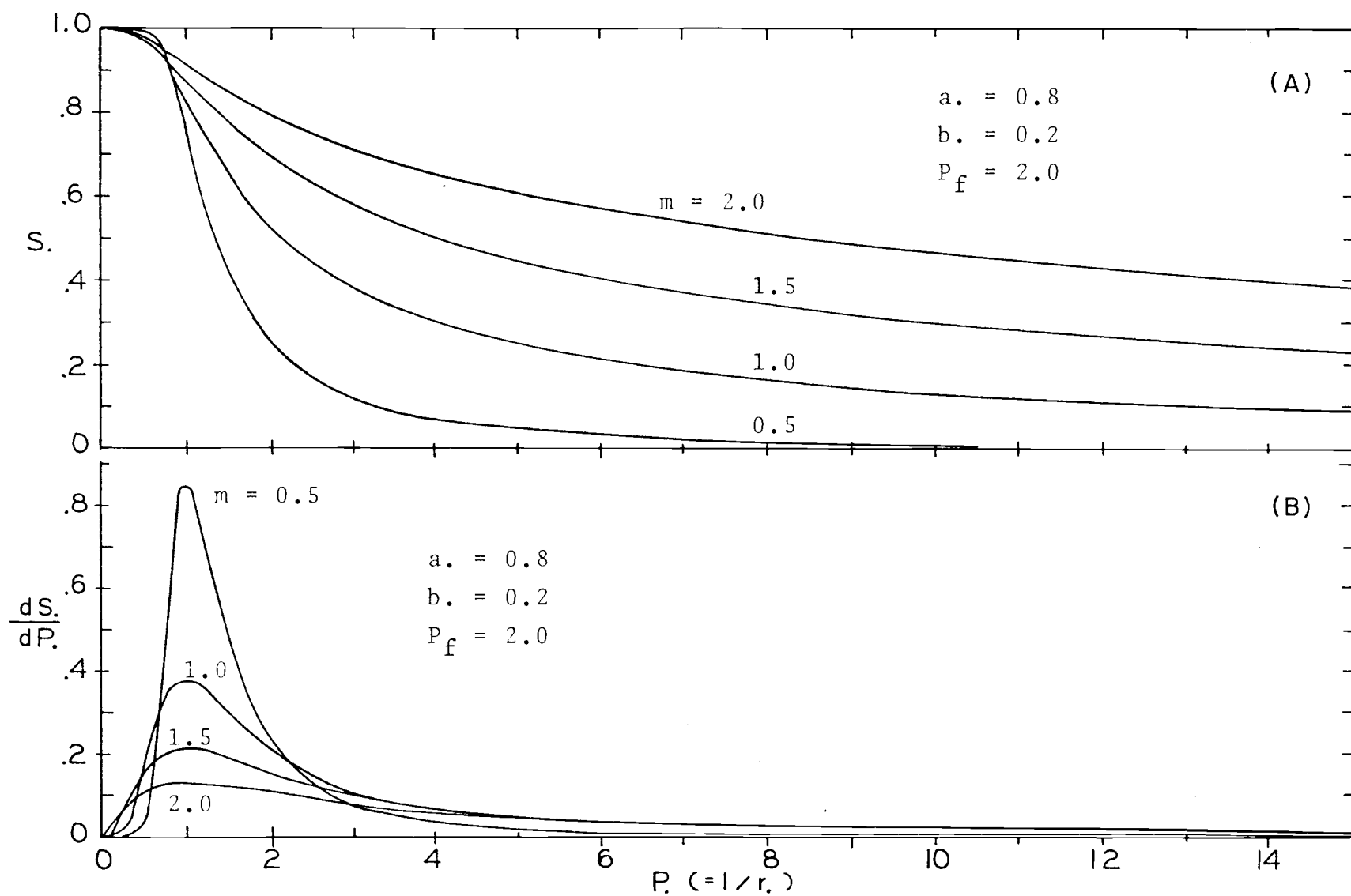


Figure 10. Hypothetical retention and pore-size distribution curves of media with various values of m . 38

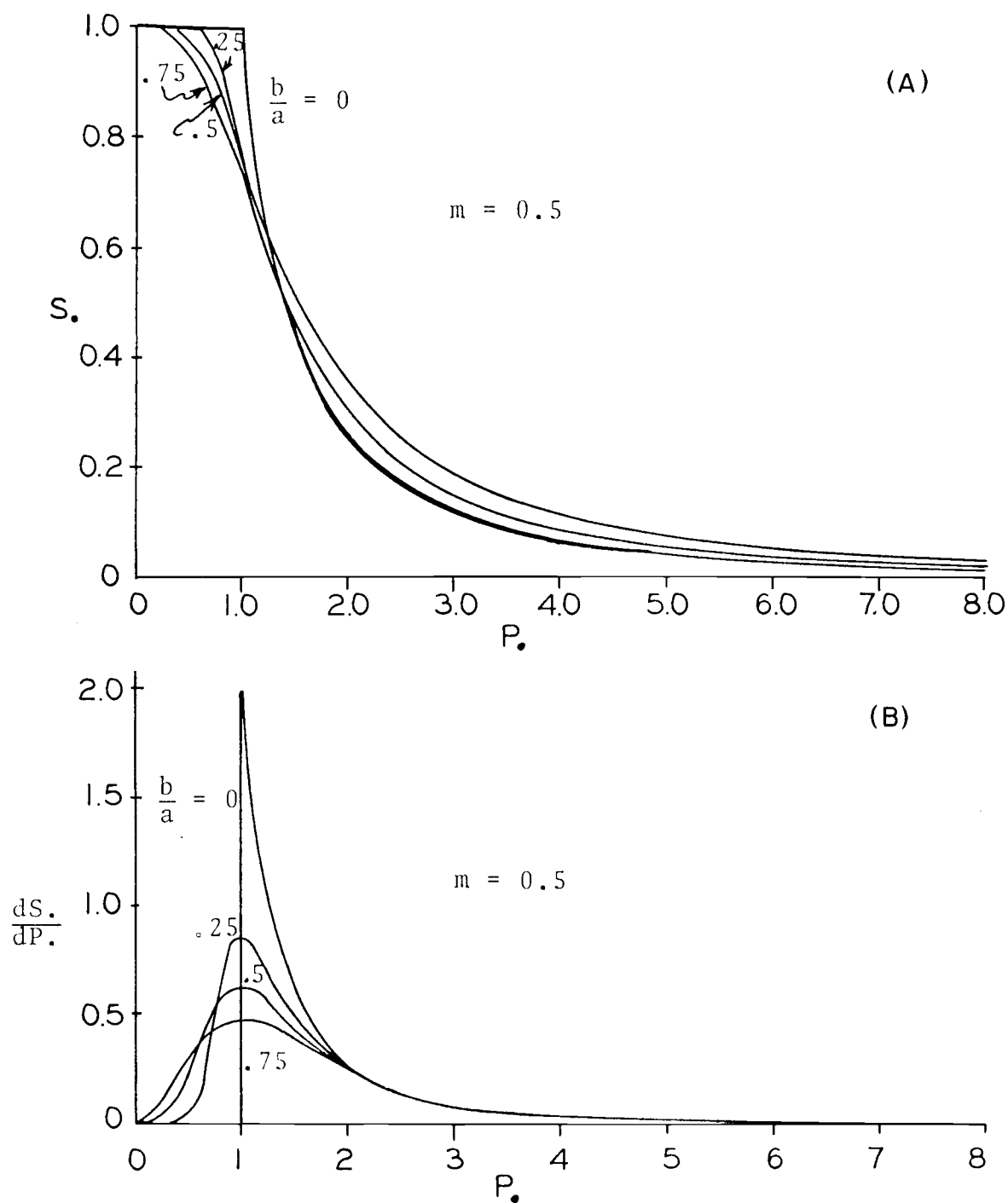


Figure 11. Theoretical curves of scaled saturation and scaled frequency of pore sizes as functions of scaled capillary pressure for hypothetical media having various values of b/a and $m = 0.5$.

abscissa as that for the scaled retention curve shown in Figures 10 and 11. The utility of this type of probability density function will become apparent in subsequent discussions. Figure 12 shows the relative position of the curves of $dS./dr.$ vs $r.$, and $dS./dP.$ vs $P.$ with the same values of m and b/a .

In Figure 10(A), $b/a = 0.25$ is held constant while m varies from 0.5 to 2.0. Obviously the value of m greatly affects the shape of the retention curve. In Figure 10(B), for $m = 0.5$, the maximum frequency of pore sizes ($dS./dP. = \text{max.}$) at $P. = 1.0$ is far greater than that for $m = 2.0$. Since the areas under the pore size frequency curves must be equal to each other and to unity, it follows that the curve for $m = 2.0$ must extend over a far greater range of values of $P.$ than that for $m = 0.5$. Hence, the curve for $m = 2.0$ covers a wider range of pore sizes than that for $m = 0.5$. It is clear that when b/a is constant, m is a measure of the distribution of pore sizes. When m is large, the distribution of pores covers a wide range, while for small values of m the distribution of pores covers a narrow range. The greatest frequency of pore always occurs at $P. = 1.0$.

Figure 11 shows the effect of the other pore-size distribution parameter, b/a , upon the retention curve and upon the frequency of pores. In Figure 11(A) where scaled saturation is plotted as a function of scaled capillary pressure,

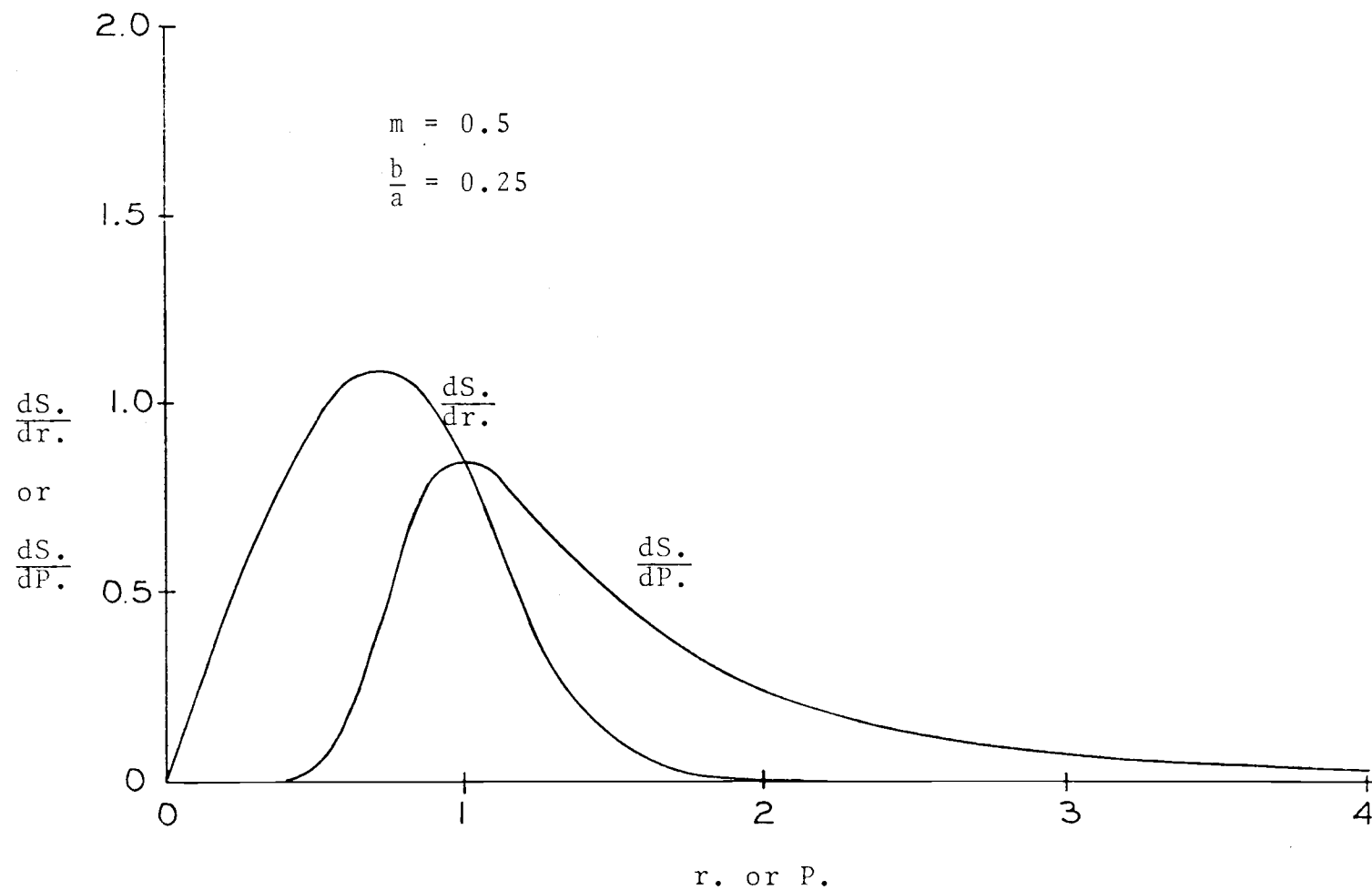


Figure 12. Comparison of the theoretical pore-size distribution function, $dS./dr.$, and the function, $dS./dP.$ for $m = 0.5$ and $b/a = 0.25$.

$m = 0.5$ is held constant and b/a varies from 0 to 0.75. Since m is the same for all curves, the shapes of the retention curves are nearly alike. The downward concavity of the curves increases as b/a increased while the upward concavity decreases as b/a increases.

In Figure 11(B), the maximum frequency of pores is greatly reduced as b/a increases from 0 to 0.75. The family of curves in Figure 11(B) is similar to the family of curves in Figure 10(B). Apparently this pore-size distribution parameter, b/a exerts a similar effect upon the maximum frequency of pore sizes as does m . Yet, it does not seem to be very apparent from the cursory observation of the retention curves. If one compares the retention curve with $b/a = 0$ and $b/a = 0.25$ in Figure 11(A), these curves seem to become nearly coincident at scaled saturation of 0.55. If one assumes that the curve with $b/a = 0$ (step type function of Brooks and Corey (1964)) approximates the curve with $b/a = 0.25$, the permeability of the media would be greatly overestimated by the approximate function according to the maximum frequencies of pore sizes shown in Figure 11(B).

F. Effect of the Pore-Size Distribution Parameters Upon Permeability and Diffusivity

The effect of m and b/a upon permeability and diffusivity

is shown in Figures 13-16. In Figure 13 relative permeability is plotted as a function of scaled saturation for $b/a = 0.25$ and m varies from 0 to 1.5. The envelope curve in this figure is the one with $m = 0$ which reduces the permeability function to $k_r = (S_r)^3$. As m increases in value, there is a precipitous change in the relative permeability.

A similar change in permeability occurs when the other pore-size distribution parameter, b/a , increases as shown in Figure 14. Here, the envelope curve is the one with $b/a = 0$ which reduces the permeability function to the Brooks-Corey permeability function given by $k_r = (S_r)^{2m+3}$. As b/a increases from zero to 0.75, the permeability is greatly reduced at high saturation.

In Figures 15 and 16, scaled diffusivity is plotted as a function of scaled saturation. In Figure 15, $b/a = 0.25$ is held constant as m varies from 0.5 to 2.0, while in Figure 16, $m = 0.5$ is held constant as b/a varies from zero to 0.75.

Figure 15 shows the smaller the value of m , the more steep the slope of the diffusivity curve becomes for all values of S_r . The diffusivity is finite for all values of S_r when $b/a = 0$; however, when $b/a = 0.05$, the scaled diffusivity becomes infinite as S_r approaches unity as shown in Figure 16.

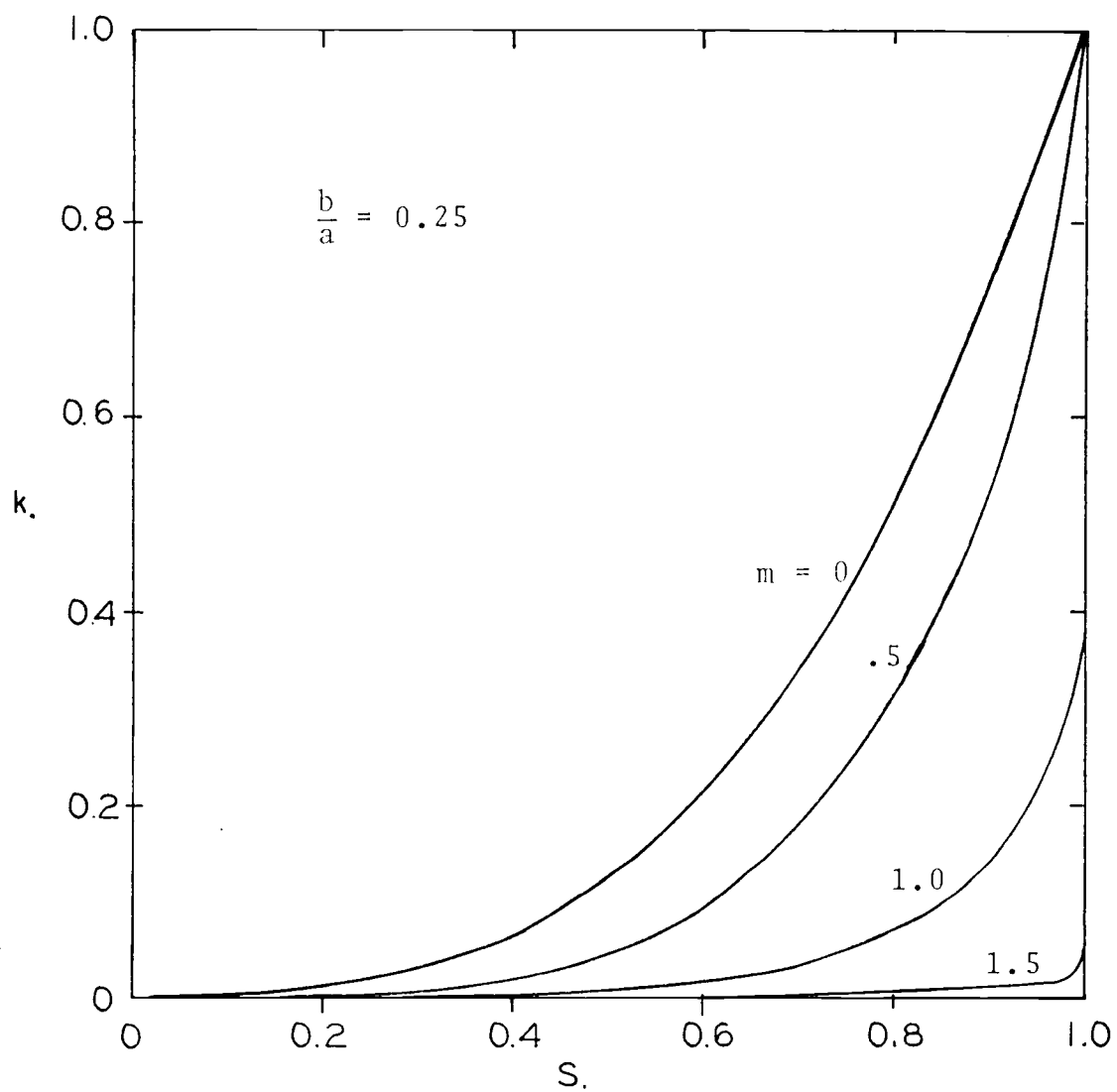


Figure 13. Theoretical relative permeability curves for hypothetical media having various values of m and $b/a = 0.25$.

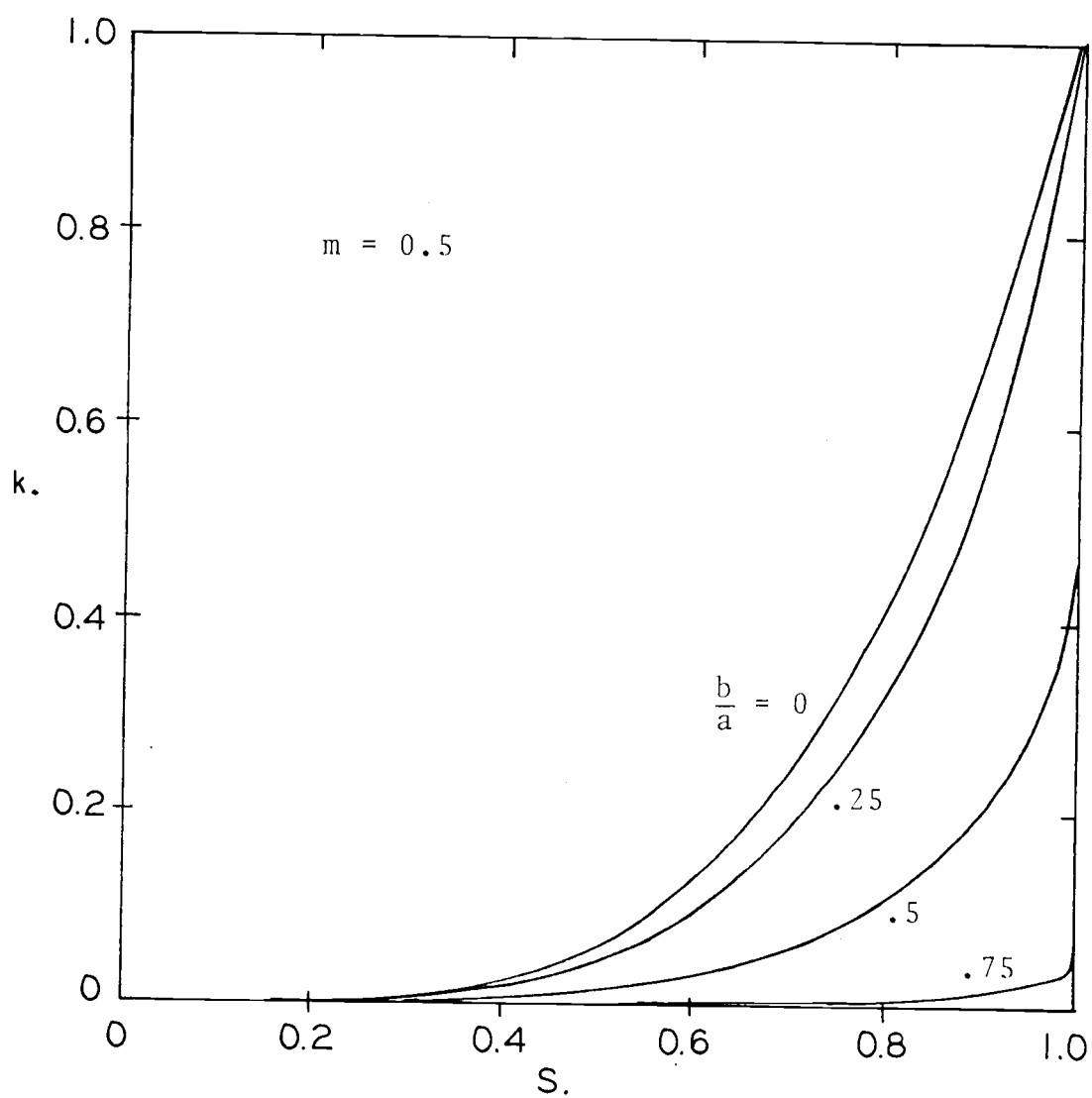


Figure 14. Theoretical relative permeability curves for hypothetical media having various values of b/a and $m = 0.5$.

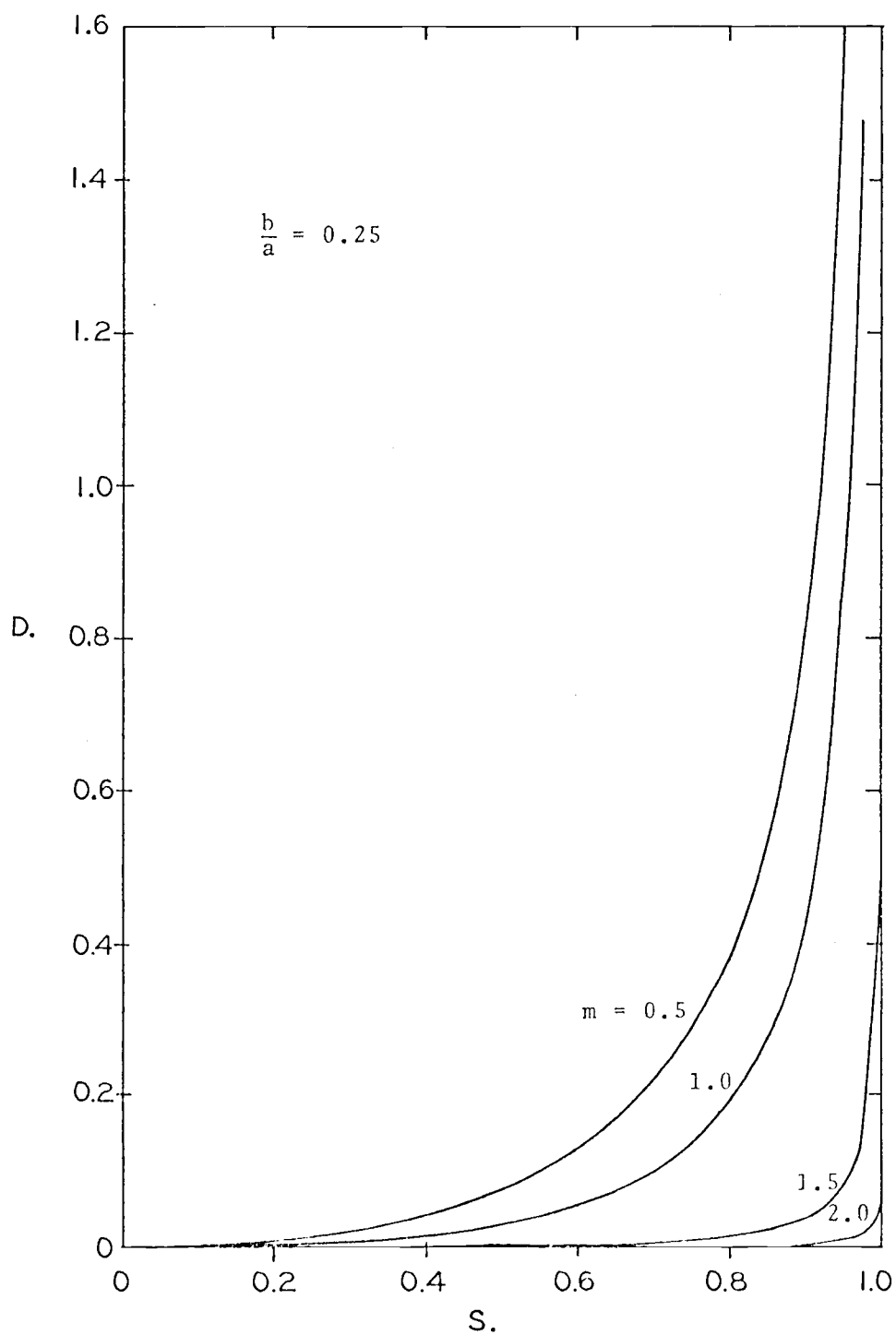


Figure 15. Theoretical scaled diffusivity as a function of scaled saturation for various values of m and for $b/a = 0.25$.

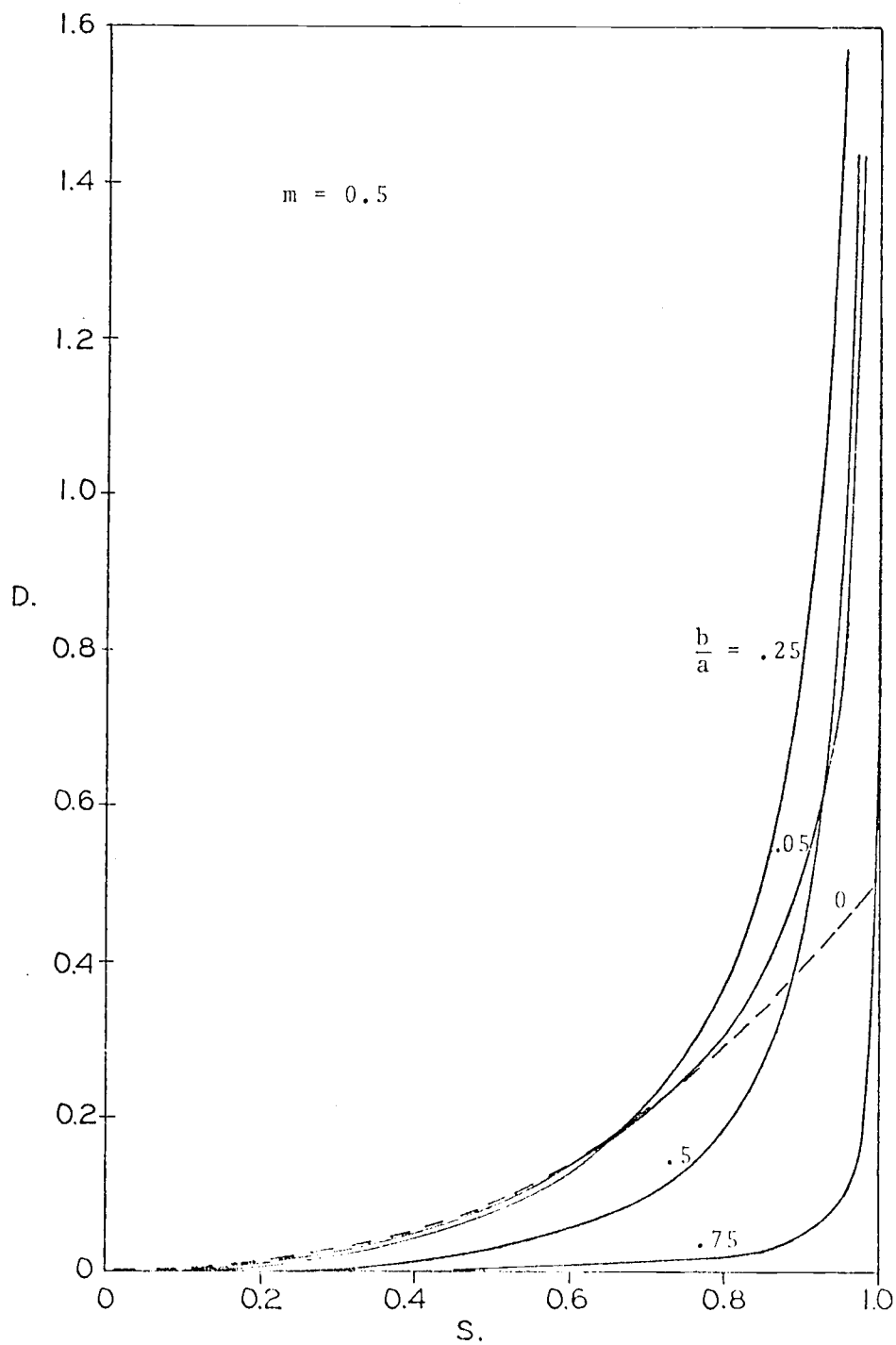


Figure 16. Theoretical scaled diffusivity as a function of scaled saturation for various values of b/a and for $m = 0.50$.

Due to the fact that the retention function takes into account the downward concavity of the retention data, the derivative of P . with respect to S . becomes infinite as S . approaches unity. When b/a and m are small, the value of diffusivity may be very large near unit saturation. This has been an insurmountable difficulty in the solution of boundary value problems by numerical schemes that have been written in terms of diffusivity and the theoretical functions proposed herein.

G. Hysteresis and Air Entrapment

The hysteresis envelopes for two soils are shown in Figures 17 and 18 where scaled saturation is plotted as a function of scaled capillary pressure. The drainage branches were obtained from soils at apparent initial saturation, i.e., the air entrapped at zero capillary pressure is regarded as part of the solid matrix of the porous media. The capillary pressures for both branches of the retention curve were scaled by the P_i of the drainage branch of the respective soil.

Directly below the retention curves, based on the same capillary pressure scale for the abscissa, the frequency of pore sizes is plotted for both branches of the retention curves. Since the total areas under each of the pore-size frequency curves must be identical, the area CDE must be

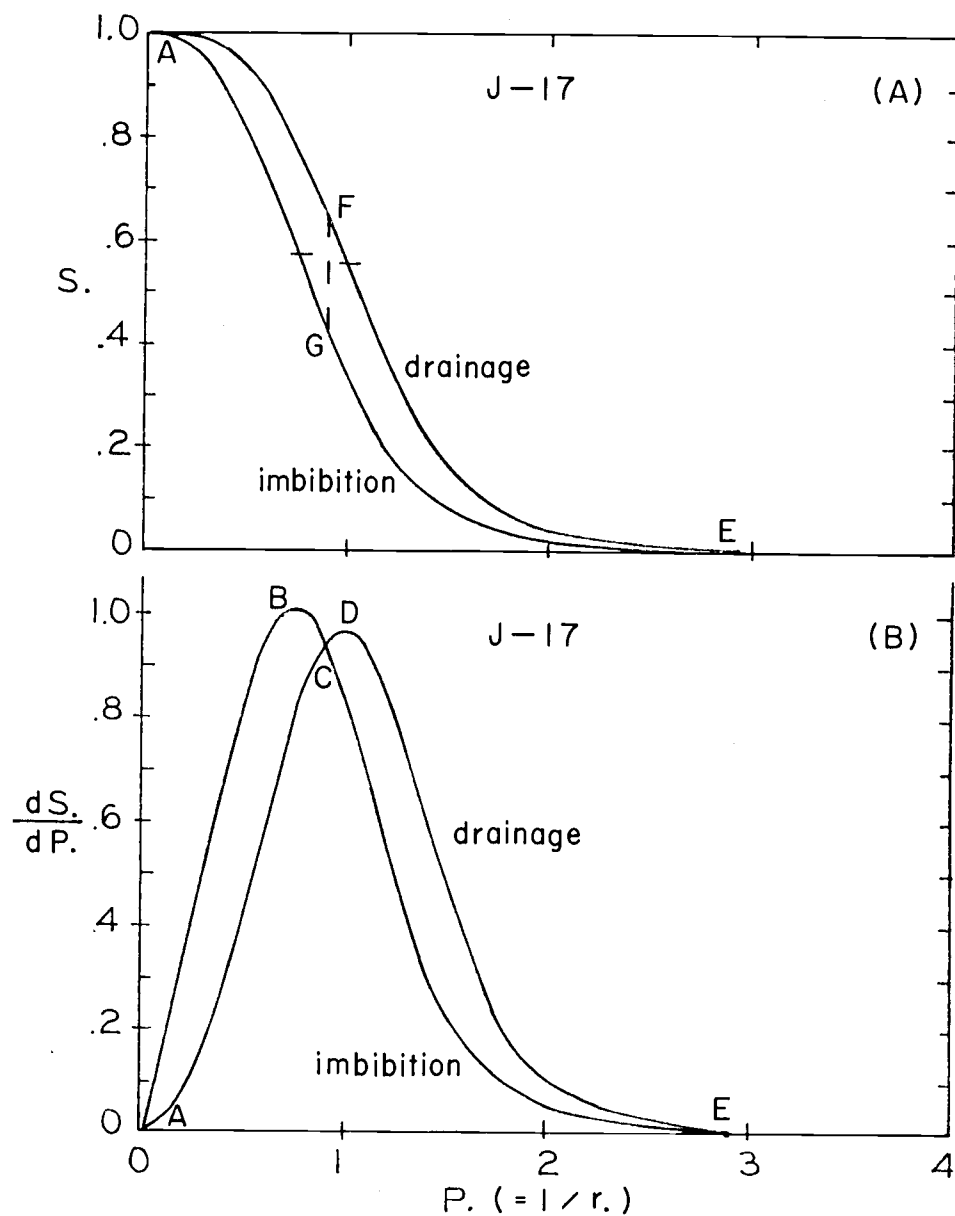


Figure 17. (A) Theoretical scaled retention curves forming the hysteresis envelope and
 (B) the scaled frequency of pore sizes as a function of scaled capillary pressure for the hysteresis envelope shown in (A).

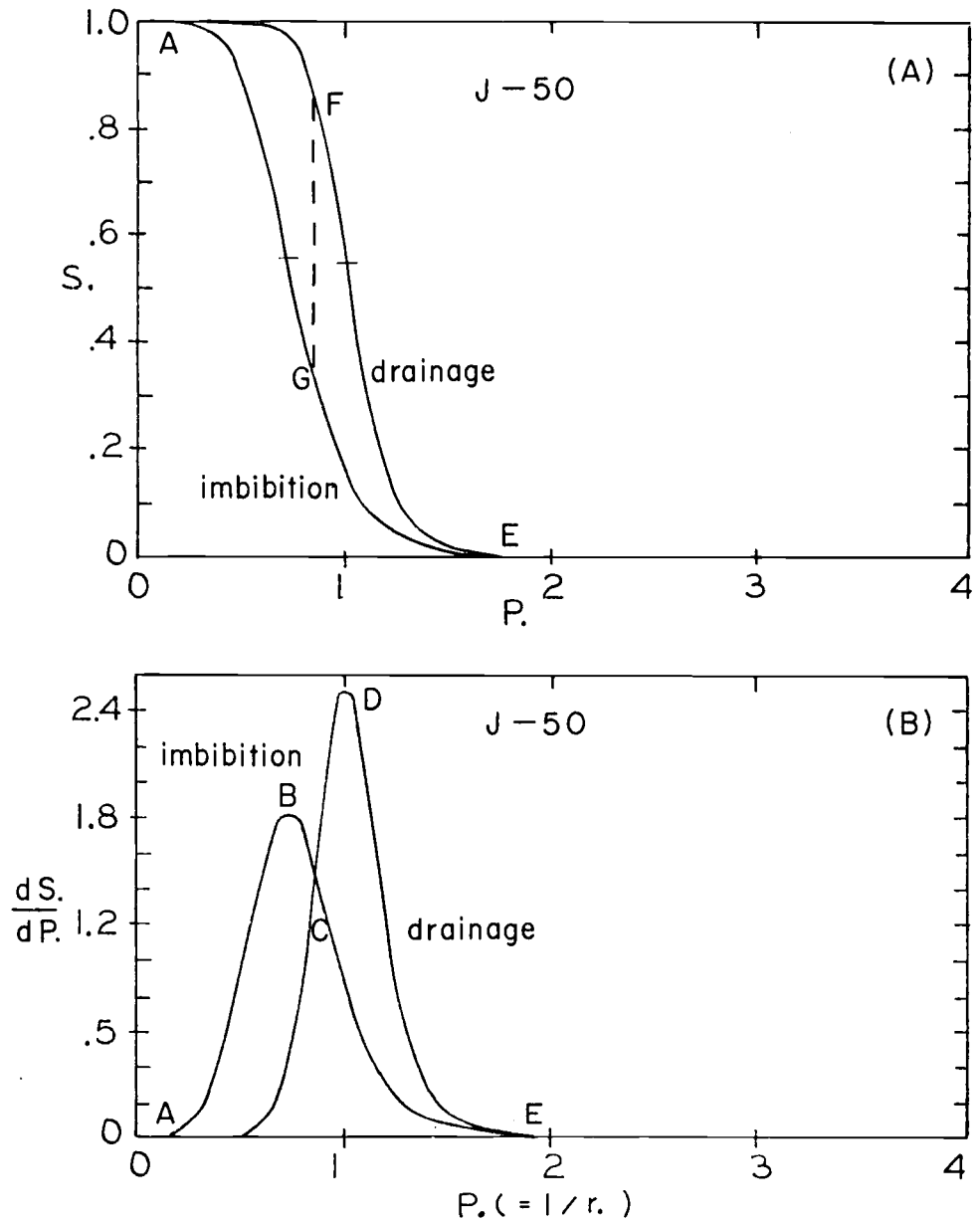


Figure 18. Theoretical scaled retention curves and theoretical scaled pore-size distribution curves for the hysteresis envelope.

equal to the area ABC in Figures 17(B) and 18(B). The area CDE represents the total volume of air entrapped as the medium undergoes imbibition down to the particular capillary pressure related to the point C. In other words, the maximum air entrapment occurs at the capillary pressure related to the intersection of the two pore-size frequency curves. At that capillary pressure indicated by point C, the entrapped air begins to move out of the medium. Consequently, the amount of the remaining entrapped air in the medium is reduced until the value of P_c equal to zero is reached. The value of P_c at the intersection C is always less than the P_{i1} of the drainage branch and greater than the P_{i2} of the imbibition branch.

H. The Concept of Energy

The area under the retention curve may be used to represent the energy stored in the liquid phase at a certain degree of saturation. Assuming the pressure of the air phase is zero, one can regard the capillary pressure as the pressure of the liquid phase. The dimension of pressure is $(\text{Force})/(\text{Length})^2$ and the definition of saturation is $(\text{Volume of liquid})/(\text{Total pore volume})$. Therefore, the product of pressure and saturation has dimensions of $(\text{Energy})/(\text{Total pore volume})$. Thus, energy stored in the liquid phase at a certain saturation is

$$E = V_t \int_0^S P.(S.)dS.,$$

where V_t is the total pore volume. Similarly, if the dependent and the independent variables are interchanged, the area under the new S.-P. curve still represents energy per total pore volume. Hence, energy stored in the liquid occupying pores smaller than a given size is

$$E = V_t \int_{\infty}^P S.(P.)dP. \quad .$$

It is postulated from an energy viewpoint that as liquid leaves the pores from an initial saturation of unity, the energy of the liquid decreases. The energy of the liquid is near its minimum value as residual saturation is approached. If some liquid is added to the pores, the energy of the liquid in the pores is increased.

In Figure 18(A), as liquid is added to the pores to increase the pressure to a point denoted by G, (point of maximum air entrapment), the volume of liquid in the pores is less than it was for the same pressure on the drainage branch. The difference in saturation is given by FG and must be due to the presence of entrapped air. The entrapped air will be at a pressure greater than zero and possesses energy. Therefore, the air obtained its energy from imbibition. Consequently, when energy is added to the medium

by adding liquid, part of the energy is utilized to trap air and part goes into the liquid itself. The difference in area under the drainage and imbibition branches of the retention curve, i.e., area EFG in Figure 18(A), represents the energy required to entrap the maximum volume of air. As additional liquid is imbibed into the media, the volume of air entrapped decreases. This implies that air is being expelled. As air is expelled into the atmosphere, energy is returned to the liquid. The liquid increases its energy until it reaches the same energy level as it possesses on the drainage branch at $P. = 0$. Therefore, the area AFG must be equal to the area EFG as the energy released from expulsion of air is exactly equal to that required for air entrapment based on law of conservation of energy.

The area EDC in Figure 18(B) represents the volume of air entrapped as the capillary pressure is decreased while area ABC represents the volume of air expelled from the medium after the maximum air entrapment occurs at C.

The retention function and the probability density function of pore sizes have made it possible to explain the phenomenon of air entrapment during imbibition. It now appears possible to explain the field method of measuring "Air Entry Value" proposed by Bouwer (1966), in which imbibition is allowed to occur under a completely sealed circular infiltrometer. The pressure is measured

when the first air bubbles enter the sealed chamber above the soil surface. This pressure may indeed be the pressure at maximum air entrapment, which is less than the capillary pressure at the inflection point of the drainage branch of the retention curve.

CHAPTER VII

CONCLUSIONS

A. Summary

Based upon the Pearson Type VIII distribution function, a retention function which describes the retention of fluids in porous media has been developed. The function was verified experimentally and could accurately relate capillary pressure to saturation on the drainage branch for porous media either initially vacuum-saturated or apparently saturated. In the latter case, the pores of the media are filled with entrapped air as well as liquid as they are found under normal field conditions at zero capillary pressure. The function was also proved to precisely define the imbibition curves for media with an initial saturation near residual saturation or field capacity. However, no attempt has been made to interrelate the two branches of the retention curve, i.e., drainage and imbibition, except the same descriptive terms are used for both.

The Burdine integrals are assumed valid for computing the permeability of the porous medium from retention data obtained in the laboratory. Since the retention function developed herein precisely fits experimental data, the permeability calculated from the permeability function based

upon the Burdine integrals should fit the experimental data precisely also. From the differentiable retention function and the permeability function, a pore-size distribution and a diffusivity function were further obtained.

An experimental apparatus and procedure have been developed for expediting the acquisition of the retention data on both drainage and imbibition branches in the laboratory. The equipment is simple, and the procedure is easy to follow and consumes less time than the conventional methods.

The retention function possesses parameters which have physical significance, and may be easily assessed from retention data by the numerical method devised in this thesis. The domain of saturation, A, from the saturation at the inflection point to the residual saturation is the one where the retention curve is concave upward. In the domain, B, from the saturation at the inflection point to the unit saturation, the retention curve is concave downward. The ratio of b/a and the value of m were demonstrated to be pore-size distribution parameters. The quantity m is the dominant factor governing the shape of the retention curve.

It is postulated that the saturation at the inflection point, S_i , is the critical point at which the non-wetting phase becomes continuous on the drainage branch and discontinuous on the imbibition branch. From a statistical

viewpoint, the critical saturation should correspond to the mode of the pore-size distribution of the soil. Equations in terms of the hydraulic properties, a , b , m , and P_f of the soil were derived to determine the values of the critical saturation and its corresponding capillary pressure.

The criteria set forth for affinity between porous media are similar to those previously established by Brooks and Corey (1964) except the new criteria includes one additional parameter. Two media are said to be affine if the b/a ratios and the values of m are identical. The standard scaling length for the external dimension of the model was chosen to be the capillary pressure head at the inflection point of the retention curve, i.e., P_i/γ .

The effect of the downward concavity of the retention curve upon the values of permeability and diffusivity was demonstrated in this thesis. It appears that if the pore-size distribution parameter b/a is ignored, the solutions of boundary value problems involving imbibition may be erroneous, particularly if the soil has a wide range of pore sizes.

The use of the scaled retention and pore-size distribution functions enables one to more rigorously examine and further explore theories and hypotheses regarding water movement in partially saturated media. For example, this thesis presents a discussion on the phenomenon of air

entrapment in porous media during imbibition through an energy concept based upon the scaled retention and pore-size distribution curves.

To the hydrologist, the major application of the theories presented herein is the use of the hydraulic functions of retentivity, permeability and diffusivity in the general flow equation governing the movement and distribution of water in the subsurface of the watershed. With these functions at hand, theoretical understanding of the soil-water system in the watershed may be enlarged. However, a paradox exists in which problems formulated in terms of diffusivity cannot be solved by numerical schemes presently available. Obviously, the difficulty arises from the fact that the diffusivity becomes infinite as the saturation approaches unity. Some problems of infiltration may be solved by resorting to the step type function proposed by Brooks and Corey (1964), which completely ignores the downward concavity of the retention data and always has a finite value of diffusivity. It should be noted, though, that the solution therefrom may be greatly in error if the downward concavity of the retention data is pronounced. Secondly, the pore-size distribution parameters, m and b/a , defined herein may be employed by hydrologists to characterize hydrologically the soil types in the watershed.

Thus, the parameters will become very helpful when it comes to exploring the possibility of transferring an existing lumped-parameter hydrological model from one watershed to another.

B. Significant Findings

1. A simple and yet complete retention function has been discovered. This function is completely adaptable to any kind of disturbed porous materials, and its parameters are easy to assess.

2. Based upon the exact retention function and the Burdine integrals, a permeability function in terms of the incomplete Beta function ratio is derived. If tables of the incomplete Beta function ratios are made available, the computation of exact permeability values from measured retention data becomes a very simple operation.

3. From the retention function, a general probability density function of pores for porous media is obtained. Since the most important hydraulic variables of porous media, e.g., permeability, are closely related to the pore-size distribution, the realization of this general probability density function will enable meaningful and constructive examinations of existing theories regarding those variables in the event of their inadequacy.

4. The established criteria of affinity between porous media will refine the procedure of physical modeling, especially the selection of proper material for use in models.

5. Although the effect of the value of b/a upon the shape of the retention curve does not appear as influential as that of the value of m , its effect upon the permeability is as pronounced as that of m . This leads one to believe that the downward concavity is an important property of the retention curve, which cannot be arbitrarily neglected when it comes to computing the permeability from retention data. The value of b/a is the dominant factor governing the downward concavity.

6. The importance of the boundary effect of the retention cell on the downward concavity of the retention curve is proportional to the non-porous surface of the retention cell and inversely to the drainable porosity of the soil. Care should be exercised when obtaining retention data of soils having high residual water content in the laboratory.

7. The acquisition of the retention data on the imbibition branch is less time-consuming than that on the drainage branch. Equilibrium of the pressure difference across the air-liquid interface in the porous medium is readily reached during imbibition.

C. Needs of Future Research

Hopefully the exact expressions developed herein will stimulate the mathematician and the others engaging in the modeling of flow systems in porous media to develop the capability of handling these expressions in the solutions of flow problems. In addition, the findings have opened up the possibility of dealing with the hysteresis in porous media in mathematical terms. For example, it now seems likely to relate the drainage branch to the imbibition branch of the hysteresis envelope. With this, the scanning loops may also be explained physically and mathematically.

Since both of the pore-size distribution parameters, b/a and m , relate to the shape of the retention curve, a single pore-size distribution index may be derived through the finding of a relationship between b/a and m .

Finally, the postulate that the critical saturation at the inflection point of the retention curve is the saturation at which the non-wetting phase becomes continuous or discontinuous needs to be experimentally verified. Such a finding would be important to agricultural engineers dealing with drainage problems. According to observations made by White (1968) on media with narrow ranges of pore sizes, the postulate is valid. Therefore, a wide range of different types of media needs to be studied, i.e., media that have widely varying dissimilar properties.

BIBLIOGRAPHY

- Abramowitz, M. and I. A. Stegun (editors). 1970. Handbook of mathematical functions with formulas, graphs, and mathematical tables. National Bureau of Standards. U.S. Government Printing Office. p. 258, p. 263, and pp. 944-945.
- Baver, L. D. 1938. Soil permeability in relation to non-capillary porosity. Soil Science Society of America Proceedings. 3:52-56.
- Bear, Jacob. 1972. Dynamics of fluid in porous media. American Elsevier Publishing Company, Inc. New York, New York. 764 pp.
- Bouwer, H. 1966. Rapid field measurement of air entry value and hydraulic conductivity of soil as significant parameters in flow system analysis. Water Resources Research. 2(4):729-738.
- Bouwer, H. and R. D. Jackson. 1974. Determining soil properties. In: Drainage for agriculture (edited by J. Van Schilfgaarde). American Society of Agronomy. Monograph No. 17. pp. 611-672.
- Brooks, R. H. and A. T. Corey. 1964. Hydraulic properties of porous media. Hydrology Paper No. 3. Colorado State University, Fort Collins, Colorado. 27 pp.
- Brooks, R. H. 1965. Hydraulic properties of porous media. A Ph.D. dissertation, Colorado State University, Fort Collins, Colorado. 88 pp.
- Brooks, R. H. and A. T. Corey. 1966. Properties of porous media affecting fluid flow. Journal of the Irrigation and Drainage Division, American Society of Civil Engineers. 92(2):61-88.
- Brooks, R. H., P. J. Leclercq, R. R. Tebbs and W. Rawls. 1974. Axisymmetric infiltration. A final report submitted to the Water Resources Research Institute, Oregon State University, Corvallis, Oregon. 61 pp.
- Bruce, R. R. 1972. Hydraulic conductivity evaluation of the soil profile from soil water retention relations. Soil Science Society of America Proceedings. 36(4):555-561.

- Brust, K. J., C. H. M. Van Bavel and G. B. Stirk. 1968. Hydraulic properties of a clay loam soil and the field measurement of water uptake by roots: III. Comparison of field and laboratory data on retention and of measured and calculated conductivities. Soil Science Society of America Proceedings. 32(3):322-326.
- Brutsaert, W. 1966. Probability laws for pore-size distributions. Soil Science. 101(2):85-92.
- Brutsaert, W. 1967. Some methods of calculating unsaturated permeability. Transactions of American Society of Agricultural Engineers. 10(3):400-404.
- Brutsaert, W. 1968. The permeability of a porous medium determined from certain probability laws for pore-size distribution. Water Resources Research. 4(2):425-434.
- Buckingham, E. 1907. Studies on the movement of soil moisture. U.S. Dept. Agr. Bureau of Soils. Bulletin No. 38. 61 pp.
- Burdine, N. T. 1953. Relative permeability calculations from pore-size distribution data. American Institute of Mining and Metallurgical Engineers. Petroleum Transactions. 198:71-77.
- Campbell, G. S. 1974. A simple method for determining unsaturated conductivity from moisture retention data. Soil Science. 117(6):311-314.
- Cary, J. W. 1967. Experimental measurements of soil-moisture hysteresis and entrapped air. Soil Science. 104(3):174-180.
- Cassel, D. K., A. W. Warrick, D. R. Nielsen and J. W. Biggar. 1968. Soil-water diffusivity values based upon time dependent soil-water content distributions. Soil Science Society of America Proceedings. 32(6):774-777.
- Childs, E. C. and N. Collis-George. 1950. The permeability of porous materials. Proc. Roy. Soc. London. A201:392-405.
- Corey, A. T. 1954. The interrelation between gas and oil relative permeabilities. Producers Monthly. XIX(1):38-41.

- Corey, A. T. 1959. Evaluation of capillary-pressure field data. Petroleum Research Corporation. Research Report A-4. Denver, Colorado. 68 pp.
- Corey, A. T. and R. H. Brooks. 1975. Drainage characteristics of soils. Soil Science Society of America Proceedings. 39(2):251-255.
- Corey, G. L., A. T. Corey and R. H. Brooks. 1965. Similitude for non-steady drainage of partially saturated soils. Hydrology Paper No. 9. Colorado State University, Fort Collins, Colorado. 38 pp.
- Darcy, H. 1856. Les fontaines publiques de la ville de Dijon. Dalmont, Paris.
- Elderton, W. P. and N. L. Johnson. 1969. Systems of frequency curves. Cambridge University Press. London. 216 pp.
- Encyclopaedia Britannica, Inc. 1969. Surface tension. Encyclopaedia Britannica. 21:442-450.
- Gardner, W. R. 1956. Calculation of capillary conductivity from pressure plate outflow data. Soil Science Society of America Proceedings. 20(3):317-320.
- Gardner, W. R. and F. J. Miklich. 1962. Unsaturated conductivity and diffusivity measurements by a constant flux method. Soil Science. 93(4):271-274.
- Gates, J. I. and W. T. Lietz. 1950. A.P.I. Drilling and Production Practice.
- Green, R. E. and J. C. Corey. 1971. Calculation of hydraulic conductivity: a further evaluation of some predictive methods. Soil Science Society of America Proceedings. 35(1):3-8.
- Haring, R. E. and R. A. Greenkorn. 1970. Statistical model of a porous medium with nonuniform pores. Amer. Inst. Chem. Eng. J. 16(3):477-483.
- Jackson, R. D., C. H. M. Van Bavel and R. J. Reginato. 1963. Examination of pressure-plate outflow method for measuring capillary conductivity. Soil Science. 96(4):249-256.

- Jackson, R. D., R. J. Reginato and C. H. M. Van Bavel. 1965. Comparison of measured and calculated hydraulic conductivities of unsaturated soils. *Water Resources Research*. 1(3):375-380.
- Jackson, R. D. 1972. On the calculation of hydraulic conductivity. *Soil Science Society of America Proceedings*. 36(2):380-382.
- King, L. G. 1965. Description of soil characteristics for partially saturated flow. *Soil Science Society of America Proceedings*. 29(4):359-362.
- Klute, A. 1965. Laboratory measurement of hydraulic conductivity of unsaturated soil. In: *Methods of soil analysis, Part 1* (edited by C. A. Black). American Society of Agronomy. pp. 253-261.
- Klute, A. 1973. Soil water flow theory and its application in field situations. In: *Field soil water regime* (edited by R. R. Bruce, et al.). *Soil Science Society of America Special Publication Series No. 5*. pp. 9-35.
- Kunze, R. J., G. Uehara and K. Graham. 1968. Factors important in the calculation of hydraulic conductivity. *Soil Science Society of America Proceedings*. 32(6):760-765.
- Laliberte, G. E., R. H. Brooks and A. T. Corey. 1968. Permeability calculated from desaturation data. *Journal of the Irrigation and Drainage Division, American Society of Civil Engineers*. 94(1):57-71.
- Laliberte, G. E. 1969. A mathematical function for describing capillary pressure-desaturation data. *Bulletin of the International Association of Scientific Hydrology*. XIV(2):131-149.
- Marshall, T. J. 1958. A relation between permeability and size distribution of pores. *Journal of Soil Science*. 9(1):1-8.
- Millington, R. J. and J. P. Quirk. 1961. Permeability of porous solids. *Trans. Faraday Society*. 57(7):1200-1207.
- Moore, R. E. 1939. Water conduction from shallow water tables. *Hilgardia*. 12:383-426.

- Nielsen, D. R., D. Kirkham and E. R. Perrier. 1960. Soil capillary conductivity: comparison of measured and calculated values. Soil Science Society of America Proceedings. 24(3):157-160.
- Nielsen, D. R., R. D. Jackson, J. W. Cary and D. D. Evans (editors). 1970. Soil Water. Western Regional Research Technical Committee W-68. pp. 85-102.
- Pearson, K. 1916. Mathematical contributions to the theory of evolution-XIX. Second supplement to a memoir on skew variation. Roy. Soc. of London, Phil. Trans. A216:429-557.
- Pearson, K. (editor). 1934. Tables of the incomplete Beta-function. Cambridge University Press. London. 494 pp.
- Purcell, W. R. 1949. Capillary pressures, their measurement using mercury and calculations of permeability therefrom. Journal of Petroleum Technology. 1(2):39-46.
- Richards, L. A. 1931. Capillary conduction of liquids through porous mediums. American Physical Society. Physics. 1:318-333.
- Ritter, H. L. and L. C. Drake. 1945. Pore-size distribution in porous materials. Industrial and Engineering Chemistry. Analytical Edition. 17(12):782-786.
- Ross, W. L. and J. F. Lutz. 1940. Determination of pore-size distribution in soils. Soil Science. 49:347-360.
- Scott, V. H. and A. T. Corey. 1961. Pressure distribution during steady flow in unsaturated sands. Soil Science Society of America Proceedings. 25(4):270-274.
- White, N. F. 1968. The desaturation of porous materials. A Ph.D. dissertation, Colorado State University, Fort Collins, Colorado.
- White, N. F., H. R. Duke, D. K. Sunada and A. T. Corey. 1970. Physics of desaturation in porous materials. Journal of the Irrigation and Drainage Division, American Society of Civil Engineers. 96(2):165-191.

Wyllie, M. R. J. and M. B. Spangler. 1952. Application of electrical resistivity measurements to problems of fluid flow in porous media. American Association of Petroleum Geologists. Bulletin. 36(2):359-403.

Wyllie, M. R. J. and G. H. F. Gardner. 1958. The generalized Kozeny-Carman equation. World Oil. March and April.

APPENDIX A

NOMENCLATURE

Nomenclature

<u>Symbol</u>	<u>Description</u>	<u>Dimension</u>
a	a parameter of the retention curve	none
a.	scaled domain of saturation defined by Equation (4-2)	none
b	a parameter of the retention curve	none
b.	scaled domain of saturation defined by Equation (4-3)	none
$\beta(p,q)$	Beta function with (p,q) as its arguments	none
$\beta_x(p,q)$	incomplete Beta function	none
D	diffusivity	L^2T^{-1}
D.	scaled diffusivity	none
D ₀	scaling factor for D defined by Equation (4-13)	L^2T^{-1}
H	a quantity defined by Equation (3-17)	none
$I_x(p,q)$	incomplete Beta function ratio	none
K	partial hydraulic conductivity	LT^{-1}
K.	scaled hydraulic conductivity, K/K_1	none
K ₁	total hydraulic conductivity	LT^{-1}
K _r	relative hydraulic conductivity, $K.$	none
k	partial permeability	L^2
k.	scaled permeability, k/k_1	none

<u>Symbol</u>	<u>Description</u>	<u>Dimension</u>
k_1	total permeability	L^2
k_r	relative permeability, k/k_1	none
m	a pore-size distribution parameter, also a parameter of the retention curve	none
P	capillary pressure	FL^{-2}
$P_.$	scaled capillary pressure, P/P_i	none
P_f	capillary pressure associated with the fictitious inflection point of the retention curve, also a parameter of the curve	FL^{-2}
P_i	capillary pressure at the real inflection point of the retention curve	FL^{-2}
P_s	scaled capillary pressure, P/P_f	none
P_w	pressure of soil-water	FL^{-2}
\bar{q}	volume flux	LT^{-1}
r	radius of pore	L
$r_.$	scaled radius of pore, r/r_i	none
r_i	radius of pore related to P_i	L
S	saturation	none
$S_.$	scaled saturation, $(S-S_r)/(1-S_r)$	none
S_e	effective saturation, $S_.$	none
S_f	saturation at the fictitious inflection point of the retention curve	none

<u>Symbol</u>	<u>Description</u>	<u>Dimension</u>
S_r	residual saturation, l-a-b	none
α	contact angle between the fluid and solid boundary	radian
γ	specific weight of the fluid	FL^{-3}
∇	vector differential operator	L^{-1}
σ	coefficient of surface tension	FL^{-1}
\emptyset	porosity of the porous medium	none

APPENDIX B

STEPS

TO REDUCE THE SYSTEM OF FOUR EQUATIONS
TO A SINGLE NONLINEAR EQUATION WITH S_r AS THE UNKNOWN

Let P_1 and S_1 , P_2 and S_2 , P_3 and S_3 , and P_4 and S_4 be four pairs of experimental data. Substituting those values into the equation

$$P = P_f \left(\frac{S - S_r}{a} \right)^{-m} \left(\frac{S_m - S_r}{b} \right)^{\frac{bm}{a}}$$

where S_m is the maximum saturation with $S_m \leq 1.0$, and taking the logarithms of the equations, one has a system of four simultaneous equations

$$\ln P_1 = \ln P_f - m \ln \left(\frac{S_1 - S_r}{a} \right) + \frac{bm}{a} \ln \left(\frac{S_m - S_1}{b} \right) \quad (1)$$

$$\ln P_2 = \ln P_f - m \ln \left(\frac{S_2 - S_r}{a} \right) + \frac{bm}{a} \ln \left(\frac{S_m - S_2}{b} \right) \quad (2)$$

$$\ln P_3 = \ln P_f - m \ln \left(\frac{S_3 - S_r}{a} \right) + \frac{bm}{a} \ln \left(\frac{S_m - S_3}{b} \right) \quad (3)$$

$$\ln P_4 = \ln P_f - m \ln \left(\frac{S_4 - S_r}{a} \right) + \frac{bm}{a} \ln \left(\frac{S_m - S_4}{b} \right) \quad (4)$$

Subtracting Equation (2) from Equation (1) yields

$$\ln \left(\frac{P_1}{P_2} \right) = m \ln \left(\frac{S_2 - S_r}{S_1 - S_r} \right) + \frac{bm}{a} \ln \left(\frac{S_m - S_1}{S_m - S_2} \right) \quad (5)$$

Similarly,

$$\ln \left(\frac{P_3}{P_4} \right) = m \ln \left(\frac{S_4 - S_r}{S_3 - S_r} \right) + \frac{bm}{a} \ln \left(\frac{S_m - S_3}{S_m - S_4} \right) \quad (6)$$

From Equation (5), one may obtain

$$m = \frac{\ln\left(\frac{P_1}{P_2}\right)}{\ln\left(\frac{S_2 - S_r}{S_1 - S_r}\right) + \frac{b}{a} \ln\left(\frac{S_m - S_1}{S_m - S_2}\right)} \quad (7)$$

Similarly from Equation (6),

$$m = \frac{\ln\left(\frac{P_3}{P_4}\right)}{\ln\left(\frac{S_4 - S_r}{S_3 - S_r}\right) + \frac{b}{a} \ln\left(\frac{S_m - S_3}{S_m - S_4}\right)} \quad (8)$$

Equating Equations (7) and (8), one has

$$\frac{\ln\left(\frac{P_1}{P_2}\right)}{\ln\left(\frac{S_2 - S_r}{S_1 - S_r}\right) + \frac{b}{a} \ln\left(\frac{S_m - S_1}{S_m - S_2}\right)} = \frac{\ln\left(\frac{P_3}{P_4}\right)}{\ln\left(\frac{S_4 - S_r}{S_3 - S_r}\right) + \frac{b}{a} \ln\left(\frac{S_m - S_3}{S_m - S_4}\right)}$$

or expressed in terms of b/a one has

$$\frac{b}{a} = \frac{\ln\left(\frac{P_3}{P_4}\right) \ln\left(\frac{S_2 - S_r}{S_1 - S_r}\right) - \ln\left(\frac{P_1}{P_2}\right) \ln\left(\frac{S_4 - S_r}{S_3 - S_r}\right)}{\ln\left(\frac{P_1}{P_2}\right) \ln\left(\frac{S_m - S_3}{S_m - S_4}\right) - \ln\left(\frac{P_3}{P_4}\right) \ln\left(\frac{S_m - S_1}{S_m - S_2}\right)} \quad (9)$$

Similarly, from the system of Equations (2), (3), (4) and (1),

$$\frac{b}{a} = \frac{\ln\left(\frac{P_4}{P_1}\right) \ln\left(\frac{S_3 - S_r}{S_2 - S_r}\right) - \ln\left(\frac{P_2}{P_3}\right) \ln\left(\frac{S_1 - S_r}{S_4 - S_r}\right)}{\ln\left(\frac{P_2}{P_3}\right) \ln\left(\frac{S_m - S_4}{S_m - S_1}\right) - \ln\left(\frac{P_4}{P_1}\right) \ln\left(\frac{S_m - S_2}{S_m - S_3}\right)} \quad (10)$$

Combining Equations (9) and (10), one has

$$\begin{aligned} & \frac{\ln\left(\frac{S_2 - S_r}{S_1 - S_r}\right) \ln\left(\frac{P_3}{P_4}\right) - \ln\left(\frac{S_4 - S_r}{S_3 - S_r}\right) \ln\left(\frac{P_1}{P_2}\right)}{\ln\left(\frac{S_m - S_3}{S_m - S_4}\right) \ln\left(\frac{P_1}{P_2}\right) - \ln\left(\frac{S_m - S_1}{S_m - S_2}\right) \ln\left(\frac{P_3}{P_4}\right)} \\ &= \frac{\ln\left(\frac{S_3 - S_r}{S_2 - S_r}\right) \ln\left(\frac{P_4}{P_1}\right) - \ln\left(\frac{S_1 - S_r}{S_4 - S_r}\right) \ln\left(\frac{P_2}{P_3}\right)}{\ln\left(\frac{S_m - S_4}{S_m - S_1}\right) \ln\left(\frac{P_2}{P_3}\right) - \ln\left(\frac{S_m - S_2}{S_m - S_3}\right) \ln\left(\frac{P_4}{P_1}\right)} \end{aligned}$$

or,

$$\frac{\ln \left[\frac{\left(\frac{S_2 - S_r}{S_1 - S_r} \right) \ln \left(\frac{P_3}{P_4} \right)}{\left(\frac{S_4 - S_r}{S_3 - S_r} \right) \ln \left(\frac{P_1}{P_2} \right)} \right]}{\ln \left[\frac{\left(\frac{S_m - S_3}{S_m - S_4} \right) \ln \left(\frac{P_1}{P_2} \right)}{\left(\frac{S_m - S_1}{S_m - S_2} \right) \ln \left(\frac{P_3}{P_4} \right)} \right]} = \frac{\ln \left[\frac{\left(\frac{S_3 - S_r}{S_2 - S_r} \right) \ln \left(\frac{P_4}{P_1} \right)}{\left(\frac{S_1 - S_r}{S_4 - S_r} \right) \ln \left(\frac{P_2}{P_3} \right)} \right]}{\ln \left[\frac{\left(\frac{S_m - S_4}{S_m - S_1} \right) \ln \left(\frac{P_2}{P_3} \right)}{\left(\frac{S_m - S_2}{S_m - S_3} \right) \ln \left(\frac{P_4}{P_1} \right)} \right]} .$$

That may be simplified by letting

$$A = \ln \left[\frac{\left(\frac{S_m - S_4}{S_m - S_1} \right) \ln \left(\frac{P_2}{P_3} \right)}{\left(\frac{S_m - S_2}{S_m - S_3} \right) \ln \left(\frac{P_4}{P_1} \right)} \right] , \quad B = \ln \left[\frac{\left(\frac{S_m - S_3}{S_m - S_4} \right) \ln \left(\frac{P_1}{P_2} \right)}{\left(\frac{S_m - S_1}{S_m - S_2} \right) \ln \left(\frac{P_3}{P_4} \right)} \right]$$

$$A1 = A \cdot \ln\left(\frac{P_3}{P_4}\right) \quad , \quad A2 = A \cdot \ln\left(\frac{P_1}{P_2}\right) \quad ,$$

$$B1 = B \cdot \ln\left(\frac{P_4}{P_1}\right) \quad , \text{ and } \quad B2 = B \cdot \ln\left(\frac{P_2}{P_3}\right) \quad .$$

Then,

$$\frac{\left(\frac{S_2 - S_r}{S_1 - S_r}\right)^{A1}}{\left(\frac{S_4 - S_r}{S_3 - S_r}\right)^{A2}} = \frac{\left(\frac{S_3 - S_r}{S_2 - S_r}\right)^{B1}}{\left(\frac{S_1 - S_r}{S_4 - S_r}\right)^{B2}} \quad .$$

This is a nonlinear equation with S_r as the only unknown.

APPENDIX C

COMPUTER PROGRAM

FOR DETERMINING THE PARAMETERS OF THE RETENTION FUNCTION

```

00001: C      NOTE: THE FIRST SET OF INPUT DATA IS THE
00002: C      INITIAL GUESS OF THE RESIDUAL SATURATION,
00003: C      SR=X(1), AND THE MAXIMUM SATURATION,
00004: C      SM, WHICH ARE TO BE TAKEN IN BY THE INPUT
00005: C      UNIT SPECIFIED IN THE STATEMENTS:
00006: C          READ(1,99)X(1),SM
00007: C      99  FORMAT(2(1X,F5.3))
00008: C      THE SECOND SET OF INPUT DATA IS THE COR-
00009: C      RESPONDING VALUES OF CAPILLARY PRESSURE, P,
00010: C      AND SATURATION, S, WHICH ARE TO BE TAKEN IN
00011: C      BY THE INPUT UNIT SPECIFIED IN THE STATEMENTS:
00012: C          READ(2,11)P1,P2,P3,P4,S1,S2,S3,S4
00013: C      11  FORMAT(4(1X,F6.2),4(1X,F5.3))
00014: C
00015: C      PROGRAM FP
00016: C      DIMENSION X(1)
00017: C      COMMON A1,A2,B1,B2,S1,S2,S3,S4,Q1,Q3
00018: C      READ(1,99)X(1),SM
00019: C      99  FORMAT(2(1X,F5.3))
00020: C      READ(2,11)P1,P2,P3,P4,S1,S2,S3,S4
00021: C      11  FORMAT(4(1X,F6.2),4(1X,F5.3))
00022: C      WRITE(61,97)
00023: C      97  FORMAT(1X,'INPUT DATA FOR THE RUN FOLLOW: '/')
00024: C      WRITE(61,98)X(1),SM
00025: C      98  FORMAT(1X,'INITIAL APPROXIMATION OF SR = ',F5.3,5X,
00026: C      1'MAXIMUM SATURATION = ',F5.3//)
00027: C      WRITE(61,13)
00028: C      13  FORMAT(3X,'P',5X,'S')
00029: C      WRITE(61,33)P1,S1
00030: C      WRITE(61,33)P2,S2
00031: C      WRITE(61,33)P3,S3
00032: C      WRITE(61,33)P4,S4
00033: C      33  FORMAT(1X,F6.2,1X,F5.3)
00034: C      A=ALOG((SM-S4)/(SM-S1))*ALOG(P2/P3))
00035: C      1-ALOG((SM-S2)/(SM-S3))*ALOG(P4/P1))
00036: C      B=ALOG((SM-S3)/(SM-S4))*ALOG(P1/P2))
00037: C      1-ALOG((SM-S1)/(SM-S2))*ALOG(P3/P4))
00038: C      B1=B*ALOG(P4/P1)
00039: C      B2=B*ALOG(P2/P3)
00040: C      A1=A*ALOG(P3/P4)
00041: C      A2=A*ALOG(P1/P2)
00042: C      CALL NONLIN(1,8,56,1,X,1,E-10)
00043: C      SR=X(1)
00044: C      C=((ALOG(P3/P4))*ALOG(Q1)-(ALOG(P1/P2))*ALOG(Q3))
00045: C      1/((ALOG(P1/P2))*ALOG((SM-S3)/(SM-S4))-(ALOG(P3/
00046: C      2P4))*ALOG((SM-S1)/(SM-S2)))
00047: C      XM=(ALOG(P1/P2))/ALOG(Q1)+C*ALOG((SM-S1)/(SM-S2))
00048: C      A=(SM-SR)/(1.+C)
00049: C      B=SM-SR-A
00050: C      D=ALOG(P1)+XM*ALOG((S1-SR)/A)-B*XM/A*ALOG((SM-S1)/B)
00051: C      PF=EXP(D)
00052: C      WRITE(61,77)
00053: C      77  FORMAT(///1X,'PARAMETERS OF THE RETENTION CURVE FOLLOW:')
00054: C      WRITE(61,19)SR,A,B,XM,PF
00055: C      19  FORMAT(//1X,'SR=',F5.3,4X,'A=',F5.3,4X,'B=',F5.3,4X,
00056: C      1'M=',F5.3,4X,'PF=',F7.3)
00057: C      END
00058: C      SUBROUTINE AUXFCN(X,Y,K)
00059: C      DIMENSION X(1)
00060: C      COMMON A1,A2,B1,B2,S1,S2,S3,S4,Q1,Q3
00061: C      T=X(1)
00062: C      Q1=(S2-T)/(S1-T)
00063: C      Q2=(S1-T)/(S4-T)
00064: C      Q3=(S4-T)/(S3-T)
00065: C      Q4=(S3-T)/(S2-T)
00066: C      Y=(Q1**A1)*(Q2**B2)-(Q3**A2)*(Q4**B1)
00067: C      RETURN
00068: C      END
00069: C      SUBROUTINE NONLIN(N,NUMSIG,MAXIT,IPRINT,X,EPS)
00070: C      REAL X(30),PART(30),TEMP(30),COE(30,31),RELCON,F,
00071: C      1FACTOR,HOLD,H,FPLUS,DEPMAX,TEST
00072: C      DIMENSION ISUE(30),LOOKUP(30,30)
00073: C      DELTA=1.E-7
00074: C      RELCON=10.E+8*(-NUMSIG)
00075: C      JTEST=1
00076: C      IF(IPRINT.EQ.1)PRINT 48
00077: C      48  FORMAT(1H1)
00078: C      ID 700 N=1,MAXIT
00079: C      IQUIT=0
00080: C      FMAX=0.
00081: C      M1=M-1
00082: C      IF(IPRINT.NE.1) GO TO 9

```

```

00083: PRINT 49,M1,(X(I),I=1,N)
00084:49 FORMAT(15,3E18.8/(E23.3, 2E16.6))
00085:9 DO 10 J=1,N
00086:10 LOOKUP (1,J)=J
00087: DO 500 K=1,N
00088: IF(K-1)134,134,131
00089:131 KMIN=K-1
00090: CALL BACK (KMIN,N,X,1SUB,COE,LOOKUP)
00091:134 CALL AUXFON(X,F,K)
00092: FMAX=AMAX1(FMAX,ABS(F))
00093: IF (ABS(F) .GE. EPS) GO TO 1345
00094: IQUIT=IQUIT+1
00095: IF(IQUIT .NE. N) GO TO 1345
00096: GO TO 725
00097:1345 FACTOR=.001E+00
00098:135 ITALLY=0
00099: DO 200 I=K,N
00100: ITEMP=LOOKUP (K,I)
00101: HOLD=X(ITEMP)
00102: PREC=5.F-6
00103: ETA=FACTOR*ABS(HOLD)
00104: H=AMIN1 (FMAX,ETA)
00105: IF(H .LT. PREC) H=PREC
00106: X(ITEMP)=HOLD+H
00107: IF(K-1) 161,161,151
00108:151 CALL BACK (KMIN,N,X,1SUB,COE,LOOKUP)
00109:161 CALL AUXFON (X,FPLUS,K)
00110: PART (ITEMP)=(FPLUS-F)/H
00111: X(ITEMP)=HOLD
00112: IF(ABS(PART(ITEMP)).LT.DELTA) GO TO 190
00113: IF(ABS(F/PART(ITEMP)).LE.1.E+15) GO TO 200
00114:190 ITALLY=ITALLY+1
00115:200 CONTINUE
00116: IF(ITALLY.LE.N-K) GO TO 202
00117: FACTOR=FACTOR*10.0E+00
00118: IF(FACTOR .GT. 11.) GO TO 775
00119: GO TO 135
00120:202 IF(K.LT.N) GO TO 203
00121: IF(ABS(PART(ITEMP)).LT.DELTA) GO TO 775
00122: COE(K,N+1)=0.0E+00
00123: KMAX=ITEMP
00124: GO TO 500
00125:203 KMAX=LOOKUP(K,K)
00126: DERMAT=ABS(PART(KMAX))
00127: KPLUS=K+1
00128: DO 210 I=KPLUS,N
00129: JSUB=LOOKUP(K,I)
00130: TEST=ABS(PART(JSUB))
00131: IF(TEST.LT.DERMAT) GO TO 209
00132: DERMAT=TEST
00133: LOOKUP(KPLUS,I)=KMAX
00134: KMAX=JSUB
00135: GO TO 210
00136:209 LOOKUP(KPLUS,I)=JSUB
00137:210 CONTINUE
00138: IF(ABS(PART(KMAX)).EQ. 0.0) GO TO 775
00139: 1SUB(K)=KMAX
00140: COE(K,N+1)= 0.0E+00
00141: DO 220 J=KPLUS,N
00142: JSUB=LOOKUP(KPLUS,J)
00143: COE(K,JSUB)=-PART(JSUB)/PART(KMAX)
00144: COE(K,N+1)=COE(K,N+1)+PART(JSUB)*X(JSUB)
00145:220 CONTINUE
00146:500 COE(K,N+1)=(COE(K,N+1)-F)/PART(KMAX)+X(KMAX)
00147: X(KMAX)=COE(N,N+1)
00148: IF(N.EQ.1) GO TO 610
00149: CALL BACK(N-1,N,X,1SUB,COE,LOOKUP)
00150:610 IF(M-1)650,650,625
00151:625 DO 630 I=1,N
00152: IF(ABS(TEMP(I)-X(I)).GT.ABS(X(I))*RELCON) GO TO 649
00153:630 CONTINUE
00154: JTEST=JTEST+1
00155: IF(JTEST-3) 650,725,725
00156:649 JTEST=1
00157:650 DO 660 I=1,N
00158:660 TEMP(I)=X(I)
00159:700 CONTINUE
00160: PRINT 1753
00161:1753 FORMAT(/' NO CONVERGENCE. MAXIMUM NUMBER OF ITERATIONS'
00162: 1' USED. ')
00163: IF(IPRINT .NE. 1) GO TO 800
00164: PRINT 1763

```

```

00165:1763  FORMAT(' FUNCTION VALUE AT THE LAST APPROXIMATION FOLLO'
00166:      1'WS: '/')
00167:      IFLAG=1
00168:      GO TO 7777
00169:725   IF(IPRINT.NE. 1) GO TO 800
00170:7777  DO 750 K=1,N
00171:      CALL AUXFCN(X,PART(K),X)
00172:750   CONTINUE
00173:      IF(IFLAG.NE. 1) GO TO 8777
00174:      PRINT 7788,(PART(K),K=1,N)
00175:7788  FORMAT(3E20.8)
00176:      GO TO 800
00177:8777  PRINT 751
00178:751   FORMAT(' CONVERGENCE HAS BEEN ACHIEVED. THE FUNCTION'
00179:      1' VALUE')
00180:      PRINT 7515,(PART(K),K=1,N)
00181:7515  FORMAT(' AT THE FINAL APPROXIMATION FOLLOWS: '/(3E20.8))
00182:      GO TO 800
00183:775   PRINT 752
00184:752   FORMAT(' MODIFIED JACOBIAN IS SINGULAR. TRY A DIFFEREN'
00185:      1'T')
00186:      PRINT 7525
00187:7525  FORMAT(' SET OF DATA OR DIFFERENT INITIAL APPROXIMATION.')
00188:800   MAXIT=MI+1
00189:      RETURN
00190:      END
00191:      SUBROUTINE BACK (KMIN,N,X,ISUB,COE,LOOKUP)
00192:      DIMENSION X(30),COE(30,31)
00193:      DIMENSION ISUB(30),LOOKUP(30,30)
00194:      DO 200 KK=1,KMIN
00195:      KM=KMIN-KK+2
00196:      KMAX=ISUB(KM-1)
00197:      X(KMAX)=0.0E+00
00198:      DO 100 J=KM,N
00199:      JSUB=LOOKUP(KM,J)
00200:      X(KMAX)=X(KMAX)+COE(KM-1,JSUB)*X(JSUB)
00201:100     CONTINUE
00202:      X(KMAX)=X(KMAX)+COE(KM-1,N+1)
00203:200     CONTINUE
00204:      RETURN
00205:      END

```

Example of Computer Print-Out

INPUT DATA FOR THE RUN FOLLOW:

INITIAL APPROXIMATION OF SR = .120 MAXIMUM SATURATION = .890

P	S
27.30	.262
22.10	.385
18.30	.507
10.80	.753

0	1.20000000E-01
1	1.23441716E-01
2	1.23339566E-01
3	1.23339476E-01

CONVERGENCE HAS BEEN ACHIEVED. THE FUNCTION VALUE
AT THE FINAL APPROXIMATION FOLLOWS:

2.91038305E-11

PARAMETERS OF THE RETENTION CURVE FOLLOW:

SR= .123 A= .236 B= .531 M= .186 PF= 23.014

APPENDIX D

EXPERIMENTAL DATA
PERTAINING TO THE FIGURES

GE2 Sand Imbibition

Figure 3(A)		Figure 3(B)	
$m = .244$ $S_r = .152$ $S_c = .632$ $P_f = 36.9$ $a = .476$ $P_i = 36.7$ $b = .250$		$m = .244$ $S_r = .173$ $S_c = .720$ $P_f = 36.9$ $a = .542$ $P_i = 36.7$ $b = .285$	
P (cm oil)	S	P (cm oil)	S_a
97.7	.153	97.7	.174
77.8	.190	77.8	.216
62.5	.247	62.5	.281
52.3	.324	52.3	.369
47.3	.390	47.3	.444
42.6	.480	42.6	.547
37.9	.600	37.9	.683
34.3	.690	34.3	.786
32.1	.741	32.1	.844
30.2	.786	30.2	.895
27.2	.838	27.2	.954
24.4	.846	24.4	.964
22.4	.855	22.4	.974
17.2	.871	17.2	.992
12.2	.873	12.2	.994
7.2	.878	7.2	1.000

GE3 Sand Imbibition

Figure 3(C)		Figure 3(D)	
$m = .515$ $S_r = .159$ $S_c = .711$ $P_f = 69.0$ $a = .591$ $P_i = 73.6$ $b = .116$		$m = .515$ $S_r = .184$ $S_c = .821$ $P_f = 69.0$ $a = .682$ $P_i = 73.6$ $b = .134$	
P (cm oil)	S	P (cm oil)	S_a
197.2	.266	197.2	.307
172.8	.300	172.8	.346
147.2	.342	147.2	.395
122.7	.412	122.7	.476
103.0	.496	103.0	.573
88.0	.595	88.0	.687
78.2	.675	78.2	.779
68.9	.756	68.9	.873
62.4	.803	62.4	.927
57.7	.829	57.7	.957
52.7	.845	52.7	.976
47.5	.853	47.5	.985
42.6	.859	42.6	.992
35.1	.866	35.1	1.000

Silty Clayey Sand (Figure 4(A))

Drainage			Imbibition		
m = .797	$S_r = .673$	$S_c = .935$	m = 1.42	$S_r = .637$	$S_c = .873$
$P_f = 53.7$	a = .249	$P_i = 49.2$	$P_f = 63.1$	a = .164	$P_i = 10.6$
	b = .078			b = .089	
P (cm H ₂ O)	S		P (cm H ₂ O)	S	
8.8	.998		326.2	.712	
18.6	.992		177.4	.741	
28.4	.987		99.4	.771	
38.1	.981		57.4	.801	
60.3	.903		34.5	.833	
72.5	.869		6.5	.880	
84.9	.845		0.0	.890	
100.9	.821				
118.8	.797				
145.0	.773				
179.7	.757				
326.2	.712				

J - 24 (Figure 4(B))

Drainage			Imbibition		
m = .567	$S_r = .354$	$S_c = .841$	m = .318	$S_r = .430$	$S_c = .806$
$P_f = 22.4$	a = .384	$P_i = 16.1$	$P_f = 26.3$	a = .178	$P_i = 12.3$
	b = .262			b = .352	
P (cm oil)	S		P (cm oil)	S	
1.6	.995		39.6	.510	
7.6	.958		29.7	.575	
10.2	.937		23.5	.640	
13.9	.870		18.7	.705	
18.2	.806		14.3	.770	
23.3	.737		10.1	.835	
28.5	.676		6.5	.899	
34.2	.603		0.2	.960	
42.2	.539				
49.3	.507				
54.8	.469				
67.3	.446				

J - 17 (Figure 5(A))

Drainage			Imbibition		
$m = .169$	$S_r = .128$	$S_c = .549$	$m = .188$	$S_r = .123$	$S_c = .562$
$P_f = 27.4$	$a = .260$	$P_i = 22.3$	$P_f = 23.0$	$a = .236$	$P_i = 16.7$
	$b = .502$			$b = .531$	
P (cm oil)	S		P (cm oil)	S	
13.0	.809		33.1	.203	
15.1	.762		27.3	.262	
16.9	.699		22.1	.385	
23.3	.515		18.3	.507	
29.6	.331		15.2	.630	
37.3	.202		10.8	.753	
53.7	.139		0.0	.885	

J - 50 (Figure 5(B))

Drainage			Imbibition		
$m = .098$	$S_r = .096$	$S_c = .523$	$m = .156$	$S_r = .112$	$S_c = .537$
$P_f = 21.5$	$a = .388$	$P_i = 21.1$	$P_f = 16.8$	$a = .324$	$P_i = 15.2$
	$b = .392$			$b = .440$	
P (cm oil)	S		P (cm oil)	S	
14.6	.853		23.3	.187	
17.1	.809		19.5	.297	
19.4	.717		17.3	.406	
20.5	.668		15.5	.515	
20.8	.555		13.9	.624	
21.9	.429		0.2	.876	
22.5	.316				
29.7	.124				

G - 1

Drainage (Figure 6 (A))		Rel. Permeability (Figure 6 (B))	
$m = .391$ $S_r = .161$ $S_c = .762$ $P_f = 2.17$ $a = .594$ $P_i = 2.15$ $b = .245$		Total Permeability $= 2.482 \times 10^{-8} \text{ cm}^2$	
P (cm H _g)	S	K _r	S
0.804	.980	1.000	1.000
1.41	.915	.340	.900
1.71	.855	.167	.800
2.01	.800	.078	.700
2.21	.740	.035	.600
2.41	.680	.014	.500
2.71	.580	.0045	.400
3.02	.515		
3.22	.460		
3.62	.395		
4.72	.290		
6.53	.210		
8.04	.195		

G - 4

Drainage (Figure 7 (A))		Rel. Permeability (Figure 7 (B))	
$m = .298$ $S_r = .357$ $S_c = .947$ $P_f = 3.19$ $a = .636$ $P_i = 3.28$ $b = .007$		Total Permeability $= 0.207 \times 10^{-8} \text{ cm}^2$	
P (cm H _g)	S	K _r	S
3.03	.999	1.000	1.000
3.23	.970	.550	.900
3.33	.925	.271	.800
3.43	.870	.110	.700
3.59	.799	.033	.600
3.79	.734	.006	.500
3.99	.663		
4.19	.618		
4.60	.538		
5.20	.487		
6.01	.442		
6.92	.407		
8.23	.377		

G-5 (Figure 9(A))

Crab Creek Sand (Figure 9(B))

Drainage			Drainage		
m = .279	S _r = .238	S _c = .830	m = .354	S _r = .173	S _c = .818
P _f = 3.76	a = .673	P _i = 4.00	P _f = 16.9	a = .723	P _i = 18.1
	b = .089			b = .104	
P (cm H _g)	S		P (cm oil)	S	
3.22	.995		12.0	.990	
3.52	.950		13.5	.986	
3.72	.915		14.5	.980	
3.92	.854		15.5	.974	
4.12	.789		16.0	.948	
4.32	.724		17.0	.895	
4.52	.653		17.2	.875	
4.77	.583		21.0	.638	
5.08	.523		24.8	.479	
5.38	.462		36.9	.277	
5.83	.407		67.7	.188	
6.48	.362		136.6	.158	
7.14	.327				
8.04	.291				